Norwegian University of
Science and Technology
NTNU

Department of Hydraulic and
Environmental Engineering

DYNAMICS OF THE SEASONAL SNOWCOVER IN THE ARCTIC

by

Oddbjørn Bruland

A dissertation submitted to the Faculty of Engineering Science and Technology,
the Norwegian University of Science and Technology,
in partial fulfilment of the requirements for the
degree of Doctor Engineer

Trondheim, Norway, March 2002
IVB Report B2-2002-2

URN:NBN:no-6348

URN:NBN:no-6348

ABSTRACT

Arctic snow cover is important to life on Earth from the microscale soil microarthropod population, to reindeer at the local scale and even the global scale through its impact on the global climate. There is a consensus that global warming will be enhanced towards the Arctic. This will influence the hydrology and snow cover in these regions, which in turn will provide a feedback to climate. There is still a lack of knowledge regarding the impacts to polar hydrology and snow cover; the gaps are even larger with respect to feedback mechanisms.

The objective of this study has been to improve the understanding and description of the dynamic processes of an Arctic snow cover. Here, the Arctic climate is studied from the first snow fall to the end of ablation in a series of nine publications grouped into three topics: “Snow Distribution”, “Snowmelt and Energy Balance” and “Measurement Methods”. The research is based on measurements and observations of climate, snow properties and snow distribution during the period 1992 to 2000 on the tundra in the vicinity of Ny-Ålesund at 78˚55’N, 11˚56’E at Svalbard, Norway.

Improvement of existing snowmelt models has been achieved by the implementation of energy balance calculations and improved description of the snow cover. Ground Penetrating Radar systems as a tool for snow surveying have been improved and used to measure and describe snow distributions over large areas. A snow drift model (SnowTran-3D) has been successfully tested for different scales and topography and was improved to better handle settling of the snow cover due to aging and melting.

URN:NBN:no-6348

URN:NBN:no-6348

PREFACE

This thesis is a result of a near decade long engagement in research related to snow and Polar Hydrology. I started with my diploma thesis in 1991 and continued at NTNU as a research assistant for one year and, from 1994, at SINTEF as researcher. Over these years I have been involved in many interesting projects and spent several, both laborious and magnificent, weeks in field. In 1997, I found it natural to employ my experiences and focus deeper on the topics of snow and Polar Hydrology by initiating a doctoral research programme.

This thesis is comprised of nine publications and the governing idea was to focus on different aspects of the seasonal snow cover in the Arctic at different scales. The publications result from cooperation with other scientists. I have made the principal contribution to six of these. In the publication Winther et al. (1998), I was involved in the planning and execution of the fieldwork, data handling and analysis and, finally, paper preparation. I was responsible for developing the snow radar setup and had the idea of connecting snow radar and GPS measurements described in Marchand et al. (2001a); the design of this system was worked out together with Egil Eide at NTNU. Wolf Marchand not only extensively tested and adjusted the system, he prepared the publication which describes the system and its testing. My least contribution was in the publication co-authored with Glen Liston. He was responsible for both the data analysis and the preparation of the paper whereas I was involved solely in the fieldwork on Antarctica. None the less, this was an important experience for me and this publication is included to reflect the scope of my activities during the doctoral programme.

To distinguish what has attracted me most to the subject of this thesis carrying me through year after year of studying, is not simple. Some of my favourite and most vivid memories from my childhood are connected to snow and skiing. I am grateful to both my parents and my sisters for shaping my longing for mountains and snow.

An opportunity to accommodate these longings and even amplify them, was given to me when I for the first time had the chance to experience Svalbard in the summer of 1991. Thanks to Professor Ånund Killingtveit it was possible for me to do my diploma thesis on Arctic hydrology, and to do field work on Svalbard; for it I owe him deep debt of gratitude.

URN:NBN:no-6348

Except for one year, I have been to Svalbard and Ny-Ålesund every May and late August between 1991 and 2000 for fieldwork, most of the time together with Dr. Knut Sand. A better fellow labourer in field cannot easily be found. Neither can there be a better place for doing fieldwork. Both Norwegian Polar Institute Research Station in Ny-Ålesund and Kings Bay A/S and their employees are acknowledged for their endurance.

Antarctica is one of the dreams that for most of us only are dreamt. Through Norwegian Antarctic Research Expedition of 96/97 I had the chance to realise this dream. Jan-Gunnar Winther and Knut Sand were the keys to this realisation, and to them and others involved, thank you. For five weeks I got to know Glen E. Liston when we worked as a "two man field group" in Jutulgryta, Antarctica as part of that expedition. Dr. Liston created SnowTran-3D and later taught me how to use it, for which I am grateful.

Last, I am most grateful for the funding from the Norwegian University of Science and Technology and Norwegian Research Council making this study possible.

…….……...……and thanks to Anne et al.

URN:NBN:no-6348

TABLE OF CONTENTS

URN:NBN:no-6348

Paper 1: Energy and water balance studies of a snow cover during snowmelt period at a high arctic site. *Theoretical and Applied Climatology, Vol. 70* (1-4), pp. 55-63.

Paper 2: An energy balance based HBV- Model with application to an Arctic watershed on Svalbard, Spitsbergen. *Nordic Hydrology, Vol. 33* (2).

Paper 3: Glacial mass balance of Austre Brøggerbreen modelled with the HBV-model. *Polar Research*, accepted for publishing June 2002.

Paper 4: Meltwater production in Antarctic blue-ice areas: sensitivity to changes in atmospheric forcing. *Polar Research, Vol. 18* (2), pp. 283-290.

Paper 5: Snow Distribution at a High Arctic Site at Svalbard. *Nordic Hydrology, Vol. 32 (1),* pp. 1-12.

Paper 6: Snow accumulation distribution on Spitsbergen, Svalbard, in 1997. *Polar Research, Vol. 17* (2), pp. 155-164.

Paper 7: Modelling of the snow distribution at two high arctic sites at Svalbard, Norway, and at a sub-arctic site in central Norway. Submitted to *Nordic Hydrology* Nov 2001.

Paper 8: Application of Georadar in Snow Cover Surveying. *Nordic hydrology*, *Vol. 29 (4/5),* pp. 361-370.

Paper 9: Improved Measurements and Analysis of Spatial Snow Cover by Combining a Ground Based Radar System With a Differential Global Positioning System Receiver. *Nordic Hydrology, Vol. 32 (3)*, pp. 181-194.

URN:NBN:no-6348

1 INTRODUCTION

This Ph.D. study has been carried out as a part of the project "Dynamics of the Seasonal Snow Cover in the Arctic" which was supported financially by the Norwegian Research Council under the programme "Arktisk lys og varme" (ALV – Arctic Light and Heat) and administrated by SINTEF. The project was coordinated with the ongoing ALV-project "Spectral Reflective Characteristics of Snow and Sea Ice" and the project "Regional Snow Distribution on Svalbard", both administrated by the Norwegian Polar Institute (NP), as well as the EU-funded project "Understanding Land Surface Physical Processes in the Arctic (LAPP)" coordinated by Institute of Hydrology (IH), Wallingford, England.

1.1 BACKGROUND

The hydrology of the Arctic dominated by snowmelt as the surface energy balance rapidly changes from a net loss of energy to a net gain during a period of near maximum incoming solar radiation. The hydrological regime can be divided into three distinct periods: winter, snowmelt and summer. Winter can last from eight to 10 months; its dominant processes are snow fall, accumulation and redistribution by wind, and seasonal freezing of the soil active layer with redistribution of soil moisture. In the High Arctic, 60-80% of the annual precipitation is accumulated as snow cover storage at the end of winter. The snowmelt period usually starts sometime between mid-May and mid-June. At this time the incoming solar radiation is close to its maximum. Ablation is intense and the river runoff increases from zero to peak flow within a few days. The snow cover rapidly decreases and within 10-14 days only the deep snowdrifts remain. As the snow cover depletes, evaporation from bare soil usually becomes the main mechanism of water loss throughout the rest of the summer. Major rainfall events will produce significant runoff, but the greatest volume of runoff is produced by snowmelt.

The consensus of opinion is that atmospheric warming due to increased greenhouse gases will be most pronounced at high latitudes (Vörösmarty et al., 2001). Such warming will initially affect the surface hydrology of the tundra.

URN:NBN:no-6348

The permafrost has a central role in the hydrology and is crucial in determining the vegetation type, carbon balance and the surface/atmosphere energy and water exchanges. Thus the response of the permafrost to global warming is a central component of the feedback between climate change and the tundra ecosystem. The tundra biome occupies approximately 10% of the Earth's land area and contains perhaps 33% of the global terrestrial total carbon (Lloyd et al., 1999). Warming in these regions will deepen the active soil layer, which forms above the permafrost in the summer months, providing the potential for enhanced CO_2 and CH_4 emissions.

Snow is another surface feature, which causes an important feedback to climate change. Snow cover changes the surface properties and also isolates the surface from the atmosphere during the winter. The change in the extent of snow cover due to atmospheric warming will have an important positive feedback on global warming through the radiation input (Harvey, 1988). The date of formation of the winter snow cover and the timing and rate of melt will strongly influence the thermal regime within the soil for the rest of the year and determine the start of the active season (Rouse, 1984). Melt also provides the major water source for subsequent vegetation use and is the major input to any of the regional river systems. The balance between runoff and infiltration is governed by the extent of frost depth (in the absence of continuous permafrost) and the rate of withdrawal of the permafrost horizon (Repp, 1988). The permafrost horizon creates a general lower limit for soil water drainage above which saturated and unsaturated soil horizons form. Within these soil moisture regimes, the production of methane and carbon dioxide may occur and their release into the atmosphere provides another positive feedback to global warming (Christensen, 1991; Grogan and Chapin, 2000).

Lloyd et al. (1999) found that with regard to the process of global warming, the premise that the Arctic will become a net source of CO_2 is highly dependent upon the particular climatic conditions, especially the depth of the summer snow cover, summer cloudiness and precipitation frequency. They also found that length of growing season is a the key factor for the variability of CO_2 balance over mountain birch forest in Kevonen, North Finland.

The land surface albedo has a large influence on the radiation balance of the Earth and in the Northern Hemisphere this is closely linked to snow coverage (Figure 1-1). Colman et al. (1994) states that the albedo is one of the most important parameterisation in global climate models (GCM) and better description of the snow distribution and thereby albedo can improve global climate modelling. Snow cover is the most variable land-surface condition in

URN:NBN:no-6348

both time and space (Cohen, 1994; Gutzler and Rosen, 1992) making it a viable candidate for amplifying climate anomalies (Cohen and Entekhabi, 1999). Cohen and Entekhabi (1999) and Walland and Simmonds (1997) found through GCM experiments that changes to the snow cover of the Northern Hemisphere will have strong impacts on climate. Changed albedo following changes in snow cover, leads, in first order, to air temperature changes. With this follows changes in air pressure, circulation patterns and, further on, changes in number of storm events and their intensity.

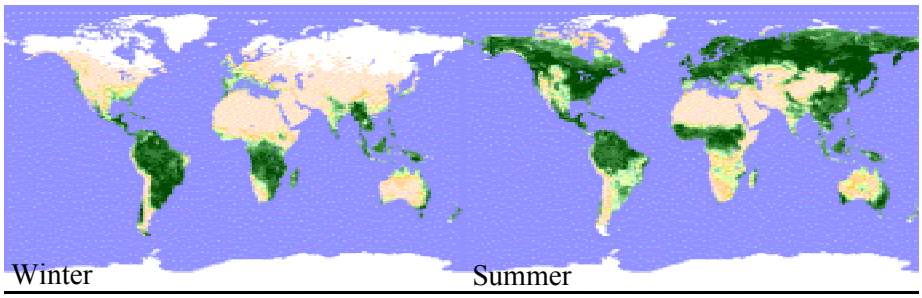

Figure 1-1 The major extent of snow and vegetation covers in 1988 shows how important these factors are to the earth's surface albedo (http://hum.amu.edu.pl/~zbzw/glob/glob1.htm, Nov. 2001)

Even at high latitudes such as Svalbard, rainfall on a cold snowpack and/or snowmelt may occur during the winter. Due to the cold content of the arctic snowpack, the liquid water will refreeze quickly and form ice layers within the snowpack. Such ice layers have been observed to be 10 cm or more thick and make finding food sources extremely difficult for Svalbard reindeer. Heavy rainfall on frozen tundra also occurs and forms a layer of basal ice which covers the vegetation. In the spring of 1994, a basal ice layer of up to 20 cm thick was observed in snow pits on the tundra in the area near Ny-Ålesund. This layer was impenetrable to reindeer hooves and during the most critical phase of their survival, it largely restricted their access to food supply leading to a severe reduction in the reindeer population of the area. This icing was due to an extreme hydrological events, but even so, the snow cover strongly influences the behaviour and survival of the reindeer population. Van Der Wal et al. (2000) showed experimentally that the timing of snowmelt influenced the foraging behaviour of Svalbard reindeer. Unlike the temperate regions, where selection of plant quality seems to be of major importance, Svalbard reindeer preferred the greater plant biomass they found in the areas that had been snow-free longest. Similarly, Johnson et al., (2001) found that the foraging behaviour of woodland caribou in British Columbia is strongly influenced by snow cover.

URN:NBN:no-6348

Figure 1-2 Basal ice impedes access to grass making Svalbard reindeer struggle for food
(photo G. Bangjord)

The seasonal snowpack and its spatial distribution determines very important conditions for plant growth; the timing of the snowmelt period determines the length of the growing season, while snowmelt probably provides the most important supply of water available to the plants. Bruland and Cooper (2001) compared snow depth distribution and vegetation distribution in a 3 km^2 typical tundra area close to Ny-Ålesund at 78˚55'N, 11˚56'E on Svalbard and found a significant correlation between these distributions. Warmer climate and longer growing seasons may lead to conditions where taller vegetation can establish. In areas where these are currently partially or totally absent, this will have a large impact on the surface albedo and thereby a positive feedback to the climatic warming in the arctic regions. This statement is supported by Chalita (1994), Douville and Royer (1997) and by Keller et al. (2000).

Impacts of a climatic warming on the hydrological regime and its influence on the biosphere has been addressed by many scientists e.g.; Sælthun et al. (1998), Woo (1986), Kane (1996), and Kane et al. (1992). Climatic warming will affect the arctic hydrology through a shift in the seasonality of the hydrologic regime. The spring flood due to snowmelt runoff, will come earlier and will influence the stability of the water column in coastal belt of the North Atlantic Ocean and the Arctic Ocean (Slagstad, 2001). This will have an influence on the timing of the primary production in these areas. The impact this may have on the fisheries in, for example, the Barents Sea which support one of the largest fisheries in the world, is unknown. Fresh water input to the Arctic Ocean also has an impact on the sea ice and thereby the oceanographic circulation (Weatherly and Walsh, 1996) and the average albedo of the Arctic Ocean. A climatic warming will also give a higher flux

URN:NBN:no-6348

of heat into the ground thus increasing the depth of the active layer. A deepening of the active layer may eventually give increased soil moisture storage capacity, improve subsurface drainage and, consequently, decrease the amount of soil moisture within the soil profile. In turn, this may decrease the total area of wetlands in the Arctic. A deeper active layer may also lead to more erosion and thereby higher sediment and nutrient transport from land to ocean (Vörösmarty et al., 2001).

The above mentioned importance of the arctic snow cover is mainly related its impact on climatic change. Snow, snow cover, snow drift and snow storage are also important in a sociological and economic context. This is emphasized in the planning and construction of roads and buildings, in planning and management of hydropower schemes and finally, to a lesser but growing extent, for ski resorts. Barth Johnson, a road engineer far ahead of his time, published a book as early as 1857 in which he described and discussed problems related to snow and snowdrift (Barth Johnson, 1857). Norem (1968) discussed methods of locating and constructing roads over mountain passes with high snow accumulation. The importance of snowdrift to the magnitude and timing of snowmelt generated runoff is emphasized by Hartman et al. (1999). Referring to Blöshl et al. (1991) and McLung and Scharer (1993), Marsh (1999) noted, "Redistribution of snow in mountainous environments is extremely important for both runoff calculation and avalanche forecasting".

Figure 1-3 Avalanche is an imminent danger in exposed areas

URN:NBN:no-6348

1.2 OBJECTIVES AND ORGANISATION

The main objective of the project "Dynamics of the seasonal snow cover in the Arctic" has been:

> "*To gain a better understanding of the dynamic processes of seasonal snow cover in an arctic area and assess its response to a climate warming*"

In order to fulfil this, the following sub-objectives were stated:

- ***To understand*** better the physical processes that control the spatial distribution of snow, the thermal processes within the snowpack, the formation of ice layers and snowmelt runoff in arctic environments.
- ***To determine*** how arctic seasonal snow cover will respond to climate warming.
- ***To investigate*** whether the seasonal snow cover will change critical conditions in arctic ecosystems due to possible changes in the length of the growing season and the availability of water.
- ***To test*** different instrumentation as well as to develop and test measurement methods and modelling schemes for hydrological studies at different scales.

The PhD study were focused on three main subjects which largely fall under the first and last of the sub-objectives listed above. The publications the thesis is compiled of can be categorised under the main subjects as follows:

URN:NBN:no-6348

Snow Distribution: mapping and modelling;	**Snow Distribution: measurement method;**	**Snowmelt modelling;**
Bruland et al. (2002) Modelling the snow distribution at two high Arctic sites at Svalbard, Norway, and at a sub-arctic site in central Norway	*Sand and Bruland (1998)* Application of Geo-radar for snow cover Surveying,	*Bruland and Killingtveit (2002)* An Energy Balance Based HBV- Model with Application to an Arctic Watershed on Svalbard, Spitsbergen,
Bruland et al. (2001b) Snow Distribution at a High Arctic Site at Svalbard	*Marchand et al. (2001a)* Improved Measure-ments and Analysis of Spatial Snow Cover by Comb-ining a Ground Based Radar System With a Differential Global Positioning System Receiver	*Bruland et al. (2001a)* Energy and water balance studies of a snow cover during snowmelt period at a high arctic site
Winther et al. (1998) Snow accumulation distribution on Spits-bergen, Svalbard, in 1997		*Bruland and Hagen (2002)* Mass Balance of Austre Brøggerbreen modelled with the HBV-model
		Liston et al. (1999a) Meltwater production in Antarctic blue-ice areas: sensitivity to changes in atmospheric forcing.

In addition to the articles included in this thesis, the author has contributed to the following publications during his doctoral research programme; Liston et al. (2000), Liston et al., (1999b), Sand et al. (2002) and Sand and Bruland (1999)

The bulk of this study has been carried out in the neighbourhood of Ny-Ålesund on Svalbard. Meteorological observations combined with detailed measurements of snow properties and snowmelt at the plot scale have been made during the ablation periods since 1992. The extensive climate and snow data sets that have been amassed have been used to compare and improve snowmelt models. Additionally, detailed measurements of snow distribution were made at the end of the accumulation period for 1998, 1999 and 2000. These data were used to describe snow distribution and to validate and improve a snow transport and redistribution model. The energy balance and snow redistribution models are crucial tools for answering the other sub-objectives in the "Dynamics of the seasonal snowcover in the Arctic".

URN:NBN:no-6348

The Ny-Ålesund study sites and fieldwork will be briefly mentioned below along with a discussion of the current state of knowledge of the three main topics of this thesis. Finally, the contents of each of the appended articles and how these articles relate to this thesis will be addressed.

1.3 STUDY SITES AND FIELD WORK

Figure 1-4 Location of Ny-Ålesund, Bayelva catchment and study areas

The field campaigns and the extensive measurements and observations of meteorological parameters, snow properties, snowmelt, and snow distribution prior to and during snowmelt has been an essential part of this study and deserve to be mentioned.

URN:NBN:no-6348

Most of the data collection and the process studies were made in the Bayelva river catchment west of Ny-Ålesund (78˚55'N, 11˚56'E), Svalbard (Figure 1-4). The first runoff plot was established in autumn 1991 on a south-facing slope of Rabben approximately 2 km west of Ny-Ålesund (Figure 1-5, Figure 1-6).

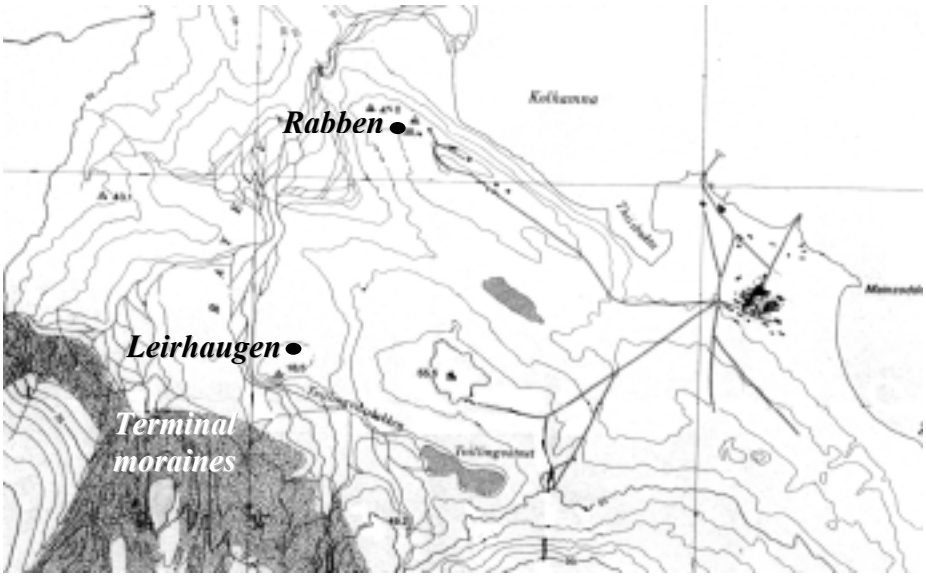

Figure 1-5 Location of the study sites

Runoff from this 40 m^2 plot was measured during the ablation periods following 1991 up to 1994. Snow depths at the plot and snow properties in adjacent snow pits were also measured (Figure 1-8). Meteorological observations were made from a 10 m high tower. Soil temperature and liquid water content were also measured. The purpose of these measurements was to study the energy and water balance of an arctic snow cover and the active layer.

URN:NBN:no-6348

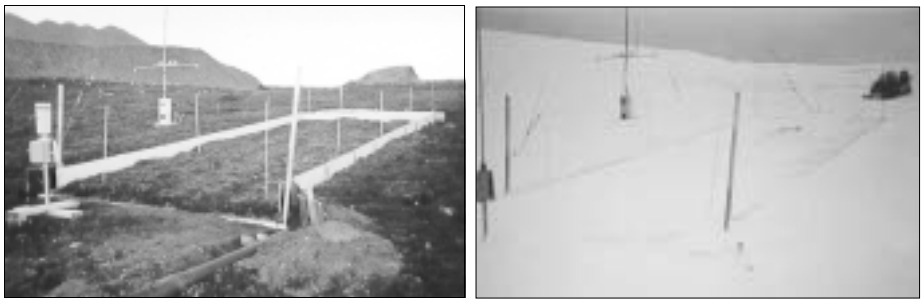

Figure 1-6 Runoff plot setup at Rabben. A gutter system collects runoff and transports it to an automatically emptied storage tank with water level recording. Snow and ice storage are measured at the stakes.

The knowledge and experience gained over these years were invaluable when similar measurements were to be carried out for both the LAPP project and this study. Disturbances near Rabben due to the extension of the adjacent airstrip, forced the plot to be relocated. In 1996 two 100 m^2 plots were established on the north-facing slope of Leirhaugen approximately one kilometre south-southeast of the previous plot (Figure 1-7). In 1998 a third 100 m^2 plot was established on the south-facing slope of Leirhaugen.

The data collected at all the sites from 1991 to 1998 are reported in Bruland (1999), and are used as a basis for the comparison of different snowmelt models in Bruland et al. (2001a).

Figure 1-7 Setup of the Leirhaugen runoff plots. A tipping bucket recorder is used to measure snowmelt.

URN:NBN:no-6348

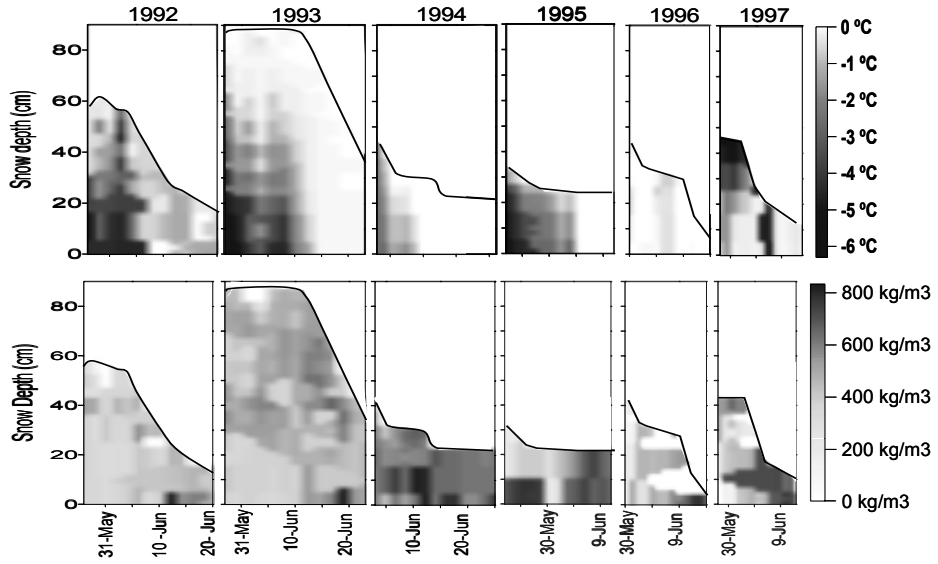

Figure 1-8 Snow temperature and density measurements in snowpits at Rabben

During measurement period at Leirhaugen (i.e., from 1996), snow depths were recorded daily each ablation season. Observations were made every five metres along a 200 metre transect running from the summit of Leirhaugen down the northern slope. Additionally, snow density and other snow properties were measured and recorded at both the deepest and shallowest parts of the transect. The snow depth before snowmelt typically ranged from 20 cm to 120 cm at the shallowest and deepest parts. These detailed measurements were used to calibrate and validate snow radar measurements made at the same time along this transect (Sand and Bruland, 1998).

Hourly soil temperatures at 5 cm depth were measured with thermistors every 5m along the same transect line (Figure 1-9). Furthermore, every 50 meters temperature was measured down to 1m depth. The purpose of these measurements was to study the dependency of soil temperature and active layer thawing on snow depth. Unfortunately, time constraints have meant that this data must wait for a future project for analysis.

URN:NBN:no-6348

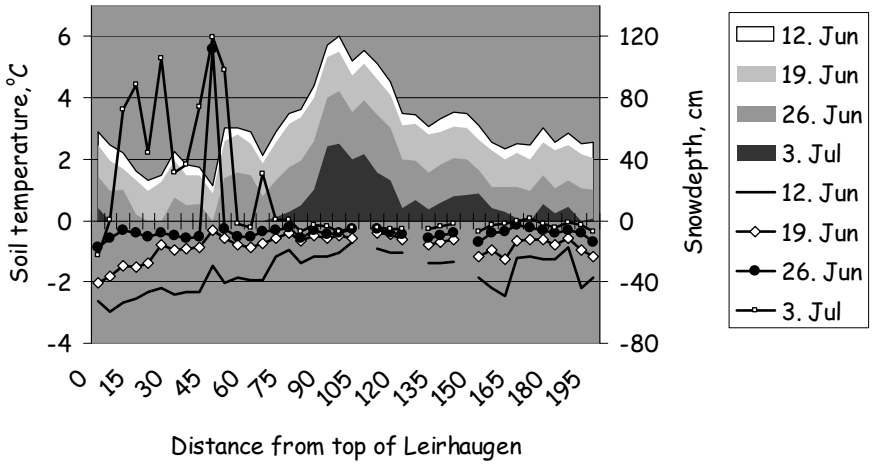

Figure 1-9 Snow depths and soil temperatures during ablation 2000.

URN:NBN:no-6348

2 SNOWMELT MODELLING

A wide variety of snowmelt models with many different levels of complexity have been developed and presented over the last decade. The complexity depends mainly on the purpose of the calculations, the availability of data and computer power. The latter has developed exponentially and has gradually opened new horizons for modellers. The availability of input data has not improved at the same rate and is today the most limiting factor for further model development.

The simplest snowmelt model, the temperature-index model, is based solely on a relationship between air temperature and melt intensity, the degree-day-factor (e.g. Bergstöm, 1975). The most complex models are based on a full description of the energy balance and layering of the snowpack (e.g. Anderson, 1976; Jordan, 1991; Brun et al.,1989). In between these two degrees of complexity are many variations with simple expressions of the energy balance (e.g. Bengtsson, 1976; Sælthun, 1996).

Anderson (1976) concludes that the temperature-index type models generally work well for average conditions and that the more physically-based energy balance models should work well under all conditions, but particularly during extreme conditions. This latter property is especially important when it comes to predicting floods, which are normally the result of extreme climatic situations. Models of different complexity have been compared by, for instance; Kane et al. (1997), Essery et al. (1999b) and Bruland et al. (2001a). The main conclusions are that the simple model works reasonably well and that even the most complex models only slightly improve runoff calculations. In an ongoing project called SnowMip (Météo-France, 2001) several model of generally high complexity will be compared.

Usually, the more complex a the model is the greater the need for input data; scaling problems increase as one moves from point measurements to large spatial representation of the input data. The scaling issue in snow hydrology is extensively discussed by Blöshl (1999). Marsh (1999) discussed the spatial variance of the different fluxes and parameters included in energy balance calculations when applied over a large area and he cited several other studies where this subject is touched on in one way or another.

URN:NBN:no-6348

2.1 TEMPERATURE-INDEX MODEL

The temperature-index model (TIM) is applied in the snow routine of the HBV-model. It is based on a simple linear relationship between air temperature and snowmelt intensity (Figure 2-1) (Bergstöm, 1975). Melt rate, refreezing index, threshold temperature for snowmelt and maximum water content in the snow, are used to calibrate the model. The model is primarily made for timing and intensity calculations of snowmelt runoff and takes into account storage and refreezing of liquid water within the snowpack. These processes only influence the water retaining capacity of the snowpack and have no effect on the melt rate.

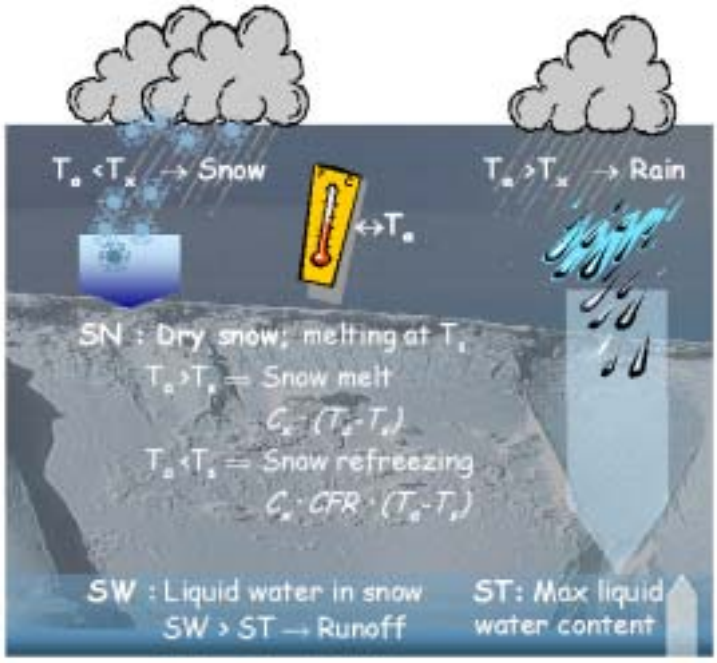

Figure 2-1 The Temperature-index (C_x) based snowmelt routine applied in the HBV-model (Killingtveit and Sælthun, 1995).

URN:NBN:no-6348

2.2 ENERGY BALANCE MODELS

The energy balance at the surface is essential to heating or cooling of any material. Properties such as thermal conductivity and capacity and surface reflectance defines how energy is absorbed, stored and transported in a material. Snow has high reflectance due to it bright white surface. Its porosity means that it insulates well and has low thermal conductivity. Much energy is needed to heat snow due to high thermal capacity.

The energy balance for a snowpack can be written as:

$$Q_m + Q_i = Q_{sh} + Q_{lo} + Q_h + Q_e + Q_g + Q_r \quad (2.1)$$

where

Q_m = energy available or used for melting snow (W/m^2),
Q_i = internal energy changes through heating or cooling of the snowpack (W/m^2),
Q_{sh} = net shortwave radiation (W/m^2),
Q_{lo} = net longwave radiation (W/m^2),
Q_h = sensible heat (W/m^2),
Q_e = latent heat (W/m^2),
Q_g = ground heat flux (W/m^2),
Q_r = heat from precipitation (W/m^2).

The sun is the source to the shortwave radiation. Atmospheric conditions and cloudiness determines how much of the extraterrestrial solar radiation will reach the earth's surface. The reflectance of the surface determines how much of this energy is absorbed. Any material emits longwave radiation proportional to the fourth power of its temperature. The atmosphere and the surroundings are sources of incoming longwave radiation and the surface temperature determines whether it looses or gains longwave radiation energy. Sensible heat flux is a result of direct contact between the surface and overlying air, the temperature differences determine the direction and the size of the flux. Latent heat energy is gained through condensation of water vapour in the air onto the snow or lost if snow sublimates or liquid water held in the snow evaporates. The boundary layer air gradually adjusts to the snow surface conditions. Thus the sensible and latent heat fluxes decrease if "old" air replenished by wind with "fresh", (for instance, warm and dry air). The rate of energy exchanges between the air and surface depends on surface roughness, wind speed and air stability. High wind speeds transport saturated "old" air away while bringing "fresh" air down to the snow surface.

URN:NBN:no-6348

A rough surface creates turbulence that leads to more efficient exchanges of boundary air masses. However, on a very rough surface with, for instance shrubs or tall vegetation, “old” air can be trapped even at high wind speeds. The air mass stability mainly influences the exchange rate when the air is calm with low wind speeds.

Ground heat flux depends on the temperature gradient between the ground surface and deeper levels. The below ground temperature is usually stable over the year at a depth of 10 to 15 metres (Williams and Smith, 1989) and the direction and size of the flux depends on the surface temperature. In the Ny-Ålesund area ground temperature was found to be stable at –4ºC 10 metres depth. Temperature of the rain or snow determines the energy flux due to precipitation. The last-mentioned two fluxes are usually of minor importance compared to the others in arctic regions and will not be discussed further.

The energy balance fluxes, especially the turbulent heat fluxes, are difficult to measure directly. For operational purposes simpler measurements are usually required. Data required to run a simple energy balance can be easily be collected. The instrumentation costs are reasonably and the measurements are easily maintained.

2.2.1 Solar radiation

Solar radiation varies with latitude, time of year and day, topography, vegetation canopy, cloud cover and atmospheric turbidity. Radiation that influences snowmelt has wavelengths between 0.2 and 100 μm; the portion that falls between 0.2 and 2.2 μm is generally considered shortwave or solar radiation (Gray and Male, 1981). Shortwave radiation can both be direct and diffuse. The diffuse (or scattered) portion is due to reflectance from the surroundings and from clouds. Depending on location and cloud formations the point value can be considerably larger on a partially cloudy day than on a clear one. Referring to Kuz'min (1961), Gray and Male (1981) state that the increase in scattered radiation over snow relative to that over bare ground ranges from 65% to 12% for solar elevations between 12° and 55° respectively. Orientation and slope affect the direct solar radiation an area receives. An example from Gray and Male (1981) shows that even with a 10° slope the effect of orientation to the solar disc is significant. At 50° N during April, a south-facing slope receives 40% more direct radiation than a north-facing slope. As the slope increases this difference becomes more pronounced. So even though the point value of shortwave radiation maybe simple to measure, up-scaling to larger areas can be far more complicated.

URN:NBN:no-6348

Net shortwave radiation (Incoming - Reflected) is calculated as the difference between either measured incoming radiation (Q_{si}) or the extra-terrestrial radiation (Q_{ex}) for a given date and latitude corrected for atmospheric effects, and reflected shortwave radiation given by the albedo of the surface. Garnier and Ohmura (1970) calculated incoming shortwave radiation on a clear day. According to Harstveit (1984) and Sand (1990) different authors (they cite Penmann, 1948; McKay, 1970; Bayne, 1978; Suckling and Hay, 1977) gave good estimates of actual radiation on cloudy days using relationships based on the potential radiation for clear conditions and information on cloudiness. Harstveit (1984) suggested a calculation of the form;

$$Q_{si} = Q_{ex} \cdot (k_{s1} \cdot C_s + k_{s2} \cdot C_s^{½} + k_{s3}), \quad (2.2)$$

where C_s = 1 – Cloudiness (0–1) and k_{s1}, k_{s2}, k_{s3} are empirical constants.

2.2.2 Albedo

The albedo of the snow (A) determines the proportion of the shortwave radiation reaching the surface that is reflected rather than absorbed by the snow. Snow albedo largely depends on the physical properties of the snow and is strongly affected by pollution and deposition on the snow surface. Fresh snow has a high albedo, often greater than 0.8, while older polluted snow may have an albedo as low as 0.2.

Gray and Male (1981) summarise the conditions and snow properties influencing the albedo of the snow. Winther et al. (1999), Winther (1993) and Gerland et al. (1999) present excellent studies of albedo variability related to changing snow properties during ablation. Several models have been suggested for calculating albedo over the snow season. Anderson (1976) found a high correlation between values simulated by a model based on the snow grain size and the extinction coefficient of clear ice suggested by Bohren and Barkstrom (1974) and albedo. Harstveit (1984) suggested a regression model of albedo based on his observations in Dyrdalen, Western Norway. He investigated the correlation between observed albedo, age of snow (days), and cloud cover. His model (Eq. 2.3) gave a multiple correlation coefficient of r = 0.77 for his data.

$$A = k_{a1} \cdot (1 - C_s) + k_{a2} \cdot \ln(d) + k_{a3}, \quad (2.3)$$

where A= albedo, d = age of snow surface in days and k_{a1}, k_{a2}, k_{a3} are empirical constants.

URN:NBN:no-6348

Sand (1990) used a model suggested by (U.S. Army Corps of Engineers, 1956) based on the cumulative maximum daily air temperature (T_{acc}). Winther (1993) was able to improve the albedo calculation (Eq. 2.4) by including solar radiation (SR) in addition to T_{acc}.

$$A = k_{W1} - k_{W2} \cdot T_{acc} - k_{W1} \cdot SR, \tag{2.4}$$

where k_{W1}, k_{W2}, k_{W3} are empirical constants.

2.2.3 Longwave radiation

The source of incoming longwave radiation is atmospheric compounds. About 16% of the extra-terrestrial solar radiation is absorbed by mainly water vapor, ozone, carbon dioxide and dust in the atmosphere, and about 4% by clouds. This absorbed energy raises the temperature of the atmosphere and is emitted from the same compounds as longwave radiation of which a portion reaches the earth surface. Incoming longwave radiation (Q_{li}) is usually calculated based on air temperature and air humidity, or air temperature and a cloud factor (U.S. Army Corps of Engineers, 1956; Bengtsson, 1976; Partridge and Platt, 1976; Swinbank, 1963; Gray and Male, 1981; Ashton, 1986; Harstveit, 1984; Sand, 1990). According to Gray and Male (1981) the most widely quoted expression was first suggested by Brunt (1952)

$$Q_{li} = \sigma T_a^4 \left(a + b\sqrt{e} \right) \tag{2.5}$$

where ů = Stefan-Boltzmann constant, T_a = air temperature (K), e = vapor pressure (Pa) and a and b are empirical constants. Harstveit (1984) and Sand (1990) included cloudiness and used a formulae for Q_{li} on the form

$$Q_{li} = k_{l1} \cdot \mathring{u} \cdot T_a^4 + k_{l2} \cdot C_s + k_{l3} \tag{2.6}$$

where k_{l1}, k_{l2}, k_{l3} is empirical constants. Outgoing longwave radiation (Q_{lo}) is determined by Stefan Bolzmann's law

$$Q_{lo} = \mathring{u} \cdot T_s^4 \tag{2.7}$$

where T_s = surface temperature (K).

URN:NBN:no-6348

2.2.4 Turbulent heat transfer

Even though the radiation exchanges represent the major fluxes in the energy balance, the sensible (Q_h) and latent (Q_e) heat fluxes often play an important role in determining the rate of melt. Both Q_h and Q_e are governed by complex turbulent exchange processes occurring in the boundary layer above the snow surface. Exact determination of these fluxes is troublesome on an operational basis as an extensive measurement set-up and high collection rate is needed. The use of the eddy correlation technique has increased during the last few years as costs have fallen (Marsh, 1999). The complexity involved and problems incurred under cold conditions has limited its use over snow surfaces, but there is an increased understanding of these problems (*ibid*). Still, the most common way to express these processes is based on relatively simple measurements of temperature, vapor and wind speed gradients. Usually the equations are of the form:

$$Q_h = D_h u_z (T_a - T_s), \tag{2.8}$$

$$Q_e = D_e u_z (e_a - e_s), \tag{2.9}$$

where D_h = bulk transfer coefficient of convective heat transfer (kJ/m^3,°C), D_e = bulk transfer coefficient of latent heat transfer (kJ/m^3,mb), u_z = wind speed at a reference height z, (m/s), and e_a and e_s = vapor pressures of air and surface, respectively (mb)

Representation of these gradients or profiles by measurements at one level is a simplification. Greater accuracy is achieved by a better description of the profile through measurements at more levels, especially closer to the surface where the gradients are largest.

Anderson (1976) represented the bulk transfer coefficients and the wind speed with an empirical wind function:

$$f(U_z) = a + bu_z \tag{2.10}$$

where a and b are empirical constants. This representation is commonly used and through several investigations different values for a and b have been found (Anderson, 1976; U.S. Army Corps of Engineers, 1956; Kuz'min, 1961; Harstveit, 1984; Sand, 1990)

The turbulent exchange coefficients are influenced by air stability and, with reference to Price and Dunne (1976), Kane et al. (1997) includes stable, neutral and unstable conditions in their calculation;

URN:NBN:no-6348

$$D_{hn} = \kappa^2 (u_z) \left(\ln \left(\frac{z - h}{z_0} \right) \right)^{-2} \quad (2.11)$$

$$D_{hs} = D_{hn} / (1 + \lambda R) \quad (2.12)$$

$$D_{hu} = D_{hn} / (1 - \lambda R) \quad (2.13)$$

$$R = [g \cdot z \cdot (T_a - T_s)] / [u_z^2 (T_a + 273.2)] \quad (2.14)$$

where D_{hn}, D_{hs}, D_{hu} = heat transfer coefficient under neutral, stable and unstable atmospheric conditions, respectively, κ = von Karman's constant (0.41), z = measurements height (m), h = snow depth (m), λ = empirical constant =10 and R = Richardson number.

2.2.5 Internal Energy

The energy balance of snow goes through a diurnal cycle. Usually, heating occurs during daytime and cooling during the night due to outgoing longwave radiation. Even though snowmelt water follows paths and channels through the snowpack major runoff occurs only when the snow is isothermal at 0°C. Male and Gray (1975) have shown that accurate measurements of internal energy are essential to successfully apply the energy balance principle to shallow snow covers. The internal energy calculation influences the timing of the snowmelt, but during ablation the magnitude of this flux compared to the radiative, latent, and sensible fluxes is quite small (Kane et al., 1997).

2.3 PAPERS RELATED TO "SNOWMELT MODELLING" PRESENTED IN THIS THESIS

As far as the author is aware, the energy balance of snow and snowmelt has not been extensively studied at Svalbard before. The first known reported study is Sand (1990). The subject has been thoroughly studied in other Arctic regions e.g. in North America and Siberia (Prowse et al., 1994). Indeed, the project that this thesis is connected to, along with other associated projects mentioned earlier, was motivated by a lack of knowledge of the snow energy balance in Svalbard. In this thesis, three papers on snowmelt and energy balance are presented. Bruland et al. (2001a) focuses on snowmelt at the plot scale and compares the performance of three models of different complexity. Based on the recommendation from this paper, a simple energy balance was incorporated into the HBV-model to simulate snowmelt for the entire Bayelva catchment (Bruland and Killingtveit , 2002).

URN:NBN:no-6348

Compared to previous simulations using the HBV-model with a temperature-index melt calculation, the result was significantly improved and more reliable due to a better physical foundation. In the third article (Liston et al., 1999a), modelling was carried out by Glen Liston. It is included here as the five weeks of fieldwork the Antarctic shelf gave experience and background valuable for the rest of this doctoral programme.

2.3.1 Paper 1:
Energy and water balance studies of a snow cover during snowmelt period at a high arctic site.

Three models of different complexity were tested in order to simulate the water and energy balances of a snow cover on the arctic tundra. The three models were: a complex numerical model (CROCUS), a simple energy balance model and a temperature-index model (TIM). The simulations were carried out for the melt periods of 1992 and 1996 as these two periods represent very different meteorological conditions. The results of these simulations exposed weaknesses in all the models. The energy balance model lacks calculation of cold content in the snowpack. This influences both the outgoing longwave radiation and the timing of melt. Due to the effect of compensating errors in the simulations, CROCUS performed better than the simple energy balance model but this model also has problems with the simulation of outgoing longwave radiation. Even considering its ease of computation, the TIM appears to be the poorest of the three. The different climatic conditions in 1992 and 1996, expose the weakness of this model. Due to long clear skies periods during the ablation of 1992, solar radiation was high whereas air temperatures were low. To simulate enough energy to match the observed snowmelt in 1992, the melt rate factor of the temperature dependent index model was much higher than needed during the cloudy and mild ablation of 1996.

2.3.2 Paper 2:
An energy balance based HBV- Model with application to an Arctic watershed on Svalbard, Spitsbergen.

In this study, an energy balance (E-bal) calculation replaces the simple TIM in a spreadsheet version of the HBV-model. Calculation of average snowpack temperatures is included, and a new method is introduced to account for uneven snow distribution and glacial melt.

The main objective of this study was to test whether a simplified energy balance model could be implemented in the HBV-model and if it could improve simulations in an Arctic catchment where radiation plays an

URN:NBN:no-6348

important role, such as in the Bayelva catchment, Svalbard. The parameter values in the energy balance equations suggested by Harstveit (1984) were used and briefly presented in this study. Simulations showed that substituting the TIM with this energy balance model and including snow temperature calculations improves both the timing and progress of the snowmelt calculations. The simplified handling of surface temperature is acceptable during ablation but will not give an exact energy balance during the rest of the year.

One of the main advantages with the energy balance based HBV-model (E-Bal HBV) is that it is more physically-based than the TIM version of the HBV-model. The parameters controlling snowmelt, such as the albedo of snow and ice and snow distribution, can be found through field investigations instead of calibration. The E-bal HBV thus needs less calibration than the original HBV-model.

The model was tested not only against observed runoff for the periods 1974 to 1978 and 1989 to 1998, but was also compared with the performance of the original HBV-model. In addition, the Norwegian Polar Institute mass balance measurements at Austre Brøgger glacier were used to validate the glacial simulations. R^2 values were generally higher for the energy balance simulations than for the original HBV-model except for two years during 1974–1978. In this period the energy balance simulation was only based on observations of cloud cover. Depending on the cloud type, solar radiation can be considerable even on days with complete cloud cover. On these occasions the simulated solar radiation component will be too low. Measuring solar radiation is fairly easy and with these data the E-bal model gives more reliable results than the original HBV-model.

It was also found that estimates of sensible heat were improved by using a function with a non-linear wind speed dependency. This improvement might as well be explained by local conditions and wind patterns as by a natural limitation of the turbulent heat flux processes as wind speeds become very high.

URN:NBN:no-6348

2.3.3 Paper 3: Glacial mass balance of Austre Brøggerbreen modelled with the HBV-model

The energy balance based HBV-model (Paper 2) was used to simulate the glacier mass balance of Austre Brøggerbreen. The results compared favourably with observations carried out by the Norwegian Polar Institute for the period 1971 to 1997. Even though the model was optimised to observed runoff from a catchment in which glaciers constitute only 50% of the area rather than observations of the glacier mass-balance, the model was able to reconstruct the trends and values of that mass balance.

The years 1994 to 1996 show deviations between simulated and observed winter accumulation of up to 160%. The best explanation found for this was extreme rainfall events during the winter leading to thick ice layers. These probably in turn make observation conditions difficult leading to questionable values of the winter accumulation. This shows how such a model can be used to control observations. To illustrate how a precipitation-runoff model can be used as a tool to estimate the consequences of a possible climatic change, the climatic forcing was changed until the average net glacial mass-balance was zero. The simulations showed that the glacier mass-balance would be in equilibrium with a summer temperature 1.2 °C lower than the average experienced over the last few decades or with a 100% increase in the winter (snow) precipitation. These are higher values than former estimates. A combined change of temperature and precipitation showed a synergistic effect and thus gave less extreme values. This paper shows also that a precipitation-runoff model can be a useful tool to calculate mass balances for glaciers without observations.

URN:NBN:no-6348

2.3.4 Paper 4:
Meltwater production in Antarctic blue-ice areas: sensitivity to changes in atmospheric forcing

In the near coastal blue-ice regions of Dronning Maud Land, Antarctica, below surface ice-melt features have been regularly observed during recent Norwegian Antarctic Research Expeditions (NARE) (Winther et al., 1996). These features and the processes behind them were further investigated at NARE 1996/97. Data collected during this expedition was used as input values for a model developed and run by Glen Liston at the Atmospheric Science Department at the University of Colorado. Low scattering coefficients of the large grained blue-ice allow penetration of solar radiation, thus providing an energy source for below surface melt significant enough to produce ice covered lakes visible on satellite images and producing an average daily runoff of 11750 m^3 from an area assumed to be about 12 km^2 (Liston et al., 1999b). The modelling showed that the ice-melt was sensitive to the atmospheric forcing. Under certain conditions more traditional surface melting could occur, whereas under others the existing melt processes could be dramatically reduced or shut of.

Another publication from this expedition, Liston et al. (1999b), in which water fluxes of the ice and snowmelt are estimated, is not included in this thesis.

URN:NBN:no-6348

3 SNOW DISTRIBUTION

Snow depth, density and coverage are the main parameters and conditions used to characterize the areal distribution of snow. For larger areas the snow coverage is probably the easiest parameter to observe, for instance from aerial photographs from aeroplanes or satellites. To collect information on snow depth average and variability for larger areas needs more extensive measurement campaigns. This applies also to snow density, but since the variability of the snow density is much lower than for snow depth, far fewer samples are needed. Even so, unfortunately density sampling is more time-consuming than snow depth sampling.

Traditionally, manual snow sounding using a graduated rod to measure depth every 5 to 10 metres over a distance of 500 to 1000 m and snow density samples taken with a snow tube, have been used in Norway to measure catchment average snow water equivalent. Over the last decades, there has been a growing interest in looking at and developing new less time consuming methods. Several of these are described by Pomeroy and Gray (1995). The extensive snow depth data set used in this study would be impossible to collect without the use of Ground Penetrating Radar (GPR). This study sought to test and improve the method for practical use. The method will be further described below.

The processes controlling snow distribution depend on the spatial scale of interest. When planning a snow surveying network and also when setting up a snow transport model, it is necessary to have knowledge of the spatial variability at different scales. It is common to refer to three scales; macroscale, mesoscale and microscale. In Pomeroy and Gray (1995) these are described as follows:

URN:NBN:no-6348

Macroscale or regional scale is areas up to 10^6 km^2 with characteristic distances of 10 km to 1000 km depending on latitude, elevation, orography, and the presence of large water bodies. At this scale dynamic meteorological effects such as standing waves in the atmosphere, the directional flow around barriers, and lake effects are important.	**Mesocale** or local scale has characteristic linear distances ranging from 100 m to 10 km in which redistribution of snow along relief features may occur because of wind and avalanches, and deposition and accumulation of snow may be related to terrain variables and to vegetation cover.	**Microscale** has characteristic distances of 10 m to 100 m over which differences in accumulation patterns result from variations in air flow pattern and transport.

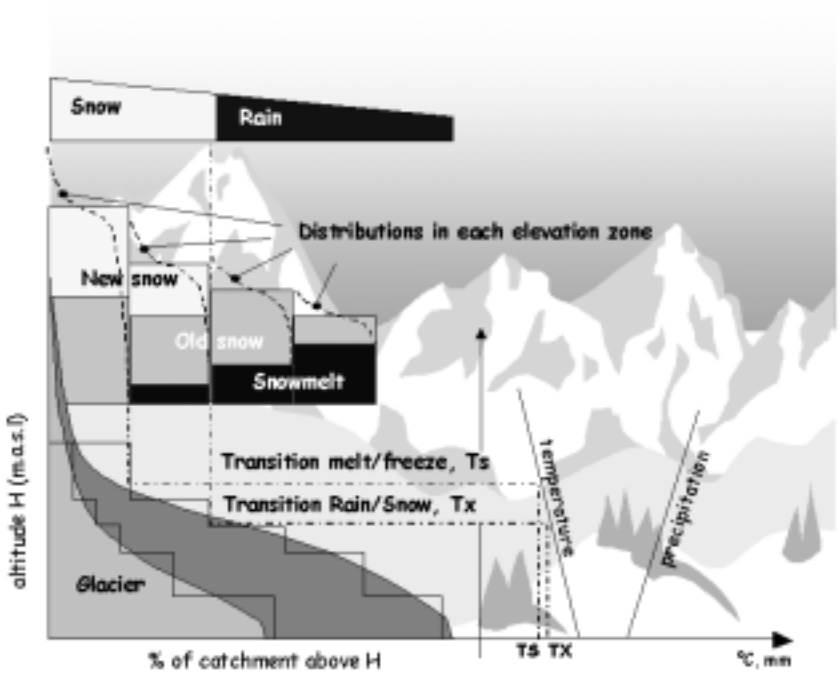

Figure 3-1 Snow distribution in the HBV-model (Killingtveit and Sælthun, 1995)

URN:NBN:no-6348

Different approaches have been applied in order to model the distribution and redistribution of snow over a terrain. In most implementations of the HBV-model a distributed snow routine is used.The catchment is separated and modelled according to elevation zones and the snow storage calculated separately for each. Within each zone the snow is unevenly distributed due to the effect of wind drift (Figure 3-1).

Several investigators have tried to develop methods and models to extrapolate sparsely observed snow depth or snow cover data into snow distribution data for larger basins. Tveit (1980) developed a method to determine the representativety of snow courses and weighted each observation based on topographical and morphological parameters. Elder and Michaelsen (1991) showed that a stratified sampling evaluated by identifying and mapping zones of similar snow properties on the basis of elevation, slope and radiation, produced superior results over random sampling. By means of snow survey data, topographical data and vegetation, Balk and Elder (2000) developed a method based on a binary-decision-tree and geo-statistics to improve the estimates of snow distribution in mountainous basins. Carroll and Cressie (1997) included geomorphic attributes in a spatial statistical model developed by National Weather Service in U.S.A. and were able to substantially improve the accuracy of the snow water equivalent estimates in areas where no observed measurements are available. Blöshl and Kirnbauer (1992) and König and Sturm (1998) investigated how topography influences snow cover depletion and how aerial photographs taken during snowmelt can be used to estimate snow water equivalent. Bahr and Meier (2000) and Shook and Gray (1997) estimated the depletion of the snow cover by assuming that snow patch size and distribution follows simple power functions and by using fractal structures.

All the methods mentioned are based upon observation of the snow cover. Another approach is to describe the processes that determine the redistribution of snow and to model the snow transport during the winter months based upon a few meteorological observations.

URN:NBN:no-6348

3.1 REDISTRIBUTION OF SNOW

The major process for the redistribution of deposited snow is aeolian transport. According to Male (1980) blowing snow occurs as often as 30% of the time on the open plains of the northern hemisphere.

The basis for and the development of the fundamental equations used to describe and quantify the wind induced snow transport is presented by Male (1980), Kind (1981), Pomeroy and Male (1987) and Pomeroy and Gray (1995), all cite earlier investigations. Pomeroy and Gray (1995) divide the transport into three modes of movement; creep, saltation and turbulent diffusion. Particles too heavy to be lifted by the wind form migrating snow waves or dunes creeping downwind proportionally to the wind speed. Referering to Tabler et al. (1990) and Kobayashi, (1971) who studied the phenomena, Pomeroy and Gray (1995) concludes that except at very low wind speeds creep comprise to a very small portion of total transport.

Saltation refers to particles moving by jumping along the snow surface. When the drag force of the wind on the surface is higher then the surface shear strength, snow particles are lifted up and follow a trajectory of up to a few centimetres in height. The trajectories of the saltating particles vary with wind speed, particle size and surface conditions. The surface shear strength depends on the properties of the grains on the surface and the bonding strength between them, which is determined by the metamorphic state of the snow surface and whether the grains have previously been moved and compacted by the wind. Air temperature, air humidity and time since snowfall are parameters influencing these conditions. The wind speed measured at 10 m, u_{10}, at which drifting is initiated, ranges from 1.9 m/s for very light dry snow, to 10.5 m/s for a wind-hardened surface with a density of approximately 350 kg/m^3 (Male, 1980). The impact of the particles when landing causes other particles to be thrown into the air. The shear stress on the surface is then both a result of the wind speed (τ_s) and the concentration of particles in the air (τ_p) (Owen, 1964). Pomeroy and Gray (1995) also consider shear stress applied to vegetation and mechanical barriers (τ_t). The resulting shear stress (τ) is:

$$\tau = \tau_t + \tau_s + \tau_p \tag{3.1}$$

The total atmospheric shear stress, τ is equal to $\rho_a u_*^2$ where ρ_a is the air density and u_* is the friction shear velocity:

URN:NBN:no-6348

$$u_* = \frac{u_z \partial}{\ln(z/z_0)} \tag{3.2}$$

where ∂ is Von Kármán constant (0.41), u_z is horizontal wind speed (m/s) at height z (m) and z_0 is the aerodynamic roughness length (m).

Saltating particles exert a drag force on the airflow similar to vegetation and thus increase the effective roughness (Kind, 1981). In Pomeroy and Gray (1995), z_0 for blowing snow over complete snow covers is expressed by number of vegetation elements pr unit area, N_s, and exposed silhouette area, A_s, given in (m^2):

$$z_0 = \frac{u_*^2}{163.3} + 0.5 N_s A_s \tag{3.3}$$

The concentration (W) and mean horizontal velocity (u_p) of saltating particles determines the transport rate (Q_s) due to saltation. In Kind (1981) the transport rate Q_s in (g/s) is expressed as:

$$Q_s = \frac{\rho_a u_*^3 C}{g}\left(1 - \frac{u_{*th}}{u_*}\right) \tag{3.4}$$

where ρ_a is density of air, $u_{*\mathrm{th}}$ is threshold shear stress and C is a constant for which Owen (1964) suggested the following experimentally derived formula:

$$C = 0.25 + \frac{w}{3u_*} \tag{3.5}$$

where w is the terminal fall velocity of the particles. Pomeroy and Gray (1995), citing Pomeroy and Gray (1990), give a general equation for the steady state saltation of a prairie snow cover (Eq. 3.6) and an empirical expression based on measured wind speed (Eq. 3.7).

$$Q_s = \frac{0.68\rho_a}{u_* g} u_{*th}\left(u_*^2 - u_{*n}^2 - u_{*th}^2\right) \tag{3.6}$$

where $u_{*\mathrm{n}}$ is shear threshold of non erodible elements and Q_s is in (kg/s).

$$Q_s = \frac{u_{10}^{1.295}}{2118} - \frac{1}{17.37 u_{10}^{1.295}} \tag{3.7}$$

URN:NBN:no-6348

Kind (1981), who refers to Kobayashi (1971), shows that the drift rates near the ground is in the order of 0.3 to 20 g/(m·s) at wind velocities between 5 and 10 m/s, respectively, measured at a level of one metre. According to Kind (1981) and Pomeroy and Gray (1995) this usually amounts to the largest portion of the total mass flux.

When the wind shear stress is higher than the shear strength, the mobility of the dominant size-group of particles exposes very fine particles to the wind action. These particles or snow dust have very low terminal fall velocity and can rise to heights above the saltating layer, become suspended and airborne by the turbulent airflow (Kind, 1981). Though the concentration in the suspended layer is low the layer may - under severe blowing conditions and where the upstream fetch distance is several kilometers in length - extend to heights of several hundred meters and thus contribute substantially to the total mass transport (Pomeroy and Gray, 1995).

According to Pomeroy and Gray (1995) transport rate of suspended flow is:

$$Q_{susp} = \frac{u_*}{\partial} \int_{h_*}^{z_b} q(z) \ln(z/z_0) dz \tag{3.8}$$

where $h_* = u_*^2 / 12.25$ and is the height of the saltation layer (Pomeroy and Gray, 1995), $q(z)$ is the mass concentration in (kg/m^3) of suspended snow at height z, and z_b is the height of the surface boundary layer of suspended flow. $q(z)$ and z_b are further described in Pomeroy and Gray (1990).

Different authors, summarized in Pomeroy and Gray (1995), have estimated the total transport rate. Except from the estimates by Budd et al. (1966) that are higher than those normally measured, there is a good agreement between the estimates. With wind speeds ranging from 5 to 30 m/s the total transport is found to be from between 1 and 10 g/s to between 1 and 6 kg/s, respectively.

The theory of sublimation of blowing snow is described by Male (1980), who also refers to a major study by Schmidt (1972), and by Pomeroy and Gray (1995) who in addition cite studies by Schmidt (1991) and Pomeroy (1988). The phenomenon is very difficult to quantify using measurements and estimates are based on theoretical assumptions. High exposure and ventilation of airborne snow crystals results in a higher sublimation rate than expected for stationary snow (Pomeroy et al., 1998). Pomeroy (1988) has developed a model called the Prairie Blowing Snow Model (PBSM) which

URN:NBN:no-6348

subsequently was used to estimate annual fluxes of blowing snow sublimation that range from 15% to 40% of the annual snowfall on the Canadian prairies (Pomeroy et al., 1993; Pomeroy and Gray, 1995). Pomeroy et al. (1998) state that at the large spatial scales of GCM grid cells, sublimation becomes the most important blowing snow flux. Essery et al. (1999b) have developed another numerical blowing snow model called PIEKTUK, which they state is innovative in that it considers the thermodynamic feedbacks for all the predictive quantities: temperature;, moisture and particle distribution. Thus, forcing is gradually reduced, and the snow sublimation was found to be self-limiting. Compared to the PBSM estimates, this led to a significant reduction in the calculated total sublimation from blowing snow.

Several model have been developed based on these theoretical descriptions and assumptions. Liston and Sturm (1998) provide a line-up of these models and their range of application. Since none were three-dimensional, they found a need for developing a model capable of producing spatially distributed maps of snow depths. They developed SnowTran-3D, a physically-based numerical snow-transport model that can be used to simulate snow depth evolution over topographically variable terrain. The model was developed for, and tested in, an Arctic –tundra landscape, but is applicable to other treeless areas such as prairies and alpine regions (Liston and Sturm, 1998). Based on a simplified version of PBSM, Pomeroy et al. (1997) developed a model using monthly mean climatological data and landscape elements to simulate end-of-winter accumulation. Essery et al. (1999a) improved this model by implementing the MS3DJH/3R terrain wind-flow model (Walmsley et al., 1982; Walmsley et al., 1986). Purves et al. (1998) developed a simple, rule- and cell-based model of snow transport and distribution.

Marsh (1999) noted that although these models work reasonably well in rolling terrain or for single species forest stands, they are not yet capable of modelling snow cover in complex mountainous terrains or multi-species forest stands. Since SnowTran-3D was developed, it has been used in several catchments with various types of terrain. Liston and Sturm (1998) found good agreement between modelled and observed snow distribution for four years in the three-by-three kilometer Imnawait Creek domain in the gently rolling foothills of the Brooks Range in Arctic Alaska. Green et al. (1999) simulated snowdrift formation using SnowTran-3D over a 2.7 km long mountain ridge including the Montgomery Pass in the northern Colorado Rocky Mountains. Prasad et al. (2001) applied the model in Reynolds Creek where one objective was to test the sensitivity of modelled snow accumulation pattern to vegetation. They found both a reasonably good

URN:NBN:no-6348

agreement between the model results and observations and that the snow held in the erosion zone is more sensitive to vegetation snow holding capacity than that held on the deposition zone. As precipitation increases, the effect becomes minor. SnowTran-3D was also used to simulate snow accumulation features on the coastal Antarctic ice sheet of Dronning Maud Land (Liston et al., 2000). In Liston and Sturm (2001), the model is applied to simulate the regional distribution of precipitation. Based on snow surveys covering a transect from the Brooks Range in south to the Arctic Ocean in north and interpolated values of available meteorological input data, they forced the precipitation input to the model until simulated snow depths agreed with the observed. Jaedicke (2001) has used parts of the SnowTran-3D model concept on Svalbard to model snow drift over complex terrains in order to explain the location of glaciers. Heused wind speed data calculated by global climate models.

Although these applications have shown that the models are able to model redistribution of snow in terrains with complex topography, lack of validation data means that for these terrains on a mesoscale, Marsh's (1999) statement is valid.

3.2 PAPERS RELATED TO "SNOW DISTRIBUTION MAPPING AND MODELLING" PRESENTED IN THIS THESIS

So far, the main purpose of snowmelt calculations in Norway has been to predict the timing and volume of the snowmelt runoff to hydropower reservoir during ablation. The calculations are usually based a temperature-index model and a standard snow distribution function originally based on studies by Tveit (1980). On average these calculations work very well, but the uncertainties connected to them have been a continuous motivation to improve the simulations. For instance, in Bruland and Killingtveit (2002) a snow cover depletion factor, f_{snow}, accounts for skew snow distribution.

$$f_{snow} = \alpha - \frac{\alpha}{\exp\left(\frac{SWE_{left}}{SWE_{\max}}\right)^{\Omega_s}} \tag{3.9}$$

where SWE_{left} is snow water equivalent left at the end of the time step, SWE_{max} is maximum snow water equivalent during the previous winter and $\breve{U}$

URN:NBN:no-6348

and q_s is snow distribution skewness factors. The method assumes that snow storage contains an even and an uneven (ŭ) distributed fraction. Assuming even snowmelt, the snow cover depletes in area when the evenly distributed fraction of the snow storage has melted. The values ŭ, $\breve{U}$ and q_s are found from snow survey data. Figure 3-2 shows how the skewness increases with increased q_s. The snow distribution is usually more skewed at higher elevation and q_s can be set differently for each elevation band or expressed as a function of elevation.

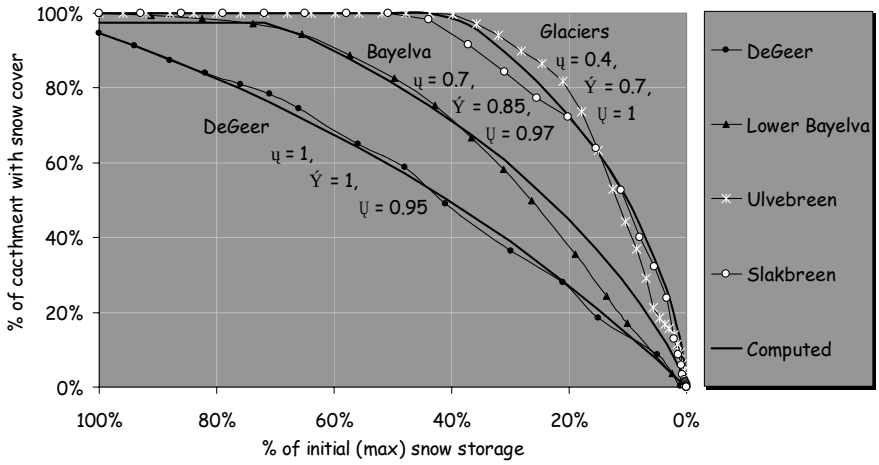

Figure 3-2 Snow depletion curves and adapted skewness factors to different locations

Updating snow storage in the model is an important subject. Remote sensing has been one approach that can improve updating of the snow coverage and to detect albedo changes and areas with snowmelt. Improving the methods and reducing the uncertainties of snow surveys is another subject. In Bruland and Sand (1997) and Sand and Bruland (1998) a strategy of how to efficiently use the SnowRadar is described. In Marchand et al. (2001a) another approach is used. So far outside the research community, modelling of snow redistribution has not been used extensively in order to improve the end of winter snow storage and distribution estimates. Bruland et al. (2002) show that SnowTran-3D, as an example of advanced numerical snow drift models, is able to recreate the snow distribution and also, to a certain degree, pin-point the drift and erosion areas in catchments with very different sizes and locations.

URN:NBN:no-6348

Snow distribution is also, as previously mentioned, an important parameter for other processes which have consequences beyond hydrology. Svalbard is for the focus of Norwegian Arctic research and the Ny-Ålesund research station is one the European Union's Large Scale Facilities. Bruland et al. (2001b) describe how snow is redistributed over typical Svalbard tundra. Though the snow distribution is interesting to study in itself, the spatial pattern is also interesting when related to other issues such as vegetation distribution (Bruland and Cooper, 2001) and reindeer studies (Aanes et al., 2000; Van Der Wal et al., 2000). Hopefully it will also be useful to other ongoing and future investigations in the Ny-Ålesund area.

Figure 3-3 Snow cover conditions make a difference to Svalbard reindeer
(photo G.Bangjord)

URN:NBN:no-6348

The meteorological observation network does not cover Svalbard very well and, as measurements of precipitation in this region are very difficult to make at the best of times and impossible with unattended equipment, the best way to describe the precipitation distribution is through end of snow accumulation season snow depth measurements. Such measurements were made for the winter accumulations of 1996/1997 (Winther et al., 1998) and 1997/1998 (Sand et al., 2002). This information is, in addition to being interesting in itself, useful basic knowledge for studies dealing with the water balance, biology, surface energy balance, climate and active layer development.

This doctoral thesis covers investigations of snow distribution on all scales: from the microscale of the 100 m^2 snow plots to the mesoscale at the one, three and 250 km^2 domains in Aursunden, Bayelva and DeGeer, respectively, and at the macroscale when looking at the Spitsbergen in its entirety.

3.2.1 Paper 4: Snow Distribution at a High Arctic Site at Svalbard

The aim of this study was to describe the snow depth variability by detailed measurement of snow distribution in a 3 km^2 site near to Ny-Ålesund and to link this to topography and climate at the location. The measurements were carried out with a grid of 100 m by 100 m cells using the SIR-2 Georadar from Geophysical Survey System Inc. (GSSI). Differential GPS was used to create a detailed Digital Elevation Model (DEM) and the snow depth data were correlated to topographic data.

Most areas with accumulation and erosion features were found to have slope exposure towards the predominant wind. Though, there are areas at some exposed ridges and slopes where it seems more likely to find erosion than an equilibrium condition. Ny-Ålesund is, as is Svalbard in general, exposed to strong winds and one should expect the snow to be strongly redistributed. This study shows that this is not necessarily the case. A variation coefficient for the area of 0.58 is close to that Tveit (1994) reported from measurements in DeGeer valley close to Longyearbyen on Svalbard, but it is low compared to normal values found in Norwegian mountainous catchments which range from 0.5 to 1.5 (Andersen et al., 1982; Marchand and Killingtveit, 1999). A snow surface exposed to strong winds rapidly develops a hard crust which prevents further erosion. The results indicate that this process is possibly more effective on Svalbard with its arctic climate than in the Norwegian mountains. The difference in average snow depths along the NW-SE and NE-SW transects would probably be reduced if the measurement grid was tighter. This difference also showed the need for having profiles in both directions.

URN:NBN:no-6348

The snow distribution found in this investigation can be a useful tool when it comes to understanding the flora in this area and explaining differences in thaw depths of the active layer. The distribution observed in this study can be compared with distributions over a larger area and for other years in the same area. If distribution can represent a larger area and is found to be similar every year, it can be a useful tool for estimation of snow depth variability in the arctic regions. The data was also very valuable for calibrating and verifying SnowTran-3D.

3.2.2 Paper 5:
Snow accumulation distribution on Spitsbergen, Svalbard, in 1997.

A survey of the regional snow accumulation variability on Spitsbergen, Svalbard, was carried out during three field campaigns in May 1997. Spitsbergen was divided into three regions, southern, middle, and northern; in each, three areas along a transect from west to east were selected (Figure 3-4). In each of these areas, wide glaciers were located and snow depth surveys carried out along a longitudinal centre profile. It was assumed that the snow depth on the glaciers is least likely to be disturbed by surroundings and thereby is the most representative for the actual area. The altitude spanned from sea level to 1000 metres elevation. Snow depth was measured with two different GPR-systems, a PulsEKKO (450 MHz) and a GSSI SIR-2 (500 MHz), and snow densities was measured at three elevations along each profile.

The gradient of winter accumulation could be estimated from the depth and density data collected. The elevation gradients varied from 3 mm/100m in the northeast to 237 mm/100m in the central south profile; the average was 104 mm/100m. The snow accumulation was 38 to 49% higher along the eastern coast than along the western and there was 55% and 40% less snow accumulation at the northern locations compared to the southern locations for the western and eastern coasts, respectively (Figure 3-4).

URN:NBN:no-6348

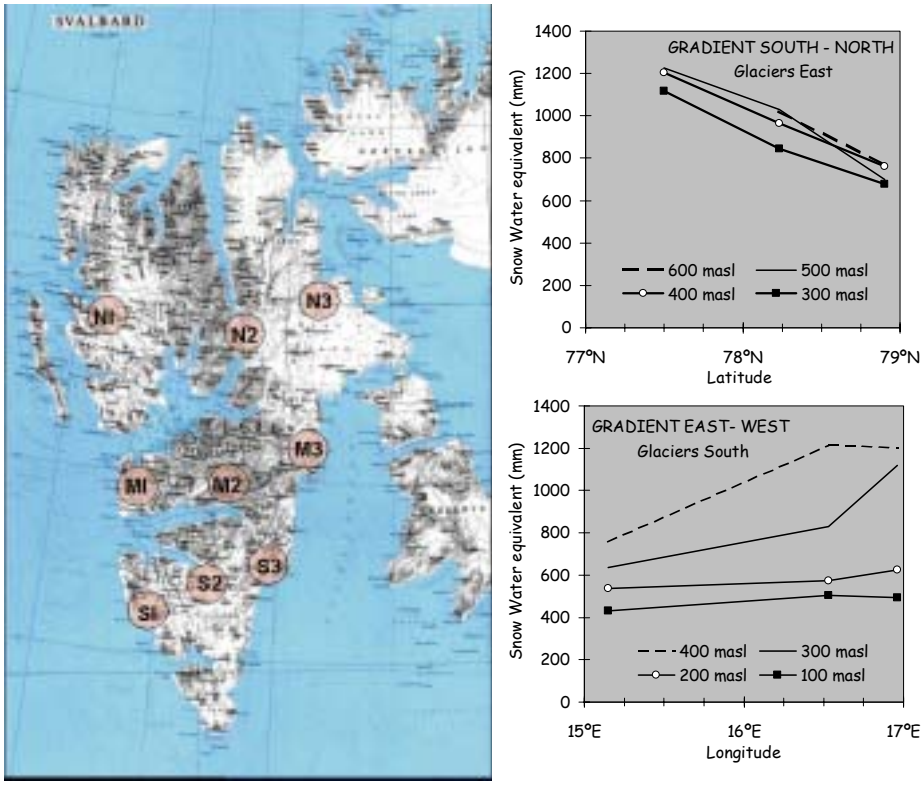

Figure 3-4 Location of the Southern, Middle and Northern transects and accumulation gradients in south and along the eastern coast.

3.2.3 Paper 6:
Modelling the snow distribution at two high arctic sites at Svalbard, Norway, and at a sub-arctic site in central Norway.

The aim of this study was to test the degree to which a numerical model is able to reproduce an observed snow distribution in sites (ranging form 1 km^2 to 250 km^2) located on Svalbard and Norway. The snow depth frequency distribution, a snow depth rank order test and location of snowdrifts and erosion areas were used as criterion for model, SnowTran3D, performance. In order to allow for spells of mild winter weather with temperatures above freezing, a snow settling calculation was included in the model. Topographic modification of wind speeds was also changed so that instead of treating the curvature of ridges and valleys independent of wind direction, the influence of curvature on the wind speed depends on wind direction. The model result was compared to an extensive observation data set for each site and the

URN:NBN:no-6348

sensitivity of main model parameters to the model result was tested. For all three sites the modelled snow depth frequency distribution was highly correlated to the observed distribution (Figure 3-5) and the snowdrifts and erosion areas located by the model corresponded well to those observed at the sites.

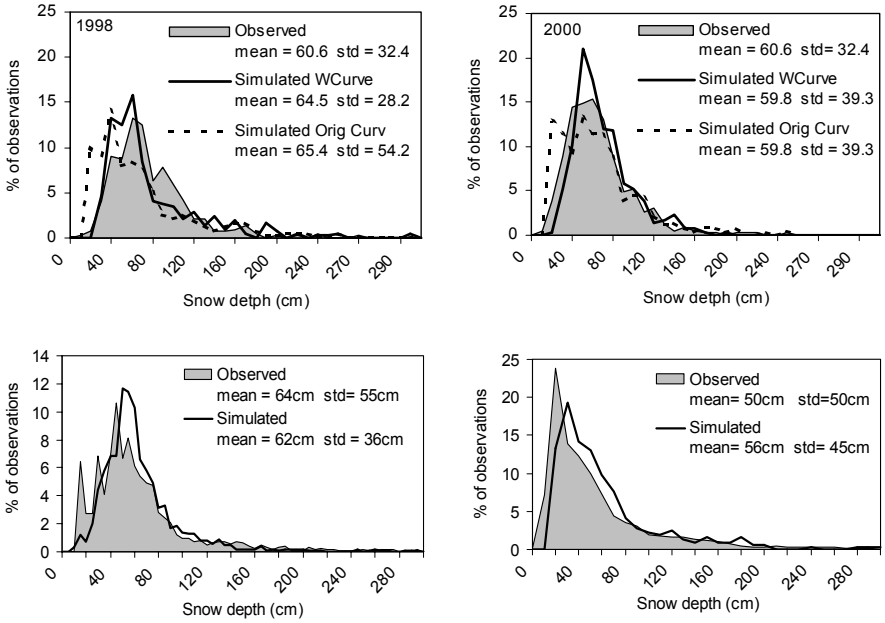

Figure 3-5 Modelled and observed snow depth frequency distributions in Bayelva (upper) and at Aursunden (below left) and the DeGeer valley (below right).

URN:NBN:no-6348

4 SNOW DEPTH MEASUREMENT

The major hindrance to validating modelled snow distribution at the mesoscale in mountainous terrains with complex topography, has been to collect extensive data sets at these scales and in these terrains. The Ground Penetrating Radar (GPR) coupled with a Global Positioning System (GPS) opens new horizons of snow distribution mapping possibilities. This technique has been developed over the two last decades, but it has only been applied extensively during recent years. According to Holmgren et al. (1998), Ellerbruch and Boyne (1980) were the first to demonstrate that a FM-CW radar could be used to determine snow depth and stratigraphy. During the 1980s a Norwegian radar system was developed and tested (Andersen et al., 1987; Killingtveit and Sand, 1988). This work was continued from the mid-1990s, but with the commercially available GPR-system, GSSI-SIR 2, and with a focus on the development of automatic transformations of the radar output files to snow water equivalent. The result was the development of the computer program SIRDAS (Susar Consulting AS, 1997), which has been used extensively in this and other studies.

In Sweden, there has also been an effort to apply GPR to snow measurements (Lundberg and Thunehed, 2000). They have focused on the use of GPR from helicopter (Ulriksen, 1989) in contrast to the Norwegian approach where the radar has been pulled by snow mobile due to rough terrain and areas inaccessible to helicopters. Marchand et al. (2001b) compared coincident measurements of airborne and ground based GPR measurements. The comparison showed in general high correlation between results of the methods. Differing results were most often found associated with small areas having shallow-snow cover or snow-free patches, and are probably connected to the larger footprint of the airborne radar.

GSSI-SIR2 is an impulse radar system. These systems are characterized by sending very short, wide band signals, allowing them to determine short ranges with high resolution. Higher antenna frequencies give greater resolutions, but also shorter ranges due to greater damping of radar signals in the snow. The electromagnetic wave transmitted from the radar antenna is reflected by objects with different dielectric properties than the surroundings.

URN:NBN:no-6348

The larger the differences, the larger the strength of the reflection. A receiving antenna intercepts these signals and a control unit stores the delay between transmission and interception of each signal (Figure 4-1). Snow depth and dielectric property of the snow determine the delay of the electromagnetic wave, or the radar signal, through the snowpack. Propagation speed *V,* of an electromagnetic wave can be calculated as

$$V = c / \sqrt{\varepsilon_r} \tag{4.1}$$

where V is the wave propagation speed, c is speed of light in vacuum (0.3 m/ns) and ε_r is the real part of the dielectric constant $\mathring{U}$

Snow density and liquid water content determines the dielectric property of snow. Lundberg and Thunehed (2000) refer to several reports where these relationships are investigated and derived equations for both dry and wet snow validating them against laboratory experiments.

$$\sqrt{\mathring{U}} = 1 + c_1 \mathcal{I}_s + c_2 d_w \tag{4.2}$$

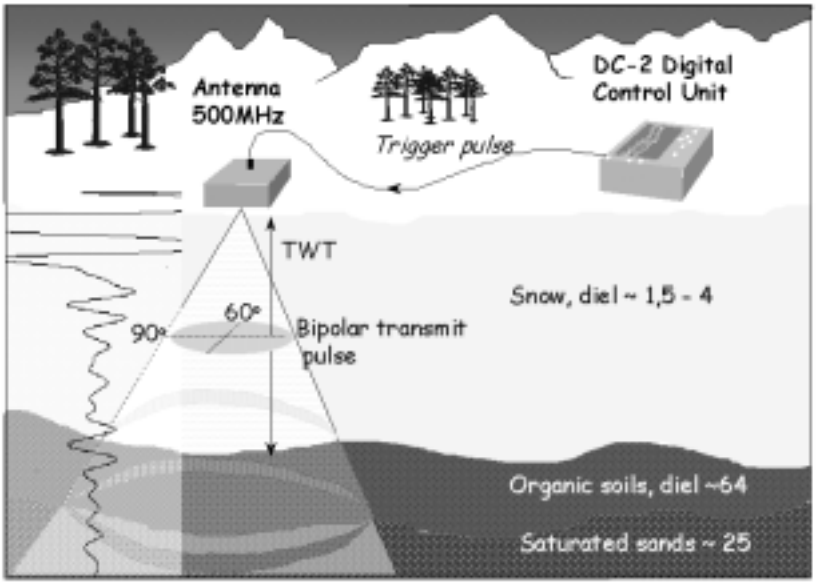

Figure 4-1 Snow radar basic principle

URN:NBN:no-6348

where $c_1 = 0.000851$, $c_2 = 7.09318$ and d_w is the liquid water content and ρ_s is the snow density. Ulaby et al. (1986) included density of ice (ρ_i) and presented the following equation for the dielectric constant in dry snow

$$\varepsilon = (1 + 0.469\rho_s/\rho_i)^3 \tag{4.3}$$

4.1 PAPERS AND WORK INCLUDED IN THIS THESIS RELATED TO THE SUBJECT "SNOW DEPTH MEASUREMENT"

Though the GPR-technique for snow measurements has been investigated over the last two decades, the SnowRadar as it is commonly called in Norway, had not been applied for extensive snow measurements in Norway before 1995. At that time it was used to measure the snow distribution in the catchment of lake Samsjøen, about 40 km south of Trondheim. This work was first presented in Bruland and Sand (1997) and later in Sand and Bruland (1998). The intention was to establish operational routines for using GPR in snow surveying for hydropower producers. Gradually after the first field and post-processing experience, the focus changed to the development of software and operational logistics. Collecting snow depths data over several tens of kilometres with a metre or less resolution creates huge amounts of data and an efficient tool to analyze and digitalize these was essential. Since the snow and ground conditions determine the quality of the data and since these conditions can be highly variable, the digitalization is not always a simple task (Figure 4-2)

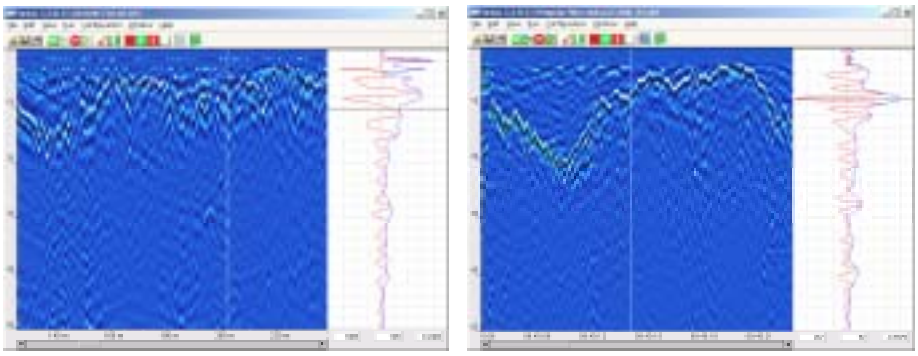

Figure 4-2 SnowRadar files of different quality. Wet snow or ice layers creates reflections (left) that make interpretation difficult

URN:NBN:no-6348

The program developed is therefore semi-automatic so that it allows the user to manually digitalize the files, correct already digitalized data or take parts of the files with inadequate quality out of the data set. The coding was carried out by a consulting company called SUSAR and resulted in the SIRDAS program (Susar Consulting AS, 1997). In order to connect the SnowRadar measurements to digital terrain models, the exact location of each measurement is needed. A system connecting GPS measurements to the SnowRadar was developed. This is described in (Marchand et al., 2001a).

4.1.1 Paper 7: Application of Georadar in Snow Cover Surveying

For two field seasons, a commercial georadar was successfully tested in the about 200 km^2 catchment to Lake Samsjøen, in Norway. During the spring of 1995, the radar ran along seventeen selected snow courses in total, covering approximately 70 km. Calibration was against manual measurements of snow depth and density along selected segments of the same snow courses. Figure 4-3 shows a section (700m) of one of the snow courses with snow water equivalent (*SWE*) values ranging from less than 200 mm to more than 1000 mm (corresponding to snow depths of approximately 60-300 cm). The figure shows good agreement between the radar measurements and the manual control measurements (R =0.76). Looking at all the control transects, the correlation coefficient varied between 0.74 and 0.90, which confirms that both the Snowradar and SIRDAS work very well for snow measurements.

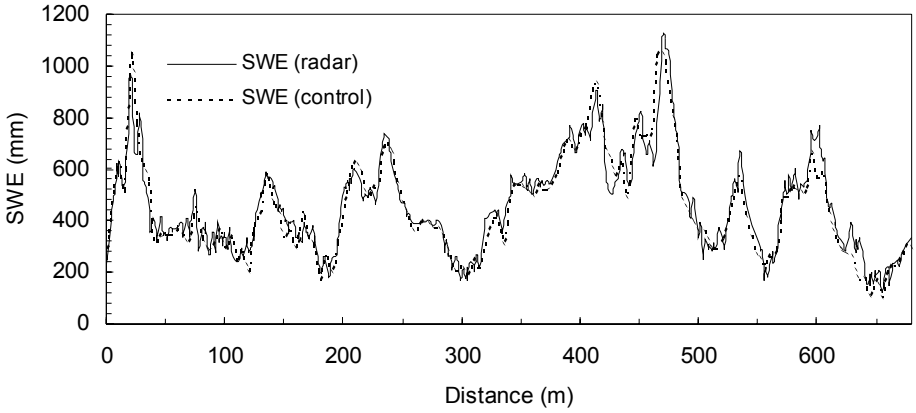

Figure 4-3 Comparison of manual and Snowradar measurements

URN:NBN:no-6348

The paper also describes the methodology and the results that were obtained during the first year of measurements. The results confirm that by using the georadar it is possible to obtain accurate estimates of mean *SWE* in the catchment area with much less time spent in the field compared to conventional measurements. Water balance calculations based on measurements of runoff, precipitation and changes in water level in the Lake Samsjøen reservoir during the snowmelt runoff season, show that snowmelt contributed 112 million m^3 of water, corresponding to an average SWE for the entire catchments of 530 mm. The snow radar survey and density measurements indicated an average SWE of 506 mm for the entire catchment in late April prior to any snowmelt, which gives a deficit of 5%.

The georadar data also gave a good description of the areal distribution of *SWE*, a task that is very time consuming by conventional survey methods. By linking the radar data to a digital terrain model (DTM), the snow distribution within individual elevation zones in the catchment were found. This is very useful if the data are to be used in a model like the HBV-model for estimating the timing of snowmelt generated runoff.

4.1.2 Paper 8: Improved Measurements and Analysis of Spatial Snow Cover by Combining a Ground Based Radar System With a Differential Global Positioning System Receiver

The paper describes the development and use of a new snow measurement system where a Ground Penetrating Radar (GPR) is connected to a Differential Global Positioning System (DGPS) receiver. The entire measuring and data collection system consists of four main parts. The GPS receiver, the differential correction-signal receiver, the georadar and the interface between the former three parts. The system is illustrated in Figure 4-4. Any GPS with communication possibilities and RTCM interface can be used. In this study a Garmin GPS 12 was used. This is a handhold, twelve-channel receiver with an update rate of one second. The GPS was connected to a Seatex DFM 200 correction-signal receiver. The differential correction-signal in Norway is transmitted from coastal beacons via commercial radio broadcasting stations. These in turn relay the correction-signal to the Norwegian Broadcasting Corporation radio channel P2, using the Radio Digital System (RDS).

URN:NBN:no-6348

Figure 4-4 Setup of the Snowradar, GPS and DFM 200 receiver.

With a FM antenna, the DFM 200 receives the correction-signal with a frequency of one second, thus both position logging and navigation can be performed in real time. In addition to giving position correction, the DFM was also used to store the current position with a time interval of 2 seconds. The accuracy of this DGPS system is 5-10 meters.

The main objective of combining the GPR and GPS is to connect each snow-depth measurement to a geographic position. This was determined by using an interface between the radar, GPS receiver and the correction-signal receiver. The GPS receiver communicates with the DFM via the interface, thus both recognize the current corrected position. Each time the DFM logs the position, it sends a signal to the interface. The signal is converted into a Transistor-Transistor Logic (TTL) pulse that is sent to the radar. When receiving a TTL pulse the radar attaches a marker to the next radar signal reflection, which is stored on the log-file together with the reflection data itself. Thus, each marker on the final radar log-file is related to a reflection and a geographic position from the DFM log-file. Since the position is logged with a time interval, the distance between two consecutive positions depends on the velocity of the snow scooter. Typically, this distance was in the range 5 to 12 metres.

URN:NBN:no-6348

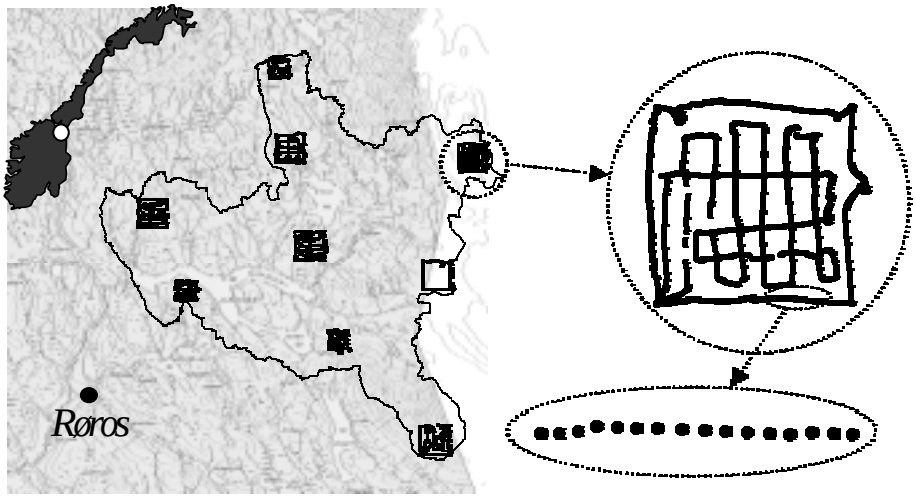

Figure 4-5 Measurements in Aursunden. (from Marchand et al. 2001a)

The system was tested during an extensive snow survey in the Aursunden catchment. The main result was 28,866 geographically referenced snow-depth values, extracted from a total of 532,192 radar shots, measured along tracks with a total length of 266 kilometres (Figure 4-5).

Since the U.S. government announced that it would remove Selective Availability (SA; see the press release "Statement by the President regarding the United States' decision to stop degrading global positioning system accuracy" May 1, 2000), the error of single measurements without corrections is reduced to 5 – 20 m. In many cases this are good enough, and the differential correction is not needed. The system described above is still useful as it links the GPS measurements to the GPR files. Since SA was removed, the Norwegian Mapping authority has stopped transmitting the RDS correction signal and developed new systems called MPOS, DPOS and CPOS. These, like the RDS signals, are based on the Mapping authority's SATREF (Satellite Reference system) services. MPOS reduces the errors to 0.5 to 1 m, DPOS to decimetres and CPOS to centimetres. A handheld GPS-receiver can be used with the MPOS system, whereas the others require more sophisticated receivers. Where high accuracy is recommended, the MPOS system can be implemented as a substitute for the RDS based DFM-100 system.

URN:NBN:no-6348

Figure 4-6 What will be the future for snow surveying?

URN:NBN:no-6348

5 SUMMARY AND FURTHER WORK

This thesis is compiled on the basis of nine papers related to snow and snow processes in the Arctic. Three of them detail mapping and modelling of snow distribution, two snow distribution measurement methods and four detail snowmelt modelling. The main objective of the doctoral study has been to understand and improve the modelling of the dynamic processes of the seasonal snow cover in the Arctic. The motivation was to better assess the Arctic's response to and influence on possible climate warming.

Snow distribution strongly influences snow cover depletion and thereby also snowmelt runoff. Snow distribution can be found through measurements or estimated by models. Georadar or snowradar was introduced during the eighties as a tool for reducing the workload of those conducting snow surveys. The method made it possible to carry out extensive measurement campaigns, however, both the logistics and data handling needed to be improved to make the method applicable for, for instance, hydropower producers. Extensive testing of the method and improvements to the logistics involved were carried out during this doctoral study. As a result, snowradar has proved to an efficient and reliable tool for snow surveying. The handling of data from several tens of kilometres of snow surveys has also become manageable through use of the program SIRDAS developed both prior to and during this study.

Extensive snow depth mapping employing the snowradar, made it possible to test and validate the performance of a numerical snow transport model. SnowTran-3D, a numerical snow transport model developed by Dr. Glen Liston at the University of Colorado, was improved in this study to better handle periods of melting and snow settling. The model was tested for three different sites with different sizes, topography and locations. The improvements proved to be successful and the simulated results were in good agreement with the observations. It has recently been stated that snow transport models are not capable of modelling snow cover evolution where there is complex mountainous terrain. On the contrary, validation of SnowTran-3D including simulation in the DeGeer valley shows that this kind of model can be used to both calculate snow depth frequency distribution and

URN:NBN:no-6348

locate snowdrifts and wind eroded areas at the regional scale and in a highly complex terrains. As far as the author is aware, models of this kind have not previously been validated to the same extent for areas with similar topography and scales. Given digital topographical information with a resolution of 100m by 100m or better, and representative weather data, these models can provide an alternative to or supplement detailed snow surveys in order to describe snow distribution.

Several detailed and extensive studies of snowmelt and energy balance over a snow cover have been performed in the Arctic regions of America and Asia. Only a few studies have been carried out in the European Arctic regions at Svalbard. Thus this thesis and the data collected at Svalbard for its preparation are original and valuable. Fieldwork in Arctic regions is in itself challenging and much experience is needed to be able to collect high quality data in these areas. Only a small amount of the data collected for the thesis and previous projects has been published to date. These data and the experience gained working in field in permafrost regions, solving all kinds of related problems, have a large potential value.

When it comes to modelling; the methods used here are well known and the testing and improvements of models carried out are less stirring. The snowmelt related papers focus on the effect of solar radiation on snowmelt and demonstrate that inclusion of a simple energy balance model can improve snowmelt calculations compared to straight temperature-index models. In this thesis, the latter is represented by the HBV model and the former by E-bal HBV. An energy balance model was especially valuable for determining the timing of the snowmelt. Simulations were also generally improved during the rest of the snow- and glacial melt period.

A new method to account for skewed snow distribution was also introduced in this thesis and used in combination with the E-bal HBV-model. A snow cover depletion factor, f_{snow}, was introduced and used to calculate the reduction of the snow area (i.e., the area contributing to snowmelt) on the tundra and the appearance of the ice surface on the glacier. The method is based on parameters that can be found from snow survey data and does not, therefore, induce more parameters that need to be calibrated. The method was validated against measurements made both on glaciers and tundra.

URN:NBN:no-6348

5.1 RECOMMENDATIONS FOR FURTHER RESEARCH

As this study has shown, snow transport models can be used alone or as supplementary tools to estimate snow distribution and snow depth frequency distribution in areas where such models were assumed to be inapplicable. This opens possibilities in other fields, for instance snowmelt runoff forecasting for hydropower production. Further research, testing and validation are however recommended before a model such as SnowTran-3D is generally applicable for those purposes.

If time and funding were not limited, the next step in this study would be to combine the snow drift model and the simple energy balance model in order to calculate distributed snowmelt and snow cover depletion. Digital video recordings of the modelled area during snow ablation would be used to validate the results. If successful, this would provide a model that could simulate the complete cycle of snow accumulation and depletion using limited meteorological data. Such a model could be a useful tool for scientist in other fields working on topics where there is a snow and snow coverage component. It could also improve forecasting of snowmelt runoff for hydropower production, and produce snow cover maps possible to validate from satellite images.

It would be valuable and innovative to combine the knowledge and modelling of snow distribution and depletion with knowledge of flora and fauna held by biologists and botanists. As the SnowTran-3D runs in the DeGeer valley shows, the model can be applied at most locations based on limited amounts of data. If understanding of the environmental (i.e. fauna, flora) impacts of snow cover where improved through multi-disciplinary research, the consequences of climate warming and changes in snow cover could be better assessed by modelling snow distribution under different climatic scenarios.

Some research is still necessary in order to optimise and simplify the use of the snow radar measurement system as a “commercial” snow survey method. The combination of the snow radar and GPS could be improved as could the SIRDAS program for data handling. These challenges are mainly of a technical character and demand the involvement of technicians and radar specialists in addition to an experienced user of the system.

URN:NBN:no-6348

"Dynamics" in the seasonal snowcover....(photo G. Bangjord)

URN:NBN:no-6348

6 REFERENCES

Aanes, R., Sæther B.-E. and N. A. Øritsland (2000) Fluctuations of an introduced population of Svalbard reindeer: the effects of density dependence and climatic variation. Ecography, Vol. 23 (4), pp. 437-443

Andersen, T., Fossdal, M. L., Killingtveit, Å. and K. Sand (1987). The Snow-radar : a new device for areal snow depth measurement. In: T. Andersen, K. Sand and Å. Killingtveit (Editors), Proceedings of Workshop on Hydropower in Cold Climates, Trondheim, pp. 1-14.

Andersen, T. L. Gottschalk, J. Harestad, Å. Killingtveit, J. Tveit and S. Aam (1982) Snow surveys in Hydropower schemes. Report A-113, Norwegian Institute of Science and technology, Trondheim. In Norwegian

Anderson, E. A. (1976) A point energy and mass balance model of s snow cover. NOAA Technical Report NWS 19, Office of Hydrology, National Weather Service, Silver Springs.

Ashton, G. D. (Editor), (1986) *River and Lake Ice Engineering*. Book Crafters Inc., Michigan, USA.

Bahr, D. B. and M. F. Meier (2000) Snow patch and glacier size distributions. *Water Resources Research, Vol. 36* (2*)*, pp. 495-501.

Balk, B. and K. Elder (2000) Combining decision tree and geostatistical methods to estimate snow distribution in a mountain watershed. *Water Resources Research, Vol. 36* (1*)*, pp. 13-26.

Barth Johnson, G.D. (1857) *Notation on drifting snow and snowdrifts and how their harmful effects on both farmland and roads can be prevented and impaired*, In Norwegian, Facsimile NTH-trykk 1969.

Bayne, D. K. (1978) The relation between Shortwave radiation and Sunshine Hours. Internal 24, University of Saskatchewan, Saskatoon.

Bengtsson, L. (1976) Snowmelt estimates from Energy budget studies. *Nordic Hydrology, Vol. 7*, pp. 3-18.

Bergstöm, S. (1975) The development of a snow routine for the HBV-2 model. *Nordic Hydrology, Vol. 6* (73-92*)*.

Blöshl, G. (1999) Scaling issues in snow hydrology. *Hydrological Processes, Vol. 13*, pp. 2149-2175.

Blöshl, G., Gutknecht, D. and R. Kirnbauer (2001) Distributed Snowmelt Simulations in an Alpine Catchment 2. Parameter Study and Model Predictions. *Water Resources Research, Vol. 27* (12*)*, pp. 3181-3188.

URN:NBN:no-6348

Blöshl, G. and R. Kirnbauer (1992) An analysis of snowcover patterns in a small alpine catchment. *Hydrological processes, Vol. 6*, pp. 99-109.

Bohren, C. F. and B. R. Barkstrom (1974) Theory of the Optical Properties of Snow. *Journal of Geophysical Research, Vol. 79* (30*)*, pp. 4527-4535.

Bruland, O. (1999) Energy and Water Balance of Active Layer 1991-1994 Understanding Land Arctic Physical Processes 1996-1998. Sintef Report STF22 A98417, SINTEF, Trondheim.

Bruland, O. and E. Cooper (2001). Snow distribution and vegetation. In: P. Kuhry (Editor), Proceedings of Arctic Feedbacks to Global Change. Rovaniemen Paintuskeskus Oy, Rovaniemi, Finland, pp. 110.

Bruland, O. and J. O. Hagen (2002) Mass Balance of Austre Brøggerbreen modelled with the HBV-model. *Polar Research,* accepted for publishing June 2002.

Bruland, O. and Å. Killingtveit (2002) An Energy Balance Based HBV-Model with Application to an Arctic Watershed on Svalbard, Spitsbergen. *Nordic Hydrology, Vol. 33* (2*)*.

Bruland, O., Liston, G. E., Sand, K. and Å. Killingtveit (2002) Modelling the snow distribution at two high Arctic sites at Svalbard, Norway, and at a sub-arctic site in central Norway. Submitted to *Nordic Hydrology,* Nov 2001.

Bruland, O., Maréchal, D., Sand, K. and Å. Killingtveit (2001a) Energy and water balance studies of a snow cover during snowmelt period at a high arctic site. *Theoretical and Applied Climatology, Vol. 70* (1-4*)*, pp. 55-63.

Bruland, O. and K, Sand (1997). Application of Georadar in Polar Hydrology. In: D. L. Kane (Editor), Proceedings of Northern Research Basin The Eleventh International Symposium and Workshop. University of Alaska, Prudhoe Bay/Fairbanks Alaska, pp. 39-48.

Bruland, O., Sand, K. and Å. Killingtveit (2001b) Snow Distribution at a High Arctic Site at Svalbard. *Nordic Hydrology, Vol. 32* (1*)*, pp. 1-12.

Brun, E., Martin, E., Simon, V., Gendre, C. and C. Coleou (1989) An energy and mass model of snow cover suitable for operational avalanche forecasting. *Journal of Glaciology, Vol. 35* (121*)*, pp. 333-342.

Brunt, D. (1952) *Physical and Dynamical Meteorology*. Cambridge University Press, Cambridge, Massachutes.

Budd, W. R., Dingle, R. and U. Radok (1966) The Bird Snowdrift Project: Outline and basic results, Studies in Antarctic Meteorology, American Geophysical Union. Antarctica Research Service, pp. 71-134.

URN:NBN:no-6348

Carroll, S. S. and N. Cressie (1997) Spatial modelling of snow water equivalent using covariances estimated from spatial and geomorphic attributes. *Journal of Hydrology, Vol. 190*, pp. 42-59.

Chalita, S. (1994) The albedo of temperate and boreal forest and the Northern Hemisphere climate: a sensitivity experiment using the LMD GCM. *Climate Dynamics, Vol. 10* (4/5*)*, pp. 231-240.

Christensen, T. R. (1991) Arctic and sub-Arctic soil emissions: possible implications for global climate change. *Polar Record, Vol. 162*, pp. 205-210.

Cohen, J. (1994) Snow cover and climate. *Weather, Vol. 49*, pp. 150-156.

Cohen, J. and D. Entekhabi (1999) The influence of Eurasian snow cover on Northern Hemisphere climate variability. In: Tranter, M., Armstrong, R., Brun, E., Jones, G., Sharp, M. and M. Williams (Editors), Interactions between the cryosphere, climate, and greenhouse gases. IAHS Press, Wallingford.

Colman, R. A., McAvaney, B. J., Fraser, J. R., Rikus, L. J. and R. R. Dahni (1994) Snow and cloud feedbacks modelled by an atmospheric general circulation model. *Climate Dynamics, Vol. 9* (4/5*)*, pp. 253-265.

Douville, H. and J. F. Royer (1997) Influence of the temperate and boreal forests on the Northern Hemisphere climate in the Météo-France climate model. *Climate Dynamics, Vol. 13*, pp. 57-74.

Elder, K. and J. Michaelsen (1991) Snow Accumulation and Distribution in an Alpine Watershed. *Water Resources Research, Vol. 27* (7*)*, pp. 1541-1522.

Ellerbruch, D. A. and H. S. Boyne (1980) Snow Stratigraphy and water equivalence measured with an active microwave system. *Journal of Glaciology, Vol. 26*, pp. 225-233.

Essery, R., Li, L. and J. Pomeroy (1999a) A distributed model of blowing snow over a complex terrain. *Hydrological Processes, Vol. 13*, pp. 2423-2438.

Essery, R., Martin, E., Douville, H., Fernandez, A. and E. Brun (1999b) A comparison of four snow models using observations from an alpine site. *Climate Dynamics, Vol. 15*, pp. 583-593.

Garnier, B.J. and A. Ohmura (1970) The evaluation of surface variation in solar radiation income. *Solar Energy, Vol. 13* , pp. 21-34.

Gerland, S., Winther, J.-G., Ørbæk, J. B., Liston, G. E., Øritsland, N. A., Blanco A. and B. Ivanov (1999) Physical and optical properties of snow covering Arctic tundra on Svalbard. *Hydrological Processes, Vol. 13*, pp. 2331-2343.

URN:NBN:no-6348

Gray, D. M. and Male, D. H., 1981. Snowcover ablation and runoff. In: D. M. Gray and D. H. Male (Editors), Handbook of Snow. Pergamon Press, Saskatchewan, 767 p.

Green, E. M., Liston, G. E. and R.A. Pielke Sr. (1999) Simulation of above treeline snowdrift formation using a numerical snow-transport model. *Cold Regions Science and Technology, Vol. 30*, pp. 135-144.

Grogan, P. and Chapin III, F.S. (2000) Initial effects of experimental warming on above- and belowground components of net ecosystem CO2 exchange in arctic tundra. Oecologia, Vol. 125 , pp. 512-520.

Gutzler, D.S. and R. D. Rosen (1992) Interannual variability of wintertime snow cover across the Northern Hemisphere. *Journal of Climate, Vol. 5*, pp. 1441-1447.

Harstveit, K. (1984) Snowmelt Modelling and Energy Exchange between the Atmosphere and a Melting Snow Cover. Ph.D Thesis, University of Bergen, Bergen, 119 p.

Hartman, M. D., Baron, J. S., Lammers, R. B., Cline, D. W., Band, L. E., Liston, G. E. and C. Taque (1999) Simulation of Snow Distribution and Hydrology in a Mountain Basin. *Water Resources Research, Vol. 35* (5*)*, pp. 1587-1603.

Harvey, L. D. D. (1988) On the role of high latitude ice, snow, and vegetation feedbacks in the climatic response to external forcing changes. *Climatic Change, Vol. 13*, pp. 191-224.

Holmgren, J., Sturm, M., Yankielun, N. E. and G. Koh (1998) Extensive measurements of snow depth using FM-CW radar. *Cold Regions Science and Technology, Vol. 27*, pp. 17-30.

Jaedicke, C. (2001) Drifting snow and snow accumulation in complex arctic terrain : field experiments and numerical modelling. Ph.D. Thesis, University of Bergen, Geophysical Institute, Bergen, 55 p.

Johnson, C. J., Parker, K. L. and D. C. Heard (2001) Foraging across a variable landscape: behavioral decisions made by woodland caribou at multiple spatial scales. *Oecologia, Vol. DOI 10.1007/ s004420000573*.

Jordan, R. (1991) A One-Dimensional Temperature Model For a Snow Cover: Technical documentation for SNTHERM.89. Technical documentation, National Technical Information Service, Springfield, Virginia.

Kane, D. L. (1996) The impact of hydrologic perturbations on arctic ecosystems induced by climate change. In: W. C. Oechel and J. J. Holten (Editors), *Global change and arctic terrestrial ecosystems*. Springer-Verlag, New York, N.Y.

URN:NBN:no-6348

Kane, D. L., Gieck, R. E. and L. D. Hinzman (1997) Snowmelt Modelling at a Small Alaskan Arctic Watershed. *Journal of Hydrologic Engineering, Vol. 2* (4*)*, pp. 204-210.

Kane, D. L., Hinzman, L. D., Woo, M. K. and K. R. Everett (1992) Hydrology of the arctic: present and future. In: S. F. Chapin III, R. Jefferies, J. Reynolds, G. Shaver and J. Svoboda (Editors), *Physiological ecology of arctic plants: implications for climate change*. Academic Press Inc., pp. 35-57.

Keller, F., Kienast, F. and M. Beniston (2000) Evidence of response of vegetation to environmental change on high-elevation sites in the Swiss Alps. *Regional Environmental Change, Vol. 1* (2*)*, pp. 70-77.

Killingtveit, Å. and N. R. Sælthun (1995) *Hydrology*. Hydropower Development, Vol 7. Norwegian University of Science and Technology, Division of Hydraulic Engineering, Trondheim, 213 p.

Killingtveit, Å. and K. Sand (1988). Snow Radar: An efficient tool for snowpack assesment. In: T. Thomsen, H. Søgaard and R. Braithwaite (Editors), Proceedings of The Seventh Northern Research Basins Symposium and Workshop. Danish Society of Arctic Technology, Ilulissat, Greenland, pp. 145-157.

Kind, R. J. (1981) Snowdrifting. In: D. M. Gray and D. H. Male (Editors), *Handbook of Snow*. Pergamon Press, Saskatchewan, pp. 338-359.

Kobayashi, S. (1971) Development and movement of wavy features on the snow surface during drifting. *Low Temperature Science Series A, Physical Sciences,* (29*)*, pp. 81-92.

König, M. and M. Sturm (1998) Mapping snow distribution in the Alaskan Arctic using aerial photography and topographic relationship. *Water Resources Research, Vol. 34* (12*)*, pp. 3471-3483.

Kuz'min, P. P. (1961) Protsess Tayaniya Shezhnogo Pokrova (Melting of Snow Cover). *Israel Prog.Sci. Transl. 1971*.

Liston, G. E., Bruland, O., Winther, J.-G., Elvehøy, H. and K. Sand (1999a) Meltwater production in Antarctic blue-ice areas: sensitivity to changes in atmospheric forcing. *Polar Research, Vol. 18* (2*)*, pp. 283-290.

Liston, G. E. and M. Sturm (1998) A snow transport model for complex terrain. *Journal of Glaciology, Vol. 44* (148*)*, pp. 498-516.

Liston, G. E., Winther, J.-G., Bruland, O., Elvehøy, H. and K. Sand (1999b) Below-surface ice melt on the coastal Antarctic ice sheet. *Journal of Glaciology, Vol. 45* (150*)*, pp. 273-285.

Liston, G. E., Winther, J.-G., Bruland, O., Elvehøy, H., Sand, K. and L. Karløf (2000) Snow and blue-ice distribution patterns on the coastal Antarctic ice sheet. *Antarctic Science, Vol. 12* (1*)*, pp. 69-79.

URN:NBN:no-6348

Liston, G. E. and M. Sturm (2001) Winter Precipitation Pattern in Arctic Alaska Determined from a Blowing-Snow Model and Snow-Depth Observations. *Journal of Hydrometeorology,* Submitted October 2001.

Lloyd, C. R., Aurela, M., Bruland, O., Fowler, D., Friborg, T., Hansen, B. U., Harding, R. J., Hargreaves, K., Nordstroem, C., Laurila, T., Tuovinen, J.-P., K. Sand and B. Vehvilainen (1999) Final Report of the Land Arctic Physical Processes (LAPP), Project. Contract No. ENV4-CT95-0093, EC DG XII Climate and Environment, Brussels.

Lundberg, A. and H. Thunehed (2000) Impulse Radar Snow Surveys - Influence of Snow Density. *Nordic Hydrology, Vol. 31* (1*)*, pp. 1-14.

Male, D. H. (1980) The Seasonal Snowcover. In: S. C. Colbeck (Editor), *Dynamics of Snow and Ice Masses*. Academic Press, New York, pp. 305-395.

Male, D. H. and D. M. Gray (1975) Problems in developing a physically based snowmelt model. *Canadian Journal of Civil Engineering, Vol. 2* , pp. 474-488.

Marchand, W.-D. and Killingtveit, Å. (1999). Statistical properties of spatial snow cover in mountainous catchments in Norway, Proceedings of Northern Research Basins, Twelfth International Symposium and Workshop, Iceland.

Marchand, W.-D., Bruland, O. and Å. Killingtveit (2001a) Improved Measurements and Analysis of Spatial Snow Cover by Combining a Ground Based Radar System With a Differential Global Positioning System Receiver. *Nordic Hydrology, Vol. 32* (3*)*, pp. 181-194.

Marchand, W.-D., Killingtveit, Å., Wilén, P. and P. Wikström (2001b) Comparison of ground-based and airborne snow-depth measurements with georadar systems, case study*,* in writing.

Marsh, P. (1999) Snowcover Formation and Melt: Recent Advances and Future Prospects. *Hydrological Processes, Vol. 12*, pp. 2117-2134.

McKay, D. C. (1970) Energy, Evaporation and Evapotranspiration. In: D. M. Gray (Editor), *Handbook on Principles of Hydrology*. Water information Centre, New York, pp. 3.1-3.66.

McLung, D. and P. Scharer (1993) *The Avalanche Handbook*. The Mountaineers, Seattle, 271 p.

Météo-France (2001). SnowMIP, Snow models Intercomparison Project. Météo-France, Centre national de recherches météorologiques, Centre d'études de la neige, 1441 rue de la Piscine, 38406 Saint Martin d'Hères CEDEX, France, http://www.cnrm.meteo.fr/ snowmip/.

URN:NBN:no-6348

Norem, H. (1968) Mapping of snow conditions on the road crossing the Strynefjellet mountain passt. Master Thesis, Norwegian University of Science and Technology, Trondheim, 104 pp.

Owen, P. R. (1964) Saltation of uniform grains in air. *Journal of Fluid Mechanics, Vol. 20*, pp. 225-242.

Partridge, G. W. and Platt, C. M. R. (1976) *Radiative Processes in Meteorology and Climatology*. Elsevier Scientific Publishing Company, Amsterdam.

Penmann, H. L. (1948) Evaporation from open water, bare soil, and grass. *Proceedings of the Royal Society Series A, Vol. 193*, pp. 120-145.

Pomeroy, J. W., Gray, D. M. and Landine, P. G. (1993) The Prairie Blowing Snow Model: characteristics, validation, operation. *Journal of Hydrology, Vol. 144*, pp. 165-192.

Pomeroy, J. W. (1988) Wind transport of Snow. Ph.D. Thesis, University of Saskatchewan, Saskatoon, 226 pp.

Pomeroy, J. W. and D. M. Gray (1990) Saltation of snow. *Water Resources research, Vol. 26* (7*)*, pp. 1583-1594.

Pomeroy, J. W. and D. M. Gray (1995) *Snow Accumulation, Relocation and Management*. National Hydrology Research Institute Science Report, 7. Minister of Environment, Saskatoon, 144 p.

Pomeroy, J. W., Gray, D. M., Shook, K. R., Toth, B., Essery, R. L. H., Pietroniro, A. and N. Hedstrøm (1998) An evolution of snow accumulation and ablation processes for land surface modelling. *Hydrological Processes, Vol. 12*, pp. 2339-2367.

Pomeroy, J. W. and D. H. Male (1987) Wind transport of seasonal snowcovers. In: H.G. Jones and W.J. Orville-Thomas (Editors), Seasonal Snowcovers: *Physics, Chemistry, Hydrology.* D. Reidel Publishing Company, pp. 119-140.

Pomeroy, J. W., Marsh, P. and D. M. Gray (1997) Application of a distributed blowing snow model to the Arctic. *Hydrological Processes, Vol. 11* (11*)*, pp. 1451-1464.

Prasad, R., Tarboton, D. G., Liston, G. E., Luce, C. and M. Seyfrid (2001) Testing a blowing snow model against distributed snow measurements at Upper Sheep Creek, Idaho, USA. *Water Resource Research, Vol. 37* (5*)*, pp. 1341-1357.

Price, A. G. and T. Dunne (1976) Energy balance computations of snowmelt in a subarctic area. *Water resources research, Vol. 12* (4*)*, pp. 686-694.

Prowse, T. D., Ommanney, C. S. L. and L. E. Watson (1994) *Northern Hydrology, International Perspective*, NHRI Science Report No.3. National Hydrology Research Institute, Saskatoon.

URN:NBN:no-6348

Purves, R. S., Barton, J. S., Mackaness, W. A. and D. E. Sugden (1998) The development of a rule-based spatial model of wind transport and deposition of snow. *Annals of Glaciology, Vol. 26*, pp. 197-202.

Repp, K. (1988). The hydrology of Bayelva, northwest Spitsbergen, Proceedings of The 7th Northern Research Basin Symposium Workshop, Ilulissat, Greenland.

Rouse, W. R. (1984) Microclimate of Arctic tree line 2. Soil microclimate of tundra and forest. *Water Resource Research, Vol. 20* (1*)*, pp. 67-73.

Sælthun, N. R. (1996) The "Nordic" HBV Model. Description and documentation of the model version developed for the project Climate Change and Energy Production. NVE Publication 7, Norwegian Water Resources and Energy Administration, Oslo.

Sælthun, N. R., Aittoniemi, P., Bergström, S., Einarsson, K., Jóhannesson, T., Lindström, G., Ohlsson, P.–E, Thomsen, T., Vehviläinen, B. and K. O. Aamodt (1998) Climate change and impacts on runoff and hydropower in the Nordic countries. TemaNord 1998:552, Nordic Council of Ministers, Copenhagen.

Sand, K. (1990) Modelling of snowmelt runoff processes in temperate and arctic environments. Ph.D. Thesis, Norwegian University of Science and Technology, Trondheim, 176 p.

Sand, K. and O. Bruland (1998) Application of Georadar for Snowcover Surveying. *Nordic hydrology, Vol. 29* (4/5*)*, pp. 361-370.

Sand, K. and O. Bruland (1999). Water balance of three high Arctic river basins in Svalbard. In: J. Elíasson (Editor), Proceedings of Northern Research Basins Twelfth International Workshop and Symposium. Engineering Research Institute University of Iceland, Iceland, pp. 270-283.

Sand, K., Winther, J. G., Maréchal, D., Bruland, O. and K. Melvold (2002) Regional Variations of Snow Accumulation on Spitsbergen, Svalbard, 1997-99. *Nordic Hydrology,* Submitted .

Schmidt, R. A. J. (1972) Sublimation of wind-transported snow - "A model". Research paper RM-90, USDA Forestry Service, Rocky Mountain Forest and Range experimental Station, Fort Collins.

Schmidt, R. A. J. (1991) Sublimation of snow intercepted in an artificial conifer. *Agriculture and forest Meteorology, Vol. 54*, pp. 1-27.

Shook, K. and D. M. Gray (1997) Synthesizing shallow seasonal snow covers. *Water Resources Research, Vol. 33* (3*)*, pp. 419-425.

Slagstad, D. (2001) Personal communication, Dag Slagstad, Senior scientist, SINTEF Fisheries and aquaculture.

Suckling, P. W. and J. E. Hay (1977) A cloud layer-sunshine model for estimating direct, diffuse and total solar radiation. *Atmosphere, Vol. 15*, pp. 194-207.

URN:NBN:no-6348

Susar Consulting AS, 1997. SIRDAS - A computer program for processing SnowRadar data, SINTEF/Statkraft, Trondheim.

Swinbank, W. C. (1963) Longwave Radiation from Clear Skies. *Quarterly Journal of the Royal Meteorological Society, Vol. 89* , pp. 339-348.

Tabler, R. D., Pomeroy, J. W. and B. W. Santana (1990) Drifting Snow. In: W. L. Ryan and R. D. Crissman (Editors), Cold Regions Hydrology and Hydraulics. American Society of Civil Engineers, New York, pp. 95-146.

Tveit, J. (1980) Representativity of snow survey systems based on topographical and morphological parameters. Ph.D. Thesis, Norwegian University of Science and Technology, Trondheim, 243 p. In Norwegian

Tveit, J. and Å. Killingtveit (1994). Snow surveys for studies of Water Budget on Svalbard, Proceedings of Tenth International Northern Research Basins Symposium and Workshop. Norwegian University of Science and Technology, Svalbard, Norway, pp. 489-509.

U.S. Army Corps of Engineers (1956) Snow Hydrology. Summary Report of Snow Investigation, Corps of Engineers, North Pacific Division, Portland.

Ulaby, F. T., Moore, R. K. and A. K. Fung (1986) *Microwave Remote Sensing: Active and Passive, Vol. III -- Volume Scattering and Emission Theory, Advanced Systems and Applications*. Artech House Inc., Dedham, Massachusetts, 1100 pp.

Ulriksen, P. (1989). Radar measurement of equivalent water content in snow measured from helicopter, Proceedings of EARSEL Workshop and Symposium. Espoo, Finland.

Van Der Wal, R., Madan N., Van Lieshout, S., Dormann, C., Langvatn, R. and S. D. Albon (2000) Trading forage quality for quantity? Plant phenology and patch choice by Svalbard reindeer. *Oecologia, Vol. 123*, pp. 108-115.

Vörösmarty C., Hinzman, L., Peterson, B., Bromwich, D., Hamilton, L., Morison, J., Romanovsky, V., Sturm, M. and R. Webb (2001) *The Hydrologic Cycle and its Role in Arctic and Global Environmental Change: A Rationale and Strategy for Synthesis Study*. Arctic Research Consortium of the U.S., Fairbanks, Alaska, 84 pp.

Walland, D. J. and I. Simmonds (1997) Modelled atmospheric response to changes in Northern Hemisphere snow cover. *Climate Dynamics, Vol. 13* (1*)*, pp. 25-34.

Walmsley, J. L., Salmon, J. R. and P. A. Taylor (1982) On the application of a model of boundary-layer flow over low hills to real terrain. *Boundary Layer Meteorology, Vol. 23* , pp. 17-46.

URN:NBN:no-6348

Walmsley, J. L., Taylor, P. A. and T. Keith (1986) A simple model of neutrally stratified boundary-layer flow over complex terrain with surface roughness modulations (MS3DJH/ 3R. *Boundary Layer Meteorology, Vol. 36*, pp. 157-186.

Weatherly, J. W. and Walsh, J. E. (1996) The effects of precipitation and river runoff in a coupled ice-ocean model of the Arctic. *Climate Dynamics, Vol. 12*, pp. 785-798.

Williams, P.J. and Smith, M.W. (1989) *The Frozen Earth*. Cambridge University Press, 306 pp.

Winther, J.-G. (1993) Short- and Long-Term Variability of Snow Albedo. *Nordic Hydrology, Vol. 24*, pp. 199-212.

Winther, J.-G., Bruland, O., Sand, K., Killingtveit, Å. and D. Maréchal (1998) Snow accumulation distribution on Spitsbergen, Svalbard, in 1997. *Polar Research, Vol. 17* (2*)*, pp. 155-164.

Winther, J.-G., Gerland, S., Ørbæk, J. B., Blanco, A., Ivanov, B. and J. Boike (1999) Spectral reflectance of melting snow in a high Arctic watershed on Svalbard: Some implications for optical satellite remote sensing studies. *Hydrological Processes, Vol. 13*, pp. 2033-2049.

Winther, J.-G., Elvehøy, H. C., Bøggild, C. E., Sand, K. and G. E. Liston (1996) Melting, runoff and formation of frozen lakes in a mixes snow and blue-ice field in Dronning Maud Land, Antarctica,. *Journal of Glaciology, Vol. 42*, pp. 271-276.

Woo, M. K. (1986) Permafrost hydrology in North America. *Atmosphere and Ocean, Vol. 24*, pp. 201-234.

URN:NBN:no-6348

APPENDICES

Paper 1: Energy and water balance studies of a snow cover during snowmelt period at a high arctic site. Theoretical and Applied Climatology, Vol. 70 (1-4), pp. 55-63.

Paper 2: An energy balance based HBV- Model with application to an Arctic watershed on Svalbard, Spitsbergen. Nordic Hydrology, Vol. 33 (2).

Paper 3: Glacial mass balance of Austre Brøggerbreen modelled with the HBV-model. Polar Research, accepted for publishing June 2002.

Paper 4: Meltwater production in Antarctic blue-ice areas: sensitivity to changes in atmospheric forcing. Polar Research, Vol. 18 (2), pp. 283-290.

Paper 5: Snow Distribution at a High Arctic Site at Svalbard. Nordic Hydrology, Vol. 32 (1), pp. 1-12.

Paper 6: Snow accumulation distribution on Spitsbergen, Svalbard, in 1997. Polar Research, Vol. 17 (2), pp. 155-164.

Paper 7: Modelling of the snow distribution at two high arctic sites at Svalbard, Norway, and at a sub-arctic site in central Norway. Submitted to Nordic Hydrology Nov 2001.

Paper 8: Application of Georadar in Snow Cover Surveying. Nordic hydrology, Vol. 29 (4/5), pp. 361-370.

Paper 9: Improved Measurements and Analysis of Spatial Snow Cover by Combining a Ground Based Radar System With a Differential Global Positioning System Receiver. Nordic Hydrology, Vol. 32 (3), pp. 181-194.

URN:NBN:no-6348

URN:NBN:no-6348

Paper 1:
Energy and water balance studies of a snow cover during snowmelt period at a high arctic site. Theoretical and Applied Climatology, Vol. 70 (1-4), pp. 55-63.

URN:NBN:no-6348

URN:NBN:no-6348

Paper 2:
An energy balance based HBV- Model with application to an Arctic watershed on Svalbard, Spitsbergen. Nordic Hydrology, Vol. 33 (2).

URN:NBN:no-6348

Nordic Hydrology, Vol. 33 (2*)* 2002 Accepted for publication.

An Energy Balance Based HBV- Model with Application to an Arctic Watershed on Svalbard, Spitsbergen.

Oddbjørn Bruland[1], Ånund Killingtveit[1]

Norwegian Univ. Of Science and Tech., N-7491 Trondheim

In several studies of snowmelt using the temperature index method from the original HBV-model, the model fails to predict the timing of the snowmelt and underestimates the intensities on occasions with high solar radiation and low air temperatures. This is especially evident at high latitudes such as catchments on Svalbard, but can also be the case for catchments at lower latitudes but at higher elevations and thus of importance to hydropower production. In this study, an energy balance calculation replaces the simple temperature index model in a spreadsheet version of the HBV-model. Calculation of average snow pack temperatures is included, and a new method is introduced to account for uneven snow distribution and glacial melt. This energy balance based HBV-model gives a better simulation of both snow and glacial melt. It was also found that estimates of sensible heat were improved by using a function with a non-linear wind speed dependency.

Introduction

The HBV-model is by far the most important precipitation-runoff model in Scandinavia, and is today considered the "standard" runoff forecasting model for hydropower utilities in Norway. It is also widely used in other countries (Bergström 1992). When moving to both higher latitudes and elevations, snow ablation gradually becomes the most important hydrological event of the year. In these areas, the solar radiation plays a more important role in ablation; especially for the timing of it (Kane *et al.* 1997). Although the simple temperature index melt model (TIM) used in the traditional HBV-model has been successfully tested and applied in several studies (Hinzman and Kane 1991; Sand 1990; Hamlin *et al.* 1998;

URN:NBN:no-6348

Vehvilänen 1992), weaknesses have been evident in situations with low temperatures and high solar radiation (Bruland et al, 2001). These situations are typical of Arctic and high mountain areas in springtime. According to Bengtsson (1986), it is physically sound to use the TIM alone only within a forest with a dense canopy. In an open area he recommends a parametric approach including both air temperature and solar radiation (Bengtsson 1984). Kane *et al.* (1997) found that a combined air temperature/radiation model did not do significantly better than the air temperature model. A similar approach within the Nordic HBV-model (Sælthun 1996) gave just slightly better results than the ordinary TIM in simulations in the Bayelva catchment at Svalbard (Bruland and Sand 1994). In this study the TIM is substituted with a surface energy balance calculation. Bruland *et al.* (2001) compared a layered numerical model, a simple energy balance model and a temperature index model. They found that on a plot scale the numerical model gave only slightly better results than the simple energy balance model, both these models where better than the TIM. Based on their conclusions, a simple energy balance calculation is combined here with internal snow temperature calculations.

Over the years a large number of studies on energy balance and snowmelt have been published and several variations of the equations for each term of the energy balance and the parameters used in these equations, have been suggested. Gray and Male (1981) summarizes some of these. Two major Norwegian studies on snowmelt and energy balance where carried out by Harstveit (1984) and Sand (1990). Harstveit (1984) tested energy balance models and TIM against lysimeter snowmelt data collected during the period 1979 to 1982 from four locations close to Bergen, Western Norway. His study includes testing and optimization of parameters used in the energy balance models. Sand performed a comparable study were he also tested Harstveit's suggestions, in an area close to Trondheim in Norway and at a plot located close to Longyearbyen at Svalbard.

The main objectives in this study is to see if a substitution of the TIM with an energy balance calculation in the HBV-model will significantly improve the simulation in Bayelva catchment and to see whether Harstveit's approach and parameters is applicable in this area.

Model Description

The HBV-Model is a conceptual precipitation-runoff model that uses precipitation, air temperature and potential evaporation data to compute snow accumulation, snow melt, actual evapotranspiration, soil moisture storage, groundwater and runoff from the catchment (Fig. 1). The model was developed in the early 1970s at the Swedish Meteorological and Hydrological Institute (SMHI) and has been documented in several reports and papers (Bergström and Forsman 1973; Bergström 1975, 1976; Lindström *et al.* 1997). In the HBV-model the catchment is divided into elevation bands and temperature and precipitation is corrected to each band. Catchment characteristics and parameters describing orographic precipitation gradient, temperature lapse rate, and threshold temperatures for snow precipitation and melt have to be found for the catchment either trough separate studies, from the literature or if no other information available; trough calibration. In addition hydrograph

URN:NBN:no-6348

characteristics and precipitation gauge catch loss corrections have to be found. In the original HBV-model, the snow and glacial melt is calculated using a TIM. The temperature index, increment for glacial melt and refreeze efficiency coefficients must be calibrated. The Nash efficiency criterion, R^2, (Nash and Suthcliffe 1970) is used to indicate model efficiency, or the agreement between the recorded and simulated hydrograph.

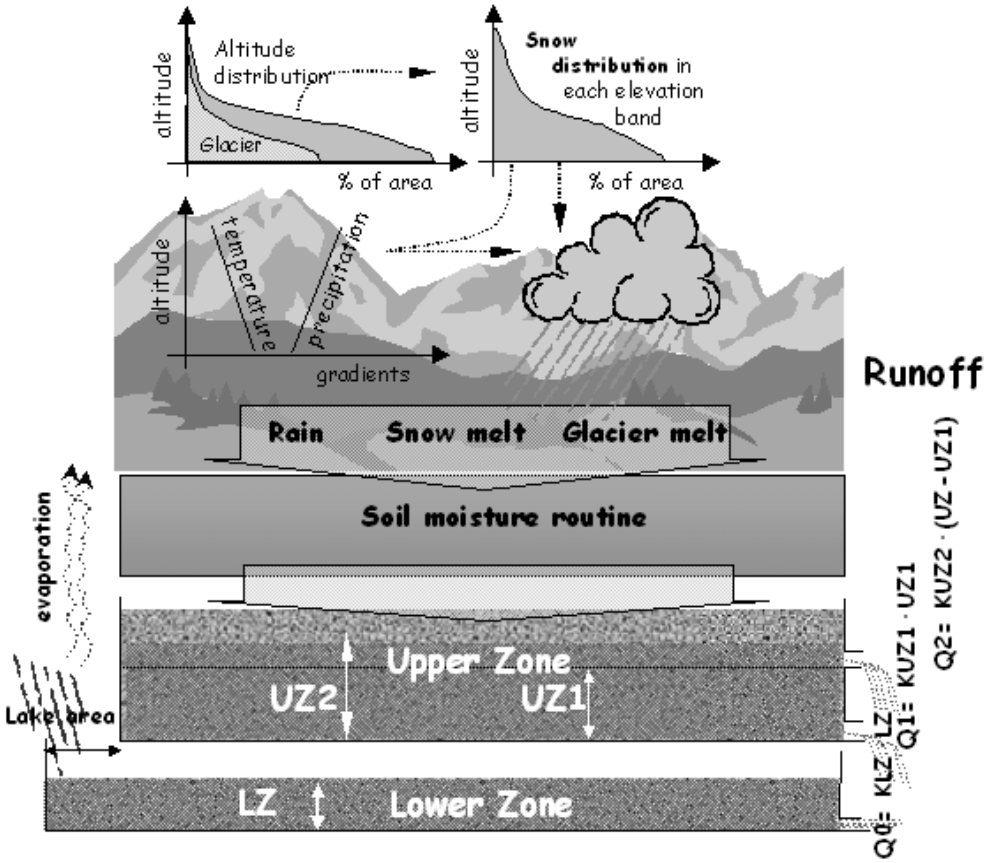

Figure 1 *The structure of the HBV-model*

URN:NBN:no-6348

Site Description and Field Measurements

Hydrological and meteorological data have been collected over a number of years in the Bayelva river catchment area close by Ny-Ålesund, on Svalbard, 78°55'N, 11°56'E (Fig. 2). Detailed measurements of snow processes in this catchment have been made since 1992 (see Bruland and Maréchal 1999).

Figure 2 *Location of Ny-Ålesund and the study area*

The catchment is 30.8 km^2 and the relief is ranging from 10 to 737 m.a.s.l with mean of 253 m.a.s.l. The catchment is 50% glaciated. The Austre and Vestre Brøgger glaciers that are bounded by steep mountains along the watershed divide, cover most of the upper catchment area. The mean altitude of the glaciers is approximately equal to the mean for the total catchment. The lower catchment consists of moraines, riverbed, tundra with a uniform lichen cover with patches of Rock Sedge (carex rupestris) and Mountain avens (Dryas octopetala). There are no trees or tall shrubs to influence either snow distribution or melt.

The Norwegian Meteorological Institute (DNMI) have made meteorological observations in Ny-Ålesund since 1961. The mean annual precipitation (1961–1990) at their station is 385 mm/year whereof approximately 74 % falls as snow or

URN:NBN:no-6348

sleet (Førland *et al.* 1996). Repp (1979) made the first time series of discharge for Bayelva catchment over the period 1974 to 1978. In 1989, the Norwegian Water Resources Administration (NVE) constructed a weir in Bayelva and reinitiated the time series. Runoff normally starts during the first week of June and lasts until mid September, and the catchment average annual runoff is 1020 mm. The large discrepancy between runoff and measured precipitation can be explained by glacial retreat, precipitation gauge catch losses and orographic rise leading to precipitation gradients (Førland *et al.* 1997). Since the Norwegian Polar Institute (NP) started mass balance studies of the Austre Brøgger glacier in 1969, there has been a steady retreat with an average negative mass balance of 423 mm water equivalent per year. As a large portion of the precipitation falls as snow during high winds, the catch losses are high. Hansen-Bauer *et al.* (1996) gives typical correction factors of 1.65–1.75, 1.05–1.10 and around 1.4 for solid precipitation (snow), for liquid precipitation and sleet (or mixed precipitation) respectively. Killingtveit *et al.* (1994) found an increase in summer precipitation of 5–10% for every 100 m increase in altitude; based on snow surveys Tveit and Killingtveit (1994) assumed a corresponding winter (snow) gradient of 14%. Hagen and Lefauconnier (1995) found, on the basis of glacial mass balance studies at the Austre Brøgger glacier, a fairly constant altitudinal increase of snow accumulation of 100 mm per 100 m; equivalent to a 25% increase per 100 m altitude. In a profile study, Førland *et al.* (1997) found that the total precipitation on the glaciers during the 1994 and 1995 summer seasons, was 45% higher than recorded at the weather station in Ny-Ålesund. It was also found that precipitation in Ny-Ålesund was strongly dependent on the wind direction. Spillover and seeder/feeder effects probably cause high precipitation events on the glaciers during winds from the South and Southwest (Førland *et al.* 1997). They estimate an increase in precipitation with altitude of 20% per 100 m up to around 300 m. Thirty to 40% of the total catchment area is above this elevation, and both Førland *et al.* (1997) and Hagen and Lefauconnier (1995) point out that a linear gradient of 20 to 25% might give too high an estimate of precipitation in these uppermost areas.

Since 1992 snow conditions have been observed daily in several snowpits during the ablation period and snowmelt has been measured from three runoff plots, together with observations of albedo, solar radiation, temperature and relative humidity. The average snowmelt intensities were found to be 14 mm/day. Average air temperature and incoming solar radiation during the ablation periods (1992–1998) were 2.1°C and 230 W/m^2 respectively.

Changes Made to the HBV-Model

Solar radiation penetrates and heats the snow to a depth several tens of centimetres below the snow surface, and snowmelt can occur even when the surface temperature is well below 0°C. In a study on the Antarctic ice sheet, Liston *et al.* (1999) found that the temperature below the snow surface could be up to 3–4°C greater than the surface temperature and that snowmelt could occur at levels from 20 to 70 cm below the surface. The conditions he used as input to his model are comparable to both those at Svalbard and at high elevations at lower latitudes. It is

URN:NBN:no-6348

obvious that a TIM can neither handle these situations, nor situations where the air temperature is below the snowmelt threshold but the surface energy balance is positive leading to a 0°C snow surface and, hence, snowmelt. The latter situation may be highly important for the ablation onset and progress. A complete numerical computation of the energy balance and snow processes as in the SNTHERM (Jordan 1991) or CROCUS models (Brun *et al.* 1989; Martin 1996) is too numerical and input demanding to be combined with an operational model for a catchment.

The energy balance model is described by Eqs. (1) to (10). Apart from the standard data used by the HBV model, the equations require only wind speed, relative humidity and cloudiness. They can also easily be adapted to the setup of a spreadsheet HBV-model. The energy balance for the snow-pack can be written

$$Qm + Qi = Qs + Ql + Qh + Qe + Qg + Qr \quad (1)$$

where

Qm = energy available for snow melt,
Qi = energy for internal heating and cooling of the snowpack,
Qs = net short wave radiation,
Ql = net long wave radiation,
Qh = sensible heat,
Qe = latent heat,
Qg = ground heat flux,
Qr = heat from preciptation.

All energy terms in Eqs. (1) to (10) have the unit W/m^2. During the ablation period in this area, with ground temperatures close to 0°C and very low precipitation, ground heat flux (Qg) and heat from precipitation (Qr) can usually be neglected for practical computations.

Short-wave Radiation

Short-wave (solar) radiation has wavelengths between 0.4–3 μm. Net short-wave radiation (Incoming - Reflected) is computed as the difference between extra-terrestrial radiation corrected for atmospheric effects and reflected shortwave radiation given by the albedo of the surface. The incoming short wave radiation can be estimated from cloudiness (Penmann,1948; McCay 1970). Harstveit (1984) used the regression model

$$Qs_{in} = Q_{ex} \cdot (kS_1 \cdot C_s + kS_2 \cdot C_s^{½} + kS_3) \quad (2)$$

where

Q_{ex} = extra-terrestrial radiation given by the date and the latitude (W/m^2),
C_s = 1 - Cloudiness, range of values is from 0 (overcast) to 1 (clear sky),
kS_1, kS_2, kS_3 = empirical constants found in studies in Dyrdalen, Western Norway, where kS_1= - 0.16, kS_2= 0.81, kS_3= 0.07.

URN:NBN:no-6348

Albedo

Snow albedo (A) largely depends on the physical properties of the snow and is strongly affected by pollution and deposition on the snow surface. Fresh snow has a high albedo, often greater than 0.8, while older polluted snow has an albedo down to 0.4. The albedo increases with cloudiness, and maximum albedo occurs for new snow and overcast weather. The calculation of the albedo in the model is based on Harstveit's (1984) regression models of albedo in Dyrdalen in Western Norway. He investigated correlation between observed albedo, age of snow (days), and cloudcover. His model Eq. (3) gave a multiple coefficient of correlation for his data of $r = 0.77$.

$$A = kA_1 \cdot (1 - C_s) + kA_2 \cdot \ln(t) + kA_3 \quad (3)$$

where

t = age of snow in days,
kA_1, kA_2, kA_3 = empirical constants found from studies in Dyrdalen, Western Norway, where $kA_1 = -0.13$, $kA_2 = -0.05$, $kA_3 = 0.87$.

The cloudiness has large-scale variability and can be taken from the nearest meteorological observatory or calculated from observations of solar radiation. In our case we have available data of solar radiation back to 1980 and cloudiness observations back to 1970.

Long-wave Radiation

Long-wave (terrestrial) radiation has wavelengths from 3 to 25 µm. Net long-wave radiation is the difference between incoming and outgoing radiation. Incoming long-wave radiation (Ql_{in}) comes from the atmosphere and surrounding objects and is strongly affected by clouds and atmospheric water vapour. Several investigators have shown that estimates of incoming long wave radiation from the atmosphere can be made from surface air temperature and vapour pressure, or surface air temperature and a cloud factor (U.S. Army corps of Engineers 1956; Partridge and Platt 1976; Swinbank 1963; Male and Gray 1981; Bengtsson 1976; Ashton 1986; Harstveit 1984). In this model the empirical formula suggested and tested by Harstveit (1984) is used (Eq. 4). His tests over 150 months of observation from Bergen, Western Norway, gave a correlation coefficient of 0.95. He also got very good agreement with Partridge and Platt's model during cloudy conditions, and Swinbank's model during clear sky conditions.

$$Ql_{in} = kL_1 \cdot \mathring{u} \cdot T_{air}^4 + kL_2 \cdot C_s + kL_3 \quad (4)$$

where

$\mathring{u}$ = Stefan-Boltzmann constant,
T_{air} = absolute air temperature (K),
kL_1, kL_2, kL_3 = empirical constants based on measurements in Bergen, $kL_1 = 1.02$, $kL_2 = 71$ and $kL_3 = -92$.

URN:NBN:no-6348

Outgoing long-wave radiation (Ql_{out}) is determined by Stefan Bolzmann's law

$$Ql_{out} = \text{ů} \cdot \text{ɸ}^{4}_{surf} \quad (5)$$

where

T_{surf} = absolute surface temperature (K).

Since surface temperature is not here measured, this has to be found through approximation. This is further discussed later.

Turbulent Heat Fluxes

Sensible heat transfer (*Qh*) depends on the temperature difference between the air and snow surface, and wind speed. Usually empirical formulas are used to compute *Qh*. Following Anderson (1976),

$$Qh = f(u) \cdot (T_{air} - T_{surf}) \quad (6)$$

where

u = wind speed (m/s)

and *f(u)* is a function of the wind speed and normally represented as

$$f(u) = kU_1 \cdot u + kU_2, \quad (7)$$

where kU_1 and kU_2 are the bulk transfer coefficients. According to Anderson (1976), Male and Gray (1981) and Sand (1990); kU_1 and kU_2 ranges from 0.9 – 7.2 and 0 – 4.0 respectively for a measurement height at 1.0 m. Harstveit's (1984) optimal transfer coefficients which this study is based on is 3.2 and 2.3 respectively.

Latent heat transfer (*Qe*) is either heat released from water vapour condensing on the snow (positive) or evaporation from the snow surface (negative). Latent heat transfer is computed in much the same way as sensible heat:

$$Qe = 1/\text{ɔ} \cdot f(u) \cdot (e_{air} - e_{surf}) \quad (8)$$

where

e_{air} = vapour pressure in the air (mb),
e_{surf} = vapour pressure at the snow surface (mb)

ɔ is the psycrometric constant (mb/K) defined as

$$\text{ɔ} = \frac{c_p \cdot P}{\text{Ů} \cdot \text{ə}} \quad (9)$$

where

c_p = specific heat of air (kJ/kg/K),
P = air pressure (mb),

URN:NBN:no-6348

Ů = ratio of molecular weigth of water wapor to that of dry air (0.622),
ॐ = latent heat of sublimation (kJ/K).

During several occasions with high wind speeds (>5 m/s), the linear wind function applied in Eq. (7) and Eq. (8) gives turbulent heat fluxes that are too high. Different values for the coefficients kU_1 and kU_2 where tested, but the best approach was found when sensible heat was calculated using the following equation

$$Qh = \ln(kU_1' \cdot u + kU_2') \cdot (T_{air} - T_{surf}). \quad (10)$$

kU_1' and kU_2' were selected to make Eq. (10) correspond to Eqs. (7) and (8) at low wind speeds where these equations gave good results. At high wind speeds the logarithmic function prevents the estimated turbulent heat fluxes from becoming unreasonably large.

Snow Surface and Snow Pack Temperatures

Since the energy balance calculations depend on the snow surface temperature, which in turn depends upon energy balance calculations, several iterations at each time step are necessary in order to solve the surface energy balance exactly. A simplification to this approach is required if the original HBV philosophy of simple computational approach with minimal data is to be maintained. Snow surface temperature is the key to solving the energy balance, here, since the energy balance calculations in this model influence only snowmelt, it is set to 0°C instead of being found through iterations. The simplified treatment of the surface temperature will have only minor effects on the performance of the model. Fig. 3 shows the surface temperature during the ablation in 1998 found when solving the energy balance through iterations. Even before any runoff is observed; the surface energy balance results in 0°C temperatures at the surface. This simplification is not applicable at sub-freezing air temperatures when the energy balance becomes negative. At these occasions, the snow surface and snowpack cool and ablation ceases. Moreover, when the temperature in the snowpack is below freezing, melt water refreezes in the snow rather than causing runoff.

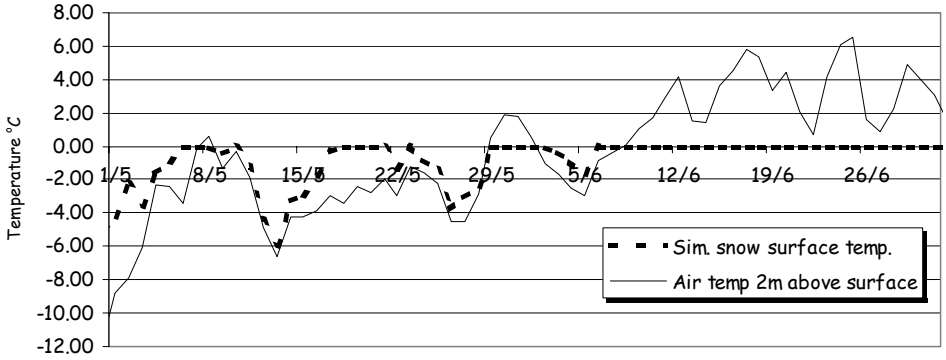

Figure 3 *Snow surface temperature found through exact solving of the surface energy balance and air temperature*

URN:NBN:no-6348

Snow surface temperature is also paramount to the calculation of snowpack cooling and again iteration is necessary if an exact solution is to be found. Here, the following equation based on snow pit observations of snow temperature, is suggested for the calculation of average snow pack temperature (T_{snow}).

$$T_{snow} = E_{refr} + T_n \tag{11}$$

E_{refr} is temperature raise due to energy released from the refreezing of melt water from the previous time step. T_n is the average of the air temperature over the previous n days where n is a function of the remaining snow depth expressed as snow water equivalent (SWE) in cm.

$$n = (SWE)^{3/4}, \tag{12}$$

where n is set to have a maximum of 15 days This approximation gave a fairly good fit to our data (Fig. 4) with a correlation coefficient of 0.77 between calculated and measured snow temperatures.

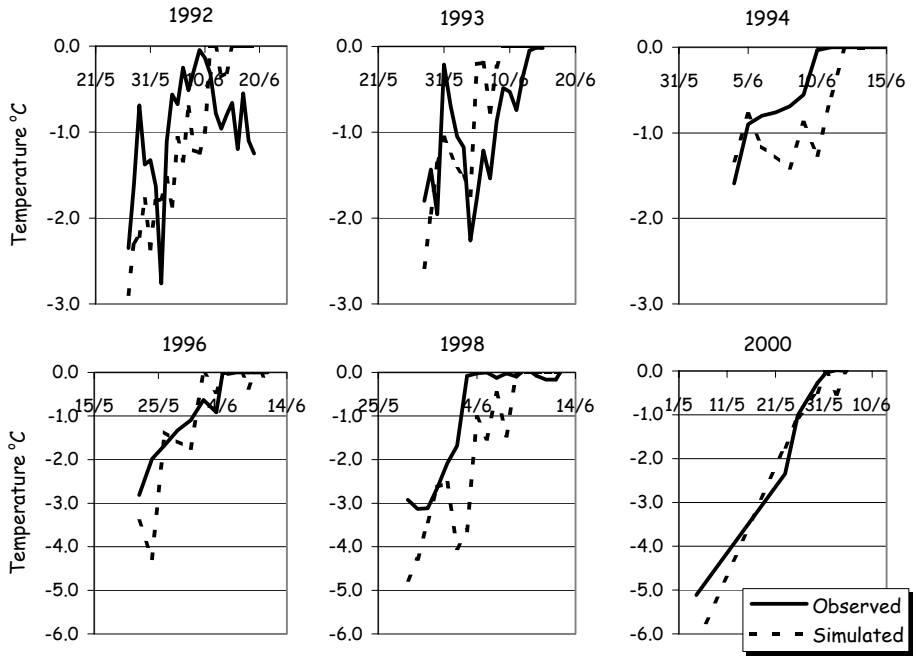

Figure 4 *Simulated average snow pack temperatures during the ablation compared with snowpack temperatures observed in snowpits. Initial snow depths (before snow melt) are noted for each year.*

T_{snow} is used to calculate the energy (Qi) necessary to heat the snow pack to isothermal condition at 0°C. As long as the temperature in the snow pack is below 0°C, any snowmelt at the surface will refreeze in the snow pack and no runoff occurs. This has a strong influence to the onset of the snowmelt runoff.

URN:NBN:no-6348

Snow Distribution

In most implementations of the HBV-model in Norway a distributed snow-routine is used to simulate the effect of an uneven or skew distribution of the snow at the defined elevation levels in the catchment (Killingtveit 1978; Killingtveit and Sælthun 1995). In this study, the effect of the skewed distribution is accounted for by reducing the snowmelt with a factor depending on snow-covered area.

$$SM = f_{\text{snow}} \cdot Qm / L_{\text{f}} \tag{13}$$

where

SM = snowmelt (kg/m^2),
f_{snow} = snow covered area (%),
Qm = energy available for snowmelt (W/m^2),
L_{f} = the latent heat of fusion (W/kg/day).

Snow covered area, f_{snow}, will be a function of initial snow distribution and snow storage depletion

$$f_{\text{snow}} = \beta - \frac{\beta}{\exp\left(\left(\frac{SWE_{\text{left}}}{\mu \cdot SWE_{\max}}\right)^{q}\right)},$$

$$\frac{SWE_{\text{left}}}{SWE_{\max}} \geq \delta \Rightarrow f_{\text{snow}} = \text{initial snow coverage} \tag{14}$$

where

SWE_{left} = snow water equivalent left at the time step,
$SWE_{\max}$ = maximum snow water equivalent during the previous winter,
β, δ, q = snow distribution skewness factors.

The values β, δ and q are found from the snow distribution in the catchment, and can be determined from snow survey data. Fig. 5 illustrates how they influence the depletion of the snow storage. The initial snow coverage determines the value β. In areas with smooth surfaces, such as on glaciers, or low snow redistribution by wind, such as in forests, the snow is more evenly distributed and it usually takes some time before the first snow free patches appear. The ŭ-value is the percentage of the total snow storage left when these patches appear and the depletion of the snow-covered area begins. q reflects the skewness in the distribution of the remaining snow. With $q = 0$ the snow is said to be evenly distributed. Snow distribution is usually more skewed at higher elevations and ŭ and q can be set differently for each elevation band or expressed as a function of elevation. In the case of a new snowfall during the ablation, a temporary new (redefined) $SWE_{\max}$ is used until this fresh snow has melted. The equation was tested against both data collected in May 2000 in the DeGeer Valley, Svalbard, and data collected on several Svalbard Glaciers by Winther *et al.* (1997). The DeGeer catchment has less than 10% glaciation and a relief ranging from 50 to 987 m.a.s.l.

URN:NBN:no-6348

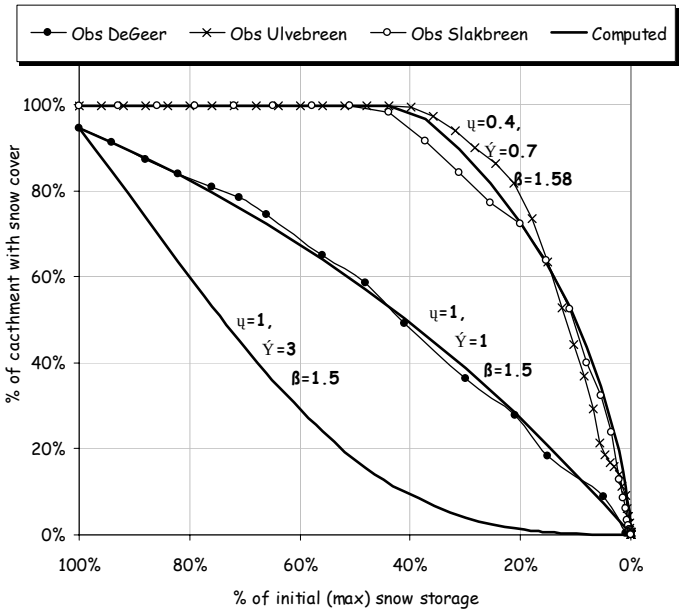

Figure 5 *Snow cover depletion curves (assuming even snowmelt) based on measured snow distribution in DeGeer Valley and two glaciers at Svalbard, compared to calculated depletion curves using Eq. (12)*

Snow surveys were carried out along 5 snow courses carefully selected to give representative snow distribution for the catchment. The snow distribution was calculated and assuming an even melt rate over the catchment the depletion curve will be as presented in Fig. 5. The computed depletion curve from Eq. (14), with β, ŭ and q values of 1.5, 1 and 1, respectively, has a high correlation (r = 0.99) with the observed data from DeGeer valley. From the snow distribution data collected by Winther *et al.* (1997) both at Slakbreen and Ulvebreen, representative values of β, ŭ and q were found for glaciers at Svalbard (Fig. 5). Since snow distribution data is only available for minor parts of Bayelva catchment, the β, ŭ and q –values for the entire catchment are found as weighted average of the values for the Svalbard glaciers and the DeGeer valley.

Glacial Melt

In the Arctic and in several Norwegian drainage catchments, glaciation can be substantial. In the Nordic HBV-model version (Sælthun 1996), glacial melt has been introduced accordingly. The glacier is described by its own elevation distribution. In the Nordic HBV-model, melt is calculated the same way as for the snow with an increased melt due to the higher albedo of exposed glacier ice. Glacial melt at an elevation level starts when the snow has completely melted. The glacier reservoir is defined as infinite, and the remaining snow at the end of the ablation is converted to ice the following year. The glacier definition is not changed in this model, however melt is calculated differently. The calculation of the energy balance is as for the snow surface with the exception of the albedo. The albedo for exposed ice is regarded as constant. According to Paterson (1994) it ranges from 0.15 for

URN:NBN:no-6348

dirty ice up to 0.51 for clean ice. A value between 0.35 and 0.45 is reasonable considering his descriptions. The timing and efficiency of the glacial melt is also changed. In reality, parts of the glacier ice are exposed long before all the snow at the particular elevation level has melted. This is accounted for by letting the percentage of the glacier with exposed ice surface or the glacial melt efficiency (f_{ice}), be a function of the snow cover depletion given by f_{snow}.

$$f_{ice} = 1 - f_{snow} \tag{15}$$

Snow is usually more evenly distributed on glacier ice due to a smooth surface, therefore the snow distribution skewness factor, q , is reduced for these areas. From the data from Ulvebreen and Slakbreen, the β, ŭ and q -values were found to be 1, 0.4 and 0.7, respectively. Fig. 6 illustrates how f_{ice} develops with the snow cover depletion and how it drops when a snowfall covers the previously exposed ice.

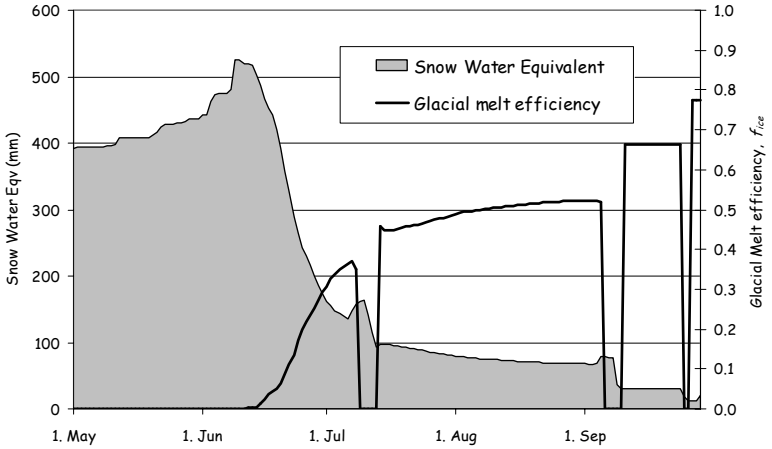

Figure 6 *Illustrated development of the glacial melt coefficient, f_{ice}.*

Results and Discussion

One of the main advantages with the energy balance based HBV-model (E-Bal HBV) is that it is more physically based than the TIM version of the HBV-model. The parameters controlling snowmelt, such as albedo of snow and ice and snow distribution, can be found through field investigations instead of calibration. The E-bal HBV thus needs less calibration than the original HBV-model. The general parameters controlling water retention in the model is the same as those found to be optimal in the original HBV-model (Bruland and Sand 1994). The model was tested not only against observed runoff for the periods 1974 to 1978 and 1989 to 1998, but was also compared with the performance of the original HBV-model. In addition, the Norwegian Polar Institute mass balance measurements at Austre Brøgger glacier are used to validate the glacial simulations.

URN:NBN:no-6348

R^2 values were generally higher for the energy balance simulations than for the original HBV-model except for two years during 1974–1978 (Table 1). In this period the energy balance simulation was only based on observations of cloudcover. Depending on the cloud type, solar radiation can be considerable even on days with complete cloudcover. On these occasions the simulated solar radiation component will be too low. Measuring solar radiation is fairly easy and with these data the E-bal model gives more reliable results than the original HBV-model. During the 1974–1978 and 1989–1992, the observed runoff data quality is poor due to a less accurate measurement technique and problems with the weir. This is also the case during the first days of ablation when the quality depends on whether and how well the weir is cleared of snow and ice and if manual control measurements are taken.

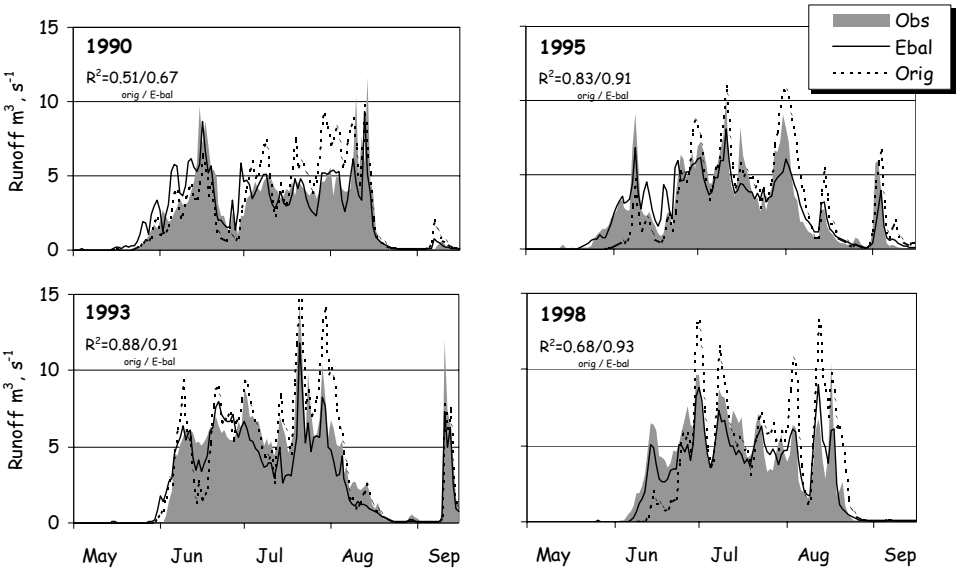

Figure 7 *Simulated runoff for the original and for the energy balance HBV-model with logarithmic wind profile, compared to observed runoff.*

In average over the years 1974 –1978 and 1989 –1998 for the period June – July the calculated short wave and long wave radiation contributed with 62.3 and -26.1 W/m^2/day respectively. Calculated sensible and latent heat contributed with 13.8 and 8.2 W/m^2/day respectively. The correlation coefficient between observed short-wave radiation in Ny-Ålesund and short-wave radiation calculated with Eq. (2) was 0.96 for the years 1992 to 1998.

URN:NBN:no-6348

Table 1 *R2 – values for the simulations with the original and two versions of the energy balance HBV-model (* The linear wind function causes an especially poor result in 1978. With this year excluded, R2 is 0.77)*

Year	Orig	E-bal Linear Wind	E-bal Log Wind	Year	Orig	E-bal Linear Wind	E-bal Log Wind	Year	Orig	E-bal Linear Wind	Log Wind
1974	0.82	0.81	0.76	1989	0.34	0.29	0.55	1994	0.76	0.75	0.81
1975	0.79	0.85	0.81	1990	0.51	0.61	0.67	1995	0.83	0.87	0.91
1976	0.62	0.76	0.74	1991	0.70	0.65	0.79	1996	0.79	0.84	0.87
1977	0.70	0.75	0.74	1992	0.82	0.88	0.89	1997	0.88	0.80	0.93
1978	0.76	0.30*	0.75	1993	0.88	0.91	0.91	1998	0.68	0.94	0.93
								Average	0.73	0.73*	

The improvement of the simulation of the snowmelt for the Bayelva catchment is especially evident during the ablation seasons of 1995 and 1998 (Fig. 7). Solar radiation was the main energy source for snowmelt but low air temperatures makes the original HBV model fail at the timing of the ablation. During the rest of the ablation seasons, the energy balance based snowmelt calculations also generally perform better. Furthermore, this seems to be the case for the glacial melt calculation too. In the years 1990, 1993, 1995 and 1998, the original HBV-model with the optimum calibrated parameters for all years, gives glacial ablation that is too high, while the E-Bal HBV-model performs satisfactorily (Fig. 7). The calculated glacial balance shows good correspondence with the observations in most years (Fig. 8). The differences between observed and simulated net balance can be explained both by the differences between calculated and observed winter accumulation and summer ablation.

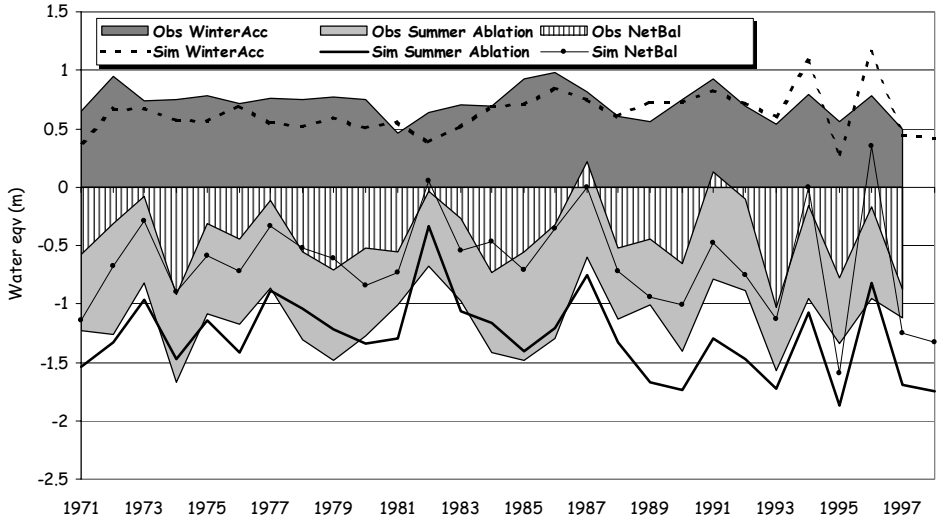

Figure 8 *Simulated and observed glacial mass balance.*

However, the observations of winter accumulation from 1993/1994 to 1995/1996 can be questioned. Rainfall events during the winter occur on rare occasions at Svalbard. At the 30th November 1993 the largest ever observed precipitation event

URN:NBN:no-6348

in Ny-Ålesund occurred when a rainfall of 57 mm was recorded at the meteorological station. The same was the case in the winter 1995 – 1996. At two occasions, the 3rd of December 1995 and 12th of March 1996, heavy rainfall was observed at days with positive air temperatures. These events resulted in conditions that made snow depth observations on the glaciers difficult. All the glacial observations were taken at the Austre Brøgger glacier. Though this amounts to approximately 50% of the glaciated area, it is not necessarily fully representative to entire glaciated area.

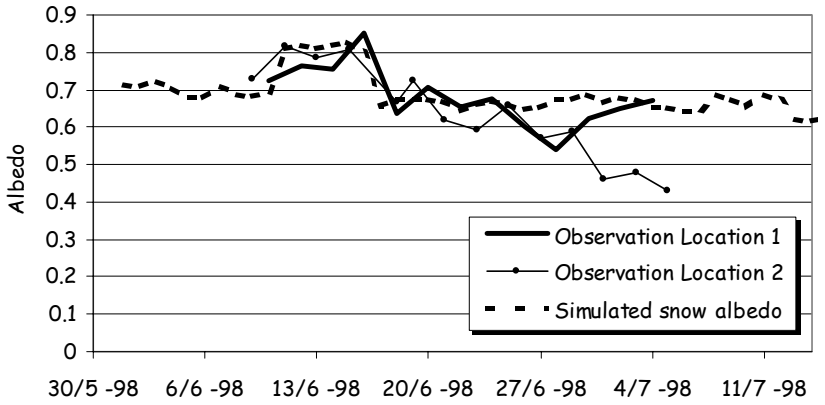

Figure 9 *Average of observed albedo values at two adjacent 100m2 large runoff plots (10 observation at each plot), compared to simulated albedo for snow during the ablation in 1998.*

Implementation of Eq. (10) improved the snowmelt and glacial balance calculations further and increased the average R^2-value from 0.73 to 0.80 (Table 1). Scaling effects and location of the wind measurements might explain the improved performance of this non-linear approach. As Fig. 2 shows, a large part of the catchment is located in between mountains and is thus less exposed to higher wind speeds than at Ny-Ålesund where observations are taken. This was evident on the 26th of June 1978 when very strong easterly winds produced a peak in snow melt, but since most of the catchment are leeward of these winds, the observed result were reduced significantly compared to the simulated result. The literature shows a large spectrum of values for the coefficients kU_1 and kU_2 in Eq. (7) (U.S. Army corps of Engineers 1956; Anderson 1976; Male and Gray (1981); Harstveit 1984; Sand 1990). Indeed, Sand (1990) found that the linear wind function gave poor results, concluding that the empirical wind function needs improvement. Albedo is a very important parameter in the energy balance calculations; Fig. 9 shows the albedo calculated by the model for the early summer of 1998 compared to observations. The deviations during late ablation at location 2 can be explained by exposed dark soil affecting the overlying snow albedo when the snow cover became shallow and translucent. Due to a generally shallow snow cover, an uneven snow distribution and strong winds, substantial amounts of dust from bare patches can be carried by wind. This dust has been found deposited at several layers in the snow leading to strong drops in the albedo when exposed.

URN:NBN:no-6348

Conclusions

The main objective of this study was to test if a simplified energy balance model could be implemented in the HBV-model and if this improves the simulations in an Arctic catchment where radiation plays an important role such as in the Bayelva catchment on Svalbard. The parameter values in the energy balance equations suggested by Harstveit (1984) is used and briefly presented in this study. Simulations presented here show that substituting the TIM with this energy balance model and including snow temperature calculations improves both the timing and progress of the snowmelt calculations. The simplified handling of surface temperature is acceptable during ablation but will not give an exact energy balance during the rest of the year.

Since the amount of the input data increases, the advantage of using an energy balance model instead of a TIM can be questioned. The temperature index ("degree-day factor") can easily be calibrated through runoff observation from the catchment during snowmelt events. A relevant question is then, if these improvements justify the need for additional data. Wind speed, air humidity and solar radiation are all simple parameters to measure. For this catchment the data needed to run the model are available from close by meteorological stations and the parameter values in the model can be determined based on several other studies in this area. The uncertainty connected to the representativity of the input data and parameters increases with the distance to the location of the observations. In this case the advantage of using the more data demanding E-bal model before a simple TIM may be reduced. Wind speed observations are, as shown in this study, least representative of large areas. The effect of the wind on catchment scale depends on the topography, but with knowledge of exposure and wind patterns this can be considered. In this study a sensible heat function with a non-linear wind dependency gave better results than a linear function.

Calibration of the parameters in the energy balance equations in order to fit observed catchment runoff data is not recommended, such calibrations should normally be based on observations on small plots or lysimeters as Harstveit and Sand did in their studies. In this paper the approach has been to use parameters in the energy balance equation previously calibrated in such specific studies, empirical parameters for snow distribution also found in specific studies and to test whether the results shows improved simulation of snowmelt runoff by implementing this into the HBV-model to compute runoff. The model results show clear improvement in most years, in particularly during the start of snowmelt and during some extreme snowmelt events where simulations with a TIM gave poorer results.

It would probably be possible to further optimise the E-bal HBV-model for this catchment by changing some of the parameters in the energy balance model. Before doing this it would be useful to do some testing of the sensitivity to changes of the parameters in the energy balance equation. This has not been an objective her, but is recommended for a further study.

URN:NBN:no-6348

Acknowledgements

The authors acknowledge the financial support of the Norwegian Research Council and the support of data and logistics in field from the Norwegian Polar Institute. The authors wish also to thank Annette Semadeni-Davies and Magne Wathne for their kind assistance and the anonymous reviewers as their comments significantly improved the quality of this paper. Last but not least the authors want to thank the company Kings Bay in Ny-Ålesund for the superb accommodation, their help and positive attitude.

References

Anderson, E. A. (1976) A Point Energy and Mass Balance Model of a Snowcover, NOOAA Technical Report, NWS-19, U.S. Department of Commerce, Washington D.C.

Ashton, G. D. (ed.) (1986) *River and Lake Ice Engineering,* Book Crafters Inc., Michigan, USA, pp. 216–233.

Bengtsson, L. (1976) Snowmelt estimates from Energy budget studies. *Nordic Hydrol., Vol. 7*, pp. 3–18.

Bengtsson, L. (1984) Modelling snowmelt induced runoff with short time resolution Proceedings of the Third International Conference on Urban Storm Drainage, Göteborg, Sweden, June 4–8, 1984 , pp. 305– 314.

Bengtsson, L. (1986) Snowmelt simulation models in relation to space and time. Modelling Snowmelt Induced Processes, Proceedings of the Budapest Symposium, July 1986, IAHS Publ. No. 155, 1986.

Bergström, S., and Forsman, A. (1973) Development of a conceptual deterministic rainfall-runoff model, *Nordic Hydrol., Vol. 16*, pp. 89–104.

Bergström, S. (1975) The development of a snow routine for the HBV-2 model, *Nordic Hydrol., Vol. 6,* pp. 73–92.

Bergström, S. (1976) Development and application of a conceptual runoff model for Scandinavian catchments, SMHI Reports Hydrology No.7, Norrköping Sweden.

Bergström, S. (1992) The HBV model – its structure and applications, SMHI Reports Hydrology No.4, Norrköping Sweden, 32 pp.

Bruland, O. and Maréchal, D. (1999) Energy- and Water Balance of Active Layer 1991–1994, Understanding Land Arctic Physical Properties 1996–1998, Project data report, SINTEF Report STF22 A98417.

Bruland, O., Maréchal, D., Sand, K., and Killingtveit, Å. (2001) Energy and water balance studies of a snow cover during snowmelt period at a high arctic site. Theoretical and Applied Climatology. LAPP/WINTEX Special Issue "Land-surface/atmosphere exchange in high-latitude landscapes", In press.

URN:NBN:no-6348

Bruland, O., and Sand, K. (1994) The Nordic HBV–model applied to an arctic watershed. Proceedings, Tenth international Northern Research Basins Symposium and Workshop, Spitsbergen, Norway, SINTEF Report STF22 A96415, pp. 594–608.

Brun, E., Martin, E., Simon, V., Gendre, C., and Coleou, C. (1989) An energy and mass model of snow cover suitable for operational avalanche forecasting, *Journal of Glaciology, Vol. 35,* No. 121, pp. 333–342.

Førland, E.J., Hansen-Bauer, I., and Nordli, P.Ø. (1997) Orographic precipitation at the glacier Austre Brøggerbre, DNMI-report 2/97 KLIMA, Norwegian Meteorological Institute, Oslo.

Førland, E. J., Hansen-Bauer, I., and Nordli, P.Ø. (1996) Climate statistics & longterm series of temperature and precipitation at Svalbard and Jan Mayen, DNMI Report No 21/97 Klima, Norwegian Meteorological Institute, Oslo, 73 pp.

Hagen, J.O., and Lefauconnier, B. (1995) Long-term glacier mass-balance investigations in Svalbard, 1950–1988, *Annals of Glaciology, Vol. 14,* pp. 102–106.

Hamlin, L., Pietroniro, A., Prowse, T., Soulis, R., and Kouwen, N. (1998) Application of indexed snowmelt algorithms in a northern wetland regime. *Hydrological Processes, Vol. 12*, pp. 1641–1657.

Hansen-Bauer, I., Førland, E.J., and Nordli, P.Ø. (1996) Measured and true precipitation at Svalbard, DNMI-report 31/96 KLIMA. Norwegian Meteorological Institute, Oslo, 44 pp.

Harstveit, K. (1984) Snowmelt modelling and energy exchange between the atmosphere and a melting snow cover. Scientific rep. no 4, Geophysical Institute, University of Bergen, 119 pp.

Hinzman, L. D., and Kane, D. L. (1991) Snow Hydrology of a headwater arctic basin-2. conceptual analysis and computer modelling. *Wat. Resour. Res., Vol. 27*, No. 6, pp. 1111–1121.

Jordan, R. (1991) A One-Dimensional Temperature Model For a Snow Cover: Technical documentation for SNTHERM.89. Available from NTIS (National Technical Information Service), Springfield , Virginia 22161.

Kane, D.L., Gieck, R.E., and Hinzman, L.D. (1997) Snowmelt modelling at Small Alaskan Arctic Watershed. *J. of Hydrol. Eng., Vol. 2*, No. 4, pp. 204–210

Killingtveit, Å. (1978) A new approach to snow accumulation modelling. Nordic hydrological conference and second Nordic IHP meeting. Hanasaari Cultural Centre July 31– august 3, 1978, Papers of sessions, Session 1a, pp. 1–12.

Killingtveit, Å., Petterson, L.E., and Sand, K. (1994) Water balance studies at Spitsbergen, Svalbard. Proceedings, Tenth international Northern Research Basins Symposium and Workshop, Spitsbergen, Norway, SINTEF Report STF22 A96415, pp. 77–94.

URN:NBN:no-6348

Killingtveit, Å. and Sælthun, N.R. (1995) Hydrology, Hydropower Development, Vol. 7. Norwegian University of Technology and Science, Divison of Hydraulic Engineering, Trondheim, 213 pp.

Lindström, G., Johansson, B., Persson, M., Gardelin, M. and Bergström, S. (1997) Development and test of the distributed HBV-96 hydrological model, *J. of Hydrol. Vol 201*(1–4), pp. 272–288

Liston, G., Winther, J.G., Bruland, O., Elvehøy, H., and Sand, K. (1999) Below-surface ice melt on the coastal Antarctic ice sheet, *Journal of Glaciology, Vol. 45*, No. 150, pp. 273–285.

Martin, E. (1996) The snow cover model CROCUS. Technical description ver 2.2. Available from Centre d'études de la neige, 1441 rue de la piscine, 38406 St Martin d'Hères, CEDEX.

Male, D.H. and Gray, D.M. (1981) Snow ablation and Runoff, *Handbook of Snow*. Ed. D.H. Male and D.M. Gray. Pergamon Press, New York, pp. 360–436.

McCay, D.C. (1970) Energy, Evaporation and Evapotranspiration, *Handbook of Principles of Hydrology*. Ed. D.M. Gray. Water Information Centre, Port Washingthon, N.Y. pp. 3.1–3.66.

Nash, J.E., and Suthcliffe, J.V. (1970) River flow Forecasting trough Conceptual Models, Part 1– a discussion of principles. *J. of Hydrol., Vol. 10*, No. 3.

Partridge, G.W., and Platt, C.M.R. (1976) *Radiative Processes in Meteorology and Climatology,* Elsevier Scientific Publishing Company, Amsterdam.

Paterson, W.S.B. (1994) *The Physics of Glaciers*. 3 rd ed. Elsevier Science Ltd. England.

Penman, H.L. (1948) Natural Evaporation from Bare Soil and Grass, Proc. Royal Society*,* London, Vol. A 193 , pp. 120–145.

Repp, K. (1979) Breerosjon, glaciohydrology og materialtransporti et høyartktisk miljø, Brøggerbreen, Vest Spitsbergen. Final Thesis, Geography, University of Oslo. (in Norwegian)

Swinbank, W.C. (1963) Longwave Radiation from Clear Skies. *Quarterly Journal of the Royal Meteorological Society*, No. 89, pp. 339–348.

Sælthun, N. R. (1996) The "Nordic" HBV Model. Description and documentation of the model version developed for the project Climate Change and Energy Production. NVE Publication 7. Norwegian Water Resources and Energy Administration, Oslo, 1996, 26 pp.

Sand, K. (1990) Modelling snowmelt runoff processes on temperate and arctic environments. Dr. Ing Thesis, IVB-report b-1990-1. Norwegian University of Technology and Science, Division of Hydraulic Engineering, Trondheim, 176 pp.

Tveit, J., and Killingtveit, Å. (1994) Snow surveys studies of water budget on Svalbard 1991–1994. Proceedings, Tenth international Northern Research

URN:NBN:no-6348

Basins Symposium and Workshop, Spitsbergen, Norway, SINTEF Report STF22 A96415, pp. 77–94.

U.S. Army corps of Engineers (1956) Snow Hydrology, Summary report of Snow Investigations, Corps of Engineers, North Pacific Division, Portland, Oregon, pp. 141–191 and plates.

Vehvilänen, B. (1992) Snowcover models in operational watershed forecasting, Publications of the Water and Environment Research Institute. National Board of Waters and Environment, Finland. No 11. 112 pp.

Winther, J.G., Bruland, O., Sand, K., Killingtveit, Å., and Maréchal, D. (1997) Snow accumulation distribution on Spitsbergen, Svalbard, in 1997, *Polar Research*, *Vol. 17*, No. 2, pp. 155–164.

URN:NBN:no-6348

URN:NBN:no-6348

Paper 3:
Glacial mass balance of Austre Brøggerbreen modelled with the HBV-model.
Polar Research, accepted for publishing June 2002.

URN:NBN:no-6348

GLACIAL MASS BALANCE OF AUSTRE BRØGGERBREEN MODELLED WITH THE HBV-MODEL

ODDBJØRN BRULAND & JON OVE HAGEN

Bruland, O. and J. O. Hagen (2002) Mass Balance of Austre Brøggerbreen modelled with the HBV-model. *Polar Research*, accepted for publishing June 2002.

An energy balance based HBV-model was calibrated to the runoff from Bayelva catchment at Svalbard, Spitsbergen. The model was used to simulate the glacier mass balance, and the results were compared to observations at Austre Brøggerbreen for the period 1971 to 1997. Even though the model was optimised to observed runoff from a catchment in which the glaciers constitutes 50% of the area, and not to the observation of glacier mass-balance, the model was able to reconstruct the trends and values of the mass balance found through observations. On average the simulation gave a negative net balance of 696 mm. The observed average is 442 mm. The simulated winter accumulation was in average for the same period 9% lower and the summer ablation 17% higher than the observed. The years 1994 to 1996 show deviations between simulated and observed winter accumulation up to 160%. This is probably due to extreme rainfall occasions during the winter leading to thick ice layers, which in turn gives difficult observation conditions and thereby questionable observation values. The higher simulated summer ablation might indicate that the glaciers in the catchment as a whole have a larger negative mass-balance than Austre Brøggerbreen. The simulations showed that the glacier mass-balance would be in equilibrium with a summer temperature 1.2 °C lower than the average over the last decades or with a 100% increase in the winter (snow) precipitation. These are higher values than former estimates. A combined change of temperature and precipitation showed a synergic effect and thereby less extreme values.

Oddbjørn Bruland, Norwegian Univ. Of Science and Tech., N-7491 Trondheim; Jon Ove Hagen University of Oslo, Dept. of Physical Geography PO Box 1042 Blindern 0316 Oslo, Norway

Introduction

In the future climate scenarios predicted by the global climate models (GCM), temperature and precipitation are the two parameters that commonly are estimated with some degree of reliability. Glacial retreat or growth depends strongly on changes in these but the response is generally very slow and the glaciers are often used as long-term climate indicators (Haeberli, 1995). Since 1969 the Norwegian Polar Institute has measured the mass balance of Austre Brøggerbreen close to Ny-Ålesund at Svalbard (Fig.1). With exception of two years, the record shows that the glacier have decreased every year at an average of 423 mm water equivalent averaged over the glacier surface (Hagen and Liestøl, 1990, Lefauconnier et.al. 1999). Lefauconnier and Hagen (1990) reconstructed the mass balance on Brøggerbreen since 1912 based on regression analysis with meteorological data and showed that the glacier has experienced a nearly constant negative mass balance since about 1920. They also showed that the negative balance was due to an increase in summer temperature during the period 1910-1920. Most of the glaciers had their maximum extension in the period 1880-1900, which was the termination of the "little ice age" in Svalbard. Since then the glaciers has

URN:NBN:no-6348

generally retreated, probably due to higher summer temperatures.

Basal melt at Austre Brøggerbreen is neglectable. The glacier is polythermal and the lowermost and thinnest part of the glacier is cold-based (Hagen and Sætrang , 1991). The runoff from the glacier is therefore entirely from surface melt during the summer and it should be possible to get good estimates of the glacier's mass balance through a precipitation-runoff model. If the model accurately reflects the observed mass balance, sensitivity analyses could reveal the effect of the summer temperature and winter precipitation. It could also be used to evaluate the effect of different climate change scenarios on the glaciers mass-balance.

In this study a variant of the "HBV-model" is applied. The HBV-model is by far the most commonly used precipitation-runoff model in Scandinavia, and is today considered the "standard" runoff forecasting model for hydropower utilities in Norway. It is also widely used in other countries (Bergström ,1992). The model has been calibrated and verified with runoff data from Bayelva, the outlet river for Austre and Vestre Brøggerbreen, for the years 1974 to 1978 and 1989 to 1997. It used meteorological input data from the Norwegian Meteorological Institute's (DNMI) observations in Ny-Ålesund for the period 1970 to 1997. The glacial mass balance calculations of the portion corresponding to Austre Brøggerbreen of the glacier in the HBV-model have been extracted from the model glacial calculations and compared to Norwegian Polar Institute's mass balance observations at Austre Brøggerbreen.

Site description and field measurements

Figure 1 Location of Ny-Ålesund, Bayelva Catchment and Brøgger breen

URN:NBN:no-6348

Hydrological and meteorological data have been collected over a number of years below the glacier in the Bayelva River catchment area near Ny-Ålesund, on Svalbard, 78° 55' N, 11° 56' (Fig. 1). Detailed measurements of snow processes in this catchment have been made since 1992 (see Bruland and Maréchal, 1999).

The catchment is 30.8 km^2 and the relief is ranging from 10 to 737 m.a.s.l with mean of 253 m.a.s.l. The catchment is 50% glaciated. The glacier Brøggerbreen, bounded by steep mountains along the watershed divide, cover most of the upper catchment area. Brøggerbreen is divided in Austre (Eastern) and Vestre (Western) Brøggerbreen where Austre alone constitutes to about 50% of the glaciated area.

The mean altitude of the glaciers is approximately equal to the mean altitude for the catchment. The lower catchment consists of moraines, riverbed, tundra with a uniform lichen cover with patches of Rock Sedge (carex rupestris) and Mountain avens (Dryas octopetala). There are no trees or tall shrubs to influence either snow distribution or melt.

DNMI have made meteorological observations in Ny-Ålesund since 1961. The mean annual precipitation (1961–1990) at their station is 385 mm/year (Førland et al., 1996). Repp (1979) made the first time series of discharge for Bayelva catchment over the period 1974 to 1978. In 1989, the Norwegian Water Resources Administration (NVE) constructed a weir in Bayelva and resumed the time series. Runoff normally starts in the first week of June and lasts until mid September. The average annual runoff from the catchment is 1020 mm. The large discrepancy between runoff and measured precipitation can be explained by glacial mass loss, precipitation gauge catch losses, and orographic induced precipitation gradients (Førland et al., 1997). A large portion of the precipitation falls as snow during high winds and the catch losses are high. Hansen-Bauer et al. (1996) suggests correction factors of 1.05–1.10 for liquid precipitation, 1.65–1.75 for solid precipitation (snow) and around 1.4 for sleet (or mixed precipitation). Killingtveit et al. (1994) found an increase in summer precipitation of 5–10% (of observed precipitation) for every 100 m increase in altitude. Based on snow surveys Tveit and Killingtveit (1994) assumed a corresponding winter (snow) gradient of 14%. Hagen and Liestøl (1990) found on the Austre Brøggerbreen, a fairly constant altitudinal increase of snow accumulation of 100 mm per 100 m; equivalent to a 25% increase per 100 m altitude. In a profile study, Førland et al. (1997) found that the total precipitation on Brøggerbreen during the 1994 and 1995 summer seasons, was 45% higher than recorded at the weather station in Ny-Ålesund. It was also found that precipitation in Ny-Ålesund was strongly dependent on the wind direction. Spillover and seeder/feeder effects probably cause high precipitation events on the glaciers during winds from the South and Southwest (Førland et al., 1997). They estimate an increase in precipitation with altitude of 20% per 100 m up to around 300 m. Thirty to 40% of the total catchment area is above this elevation, and both Førland et al. (1997) and Hagen and Lefauconnier (1995) point out that a linear gradient of 20 to 25% might give too high an estimate of precipitation in these uppermost areas.

Since 1992 snow conditions have been observed daily in several snowpits during the ablation period and snowmelt has been measured from three runoff plots, together with observations of albedo, solar radiation, temperature and relative humidity. The average snowmelt intensities were found to be 14 mm/day. Average air temperature and incoming solar radiation during the ablation periods (1992–1998) were 2.1°C and 230 W/m^2 respectively.

URN:NBN:no-6348

The threshold temperature for snowmelt was 0°C.

The snow accumulation on Austre Brøggerbreen is measured at the end of the winter, usually in the beginning of May, before snow melt. Snow survey consists of point measurements every 100 m along transects across the glacier at about every 50 m height interval. Any later snowfall is not included. The main components of summer ablation are the snowmelt and glacier melt. It is measured as changes in snow depth and surface level at stakes drilled into the ice at about 50 m altitude intervals along a central flow line.

Model Description

The HBV-Model is a conceptual precipitation-runoff model that uses precipitation, air temperature and potential evaporation data to compute snow accumulation, snow melt, actual evapotranspiration, soil moisture storage, groundwater and runoff from the catchment (Fig. 2). The model was developed in the early 1970s at the Swedish Meteorological and Hydrological Institute (SMHI) and has been documented in several reports and papers (Bergström and Forsman, 1973; Bergström, 1975, 1976; Lindström et al., 1997). In addition to catchment characteristics, several parameters describing orographic precipitation gradient, precipitation gauge catch loss corrections, temperature lapse rate, hydrograph characteristics and threshold temperatures for snow precipitation and melt have to be determined or calibrated.

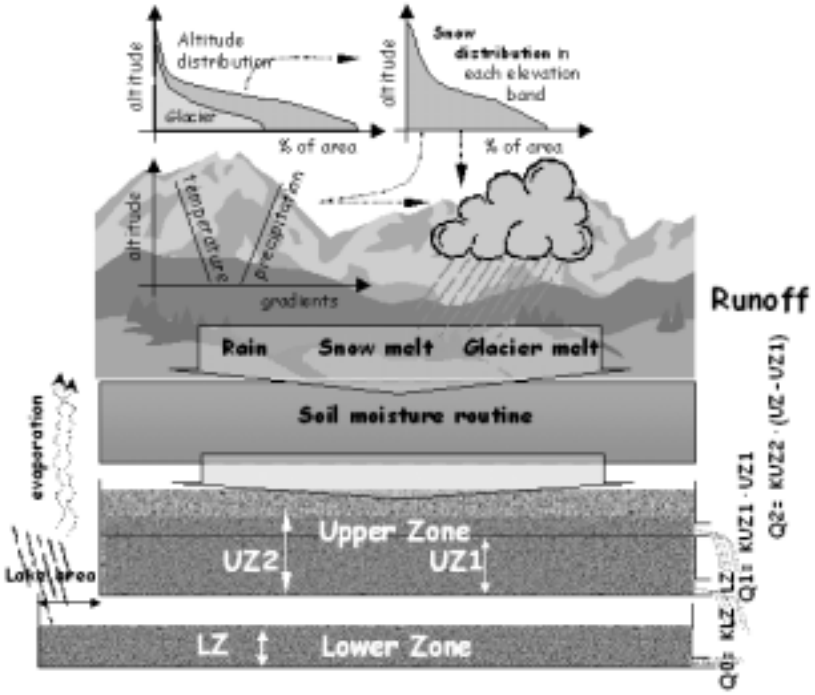

Figure 2 Main principles of the HBV-Model

URN:NBN:no-6348

In the original HBV-model, the snow and glacial melt is calculated using a Temperature Index Melt At higher latitudes and elevations, snow ablation gradually becomes the most important hydrological event of the year, and the importance of solar radiation to ablation grows; especially for the timing of runoff (Kane et al., 1997). (TIM) model. Although the simple TIM model used in the traditional HBV-model has been successfully tested and applied in several studies (Hinzman and Kane 1991; Sand, 1990; Hamlin et al., 1998; Vehvilänen, 1992), weaknesses have been evident in situations with low temperatures and high solar radiation (Bruland et al., 2001).

These situations are typical of Arctic and high mountain areas in springtime. Bruland and Killingtveit (2001) substituted the TIM with a surface energy balance calculation. They also introduced an improved description of snow distribution on the glacier and a simulation of snow temperatures. This revised version of the HBV-model, called E-bal HBV, is applied here.

Energy balance calculations

The energy balance model calculations in E-Bal HBV are based on the equations suggested by Harstveit (1984). Harstveit (1984) tested energy balance models and TIM against lysimeter snowmelt data collected during the period 1979 to 1982 from four locations close to Bergen, Norway. His study includes testing and optimization of parameters used in the energy balance models; these optimal values are used here. Bruland and Killingtveit (2001) and Bruland et al. (2001) have previously applied Harstveit's energy balance equations at Svalbard. Though the location and climate is completely different from Western Norway they concluded that the equations and Harstveit's empirical constants improved snowmelt calculations compared to simple temperature index calculations. The model is described by Eqs. (1) to (11). The energy balance for the snow-pack can be written:

$$Q_m + Q_i = Q_s + Q_l + Q_h + Q_e + Q_g + Q_r \quad (1)$$

where Qm is energy available for snow/ice melt, Qi is energy for internal heating and cooling of the snowpack, Qs and Ql is net short and long wave radiation, respectively, Qh and Qe is sensible and latent heat, respectively. During the ablation period in this area, with ground temperatures close to 0 °C and very low precipitation, ground heat flux (Qg) and heat from precipitation (Qr) can usually be neglected for practical computations. All energy terms in Eqs. (1) to (11) have the units W/m^2.

Net short-wave radiation (Incoming - Reflected) is computed as follows:

$$Qs = Qs_{in} - Qs_{out} \quad (2)$$

where Qs_{in} is extra-terrestrial radiation corrected for atmospheric effects and Qs_{out} is reflected shortwave radiation given by the albedo of the surface.

$$Qs_{in} = Q_{ex} \cdot (s_1 \cdot C_s + s_2 \cdot C_s^{1/2} + s_3) \quad (3)$$

where Q_{ex} is extra-terrestrial radiation given by the date and the latitude (W/m^2), Cs is (1 – Cloudiness) varying from 0 at complete cloud cover to 1 at clear skies, s_1, s_2 and s_3 are empirical constants found in studies in Dyrdalen, Western Norway, where $s_1 = -0.16$, $s_2 = 0.81$, $s_3 = 0.07$.

The calculation of the albedo in the model is based on Harstveit's (1984) regression models of albedo in Dyrdalen in Western Norway. He investigated correlation between observed albedo, age of snow (days), and cloudcover. His model Eq. (4) gave a multiple coefficient of correlation for his data of r = 0.77.

$$A = a_1 \cdot (1 - C_s) + a_2 \cdot \ln(t) + a_3 \quad (4)$$

where t is age of snow in days, a1, a2 and a3 is empirical constants found from studies in Dyrdalen, Western Norway, where $a_1 = -0.13$, $a_2 = -0.05$, $a_3 = 0.87$.

URN:NBN:no-6348

The cloudiness has large-scale variability and can be taken from the nearest meteorological observatory or calculated from observations of solar radiation. In our case we have available data of solar radiation back to 1980 and cloudiness observations back to 1970.

Several investigators have shown that estimates of incoming long wave radiation from the atmosphere can be made from surface air temperature and vapour pressure, or surface air temperature and a cloud factor (U.S. Army corps of Engineers, 1956; Partridge and Platt, 1976; Swinbank, 1963; Male and Gray, 1981; Bengtsson, 1976; Ashton, 1986; Harstveit, 1984). In this model the empirical formula suggested and tested by Harstveit (1984) is used (Eq. 5). His tests over 150 months of observation from Bergen, Western Norway, gave a correlation coefficient of 0.95. The equation was in good agreement with Partridge and Platt's model during cloudy conditions, and Swinbank's model during clear sky conditions.

$$Ql_{in} = l_1 \cdot \mathring{u} \cdot T_{air}^4 + l_2 \cdot C_s + l_3 \qquad (5)$$

where $\mathring{u}$ is Stefan-Boltzmann constant, T_{air} is air temperature (K), l1, l2 and l3 is empirical constants based on measurements in Bergen where $l_1 = 1.02$, $l_2 = 71$ and $l_3 = -92$. Outgoing long-wave radiation (Ql_{out}) is determined by Stefan Bolzmann's law;

$$Ql_{out} = \mathring{u} \cdot T_{surf}^4 \qquad (6)$$

where T_{surf} is surface temperature (K). Sensible heat transfer (Qh) depends on the temperature difference between the air and snow surface, and wind speed. Usually empirical formulas are used to compute Qh, mostly of the form:

$$Qh = f(u) \cdot (T_{air} - T_{surf}) \qquad (7)$$

where u is wind speed (m/s) and f(u) is a function of the wind speed. Here an empirical model based on Harstveit's (1984) studies in Norway is used:

$$Qh = (kU_1 \cdot u + kU_2) \cdot (T_{air} - T_{surf}) \qquad (8)$$

where w1 = 3.1 and w2 = 2.3.

Latent heat transfer (Qe) is either heat released from water vapour condensing on the snow (positive) or evaporation from the snow surface (negative). Latent heat transfer is computed in much the same way as sensible heat:

$$Qe = f(u) \cdot (e_{air} - e_{surf}) \qquad (9)$$

where u is wind speed (m/s), eair and esurf is vapour pressure in the air and at the snow surface (mb), respectively.

Also based on Harstveit's studies the following empirical model is used:

$$Qe = w_0 \cdot (w_1 \cdot u + w_2) \cdot (e_{air} - e_{surf}) \qquad (10)$$

where $w_0 = 1.7$ and w_1 and w_2 as in Eq. (8). During several occasions with high wind speeds (>5 m/s) simulated runoff were too high. At these wind speeds the linear wind function applied in Eq. (8) and Eq. (10) yielded too high turbulent heat fluxes. Different values for the coefficients w_1 and w_2 where tested, but the best approach was found when sensible heat was calculated using the following equation;

$$Qh = \ln(w_1' \cdot u + w_2') \cdot (T_{air} - T_{surf}) \qquad (11)$$

w_1' and w_2' were selected to make Eq. (11) correspond to Eqs. (8) and (10) at low wind speeds where these gave good results. At high wind speeds the logarithmic function prevents the estimated turbulent heat fluxes from becoming unreasonably large. The latent heat fluxes are so small that replacing the linear wind function with the logarithmic function did not have a significant influence on the simulations.

URN:NBN:no-6348

Since the energy balance calculations depend on the snow surface temperature, which in turn depends upon energy balance calculations, several iterations at each time step are necessary in order to balance the surface energy terms exactly. A simplification to this approach is required if the original HBV philosophy of simple computational approach with minimal data is to be maintained. Snow surface temperature is the key to solving the energy balance. Since the energy balance calculations in this model is most important during the ablation period, the surface temperature is set to 0 °C instead of being found through iterations. The simplified treatment of the surface temperature will have only minor effects on the performance of the model. This simplification is not applicable at sub-freezing air temperatures when the energy balance becomes negative. At these occasions, the snow surface and snowpack cool and ablation ceases. Moreover, when the temperature in the snowpack is below freezing, melt water refreezes in the snow rather than causing runoff.

Snow surface temperature is also paramount to the calculation of snowpack cooling and again iteration is necessary. Here, a simplified snow temperature calculation is suggested. The following equation was found to give snow temperatures (T_{snow}) with a fairly good fit to snow temperatures measured in snow pits (Fig. 3). The correlation coefficient was 0.77 between calculated and measured average snow temperatures.

$$T_{snow} = E_{refr} + T_n \quad (12)$$

E_{refr} is temperature increase due to energy released from refreezing of melt water from the previous time step. The equation is based on the average air temperature (T_n) over the previous n days. As snow is a good insulator the average temperature of a thick snowpack changes slower than for shallow snow pack and n is a function of the snow depth expressed as the remaining snow water equivalent (SWE) in cm at the time step. n is set to have a maximum of 15 days

$$n = (\mathrm{SWE})^{3/4}, \quad (13)$$

T_{snow} is used to calculate the energy necessary to heat the snow pack to isothermal condition at 0 °C. As long as the temperature in the snow pack is below 0 °C, any snowmelt at the surface will refreeze in the snow pack and no runoff occurs. This has a strong influence to the onset of the snowmelt runoff.

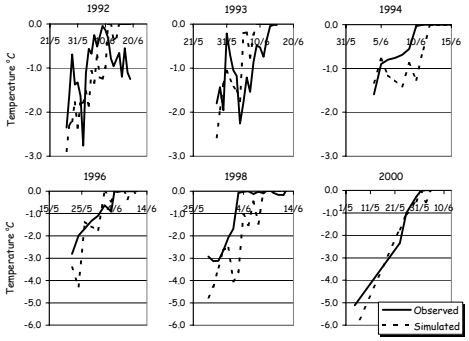

Figure 3 Mean measured and simulated Snow profile temperatures

Snow distribution

In most implementations of the HBV-model a distributed snow-routine is used to simulate the effect of an uneven or skew distribution of the snow at the defined elevation levels in the catchment (Killingtveit, 1978; Killingtveit and Sælthun, 1995). In this study, the effect of the skewed distribution is accounted for by reducing the snowmelt with a factor depending on snow-covered area.

$$SM = f_{snow} \cdot Q_m / L_f \quad (14)$$

Where SM is snowmelt (kg/m2), f_{snow} is snow covered area (%), Qm energy available for snowmelt (W/m2) and L_f is the latent heat of fusion (W/kg).

URN:NBN:no-6348

Snow covered area, f_{snow}, will be a function of initial snow distribution and snow storage depletion

$$f_{snow} = \beta - \frac{\beta}{\exp\left(\eta \cdot \left(\frac{SWE_{left}}{\delta \cdot SWE_{\max}}\right)^{\omega}\right)}, \quad (15)$$

$$\frac{SWE_{left}}{SWE_{\max}} \geq \delta \;\heartsuit\; f_{snow} = \frac{initial}{snow\,coverage}$$

where SWE_{left} is snow water equivalent left at the time step, SWE_{max} is maximum snow water equivalent during the previous winter. ß, ŭ and ą is snow distribution skewness factors.

The values ß, ŭ and ą are found from the snow distribution in the catchment, and can be determined from snow survey data. Figure 4 illustrates how they influence the depletion of the snow storage. ß is the initial snow coverage ranging from zero for no snow cover to 1.5 for a complete snow cover. In areas with smooth surfaces, such as on glaciers, or low redistribution, such as in forests, the snow is more evenly distributed and it usually takes some time before the first snow free patches appear. The ŭ-value is the fraction of the total snow storage left when these patches appear and the depletion of the snow-covered area begins. ą reflects the skewness in the distribution of the remaining snow. With ą = 0 the snow is said to be evenly distributed. Snow distribution is usually more skewed at higher elevations and ŭ and ą can be set differently for each elevation band or expressed as a function of elevation. In the case of a new snowfall during the ablation season, a temporary new (redefined) SWE_{max} is used until this fresh snow has melted.

The equation was tested against both data collected in May 2000 in the DeGeer Valley, Svalbard, and data collected on several Svalbard Glaciers by Winther et al.(1997).

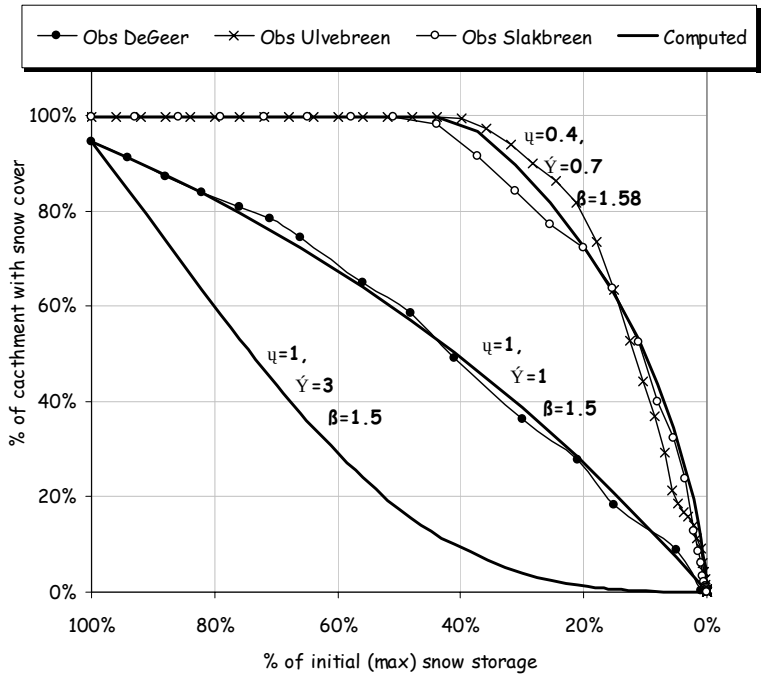

Figure 4 Observed and simulated Snow cover depletion at three different locations

URN:NBN:no-6348

The DeGeer catchment has a relief ranging from 50 to 987 m.a.s.l. Snow surveys were carried out along 5 carefully selected snow courses and the snow distribution was calculated. Assuming an even melt rate over the catchment the depletion curve will be as presented in Fig. 4. The computed depletion curve from Eq. (15), with ϐ, ŭ and ϙ values of 1.5, 1 and 1, respectively, has a high correlation (r = 0.99) with the observed data. From the snow distribution data collected at Slakbreen and Ulvebreen, representative values of ϐ, ŭ and ϙ were found for Svalbard glaciers (Fig. 4)

Glacial melt

In the Arctic and in several Norwegian drainage catchments, glaciation can be substantial. In the Nordic HBV-model version (Sælthun, 1996) glacial ice melt has been introduced accordingly. The glacier is described by its own elevation distribution. In the Nordic HBV-model, melt is calculated the same way as for the snow with an increased rate due to the lower albedo of exposed glacier ice. Glacial ice melt at an elevation level starts when the snow has completely melted. The ice thickness is assumed infinite, and the remaining snow at the end of the ablation is converted to ice the following year. The albedo for exposed ice is assumed constant. According to Paterson (1994) it ranges from 0.15 for dirty ice up to 0.51 for clean ice. 0.35 to 0.45 is a reasonable range of ice albedo values in this application. The timing and rate of the glacial melt is also changed. At any elevation band the ice surface can be exposed long before all the snow at that elevation level has melted. This is accounted for by letting the percentage of the glacier with exposed ice surface (f_{ice}) and thereby the glacial melt rate, be a function of the snow cover depletion given by f_{snow}.

$$f_{ice} = 1 - f_{snow} \quad (16)$$

Snow is usually more evenly distributed on glacier ice due to its smooth surface and the snow distribution skewness factor, ϙ, is reduced for these areas. For Ulvebreen and Slakbreen, the b, ŭ and ϙ -values were found to be 1, 0.4 and 0.7, respectively. Figure 5 illustrates how f_{ice} develops with the snow cover depletion and how it drops when a snowfall covers the previously exposed ice.

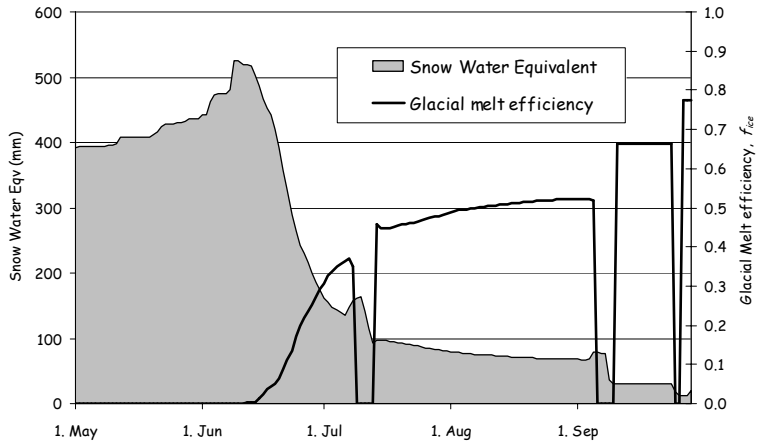

Figure 5 Snow and glacier ice ablation

URN:NBN:no-6348

Results and discussion

The model calculates the runoff from the entire catchment and is primarily calibrated to get the best fit to the runoff measurements in Bayelva. A selection of graphs presented in Fig. 6 and the R^2 – values presented in Table 1, illustrates the accuracy of the simulation.

Table 1 Godness of fit between simulated and observed runoff (R^2) for all years with observed runoff.

Year	R^2	Year	R^2	Year	
	0.76	1989	0.55	1994	0.81
1975	0.81	1990	0.67	1995	0.91
1976	0.74	1991	0.79	1996	0.87
1977	0.74	1992	0.89	1997	0.93
1978	0.75	1993	0.91	1998	0.93

The Nash efficiency criterion, R^2, (Nash and Suthcliffe, 1970) indicates the model efficiency, or the agreement between the recorded and simulated hydrograph. Compared to the original HBV-model, the modified model gave a significantly better fit to observed runoff, especially at the onset of the snowmelt. The glacial mass balance calculations were also improved.

The snow accumulation on the glaciers is controlled by the correction factors for liquid and solid precipitation, the increase of precipitation with altitude, temperature lapse rate and the threshold value for solid precipitation. The values found optimal are consistent to those suggested in the literature (Table 2).

The correction of precipitation in the model is a combination of catch loss corrections and an increment due to orographic rise (altitude correction). When using a value in the range suggested by Hansen-Bauer et al. (1996) for correction of solid precipitation, changing the altitude correction within the range from 10% – 20% did not significantly change the average R2-value.

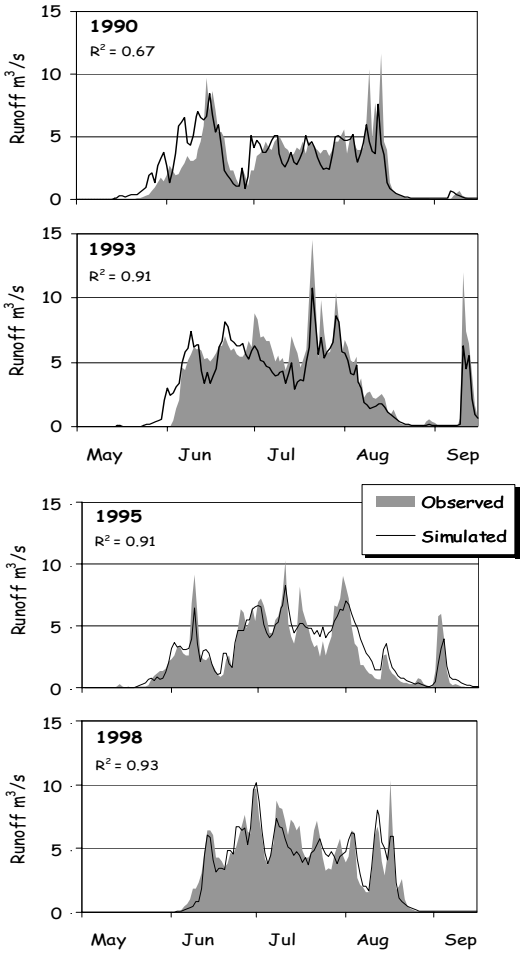

Figure 6 Simulated and observed runoff for four selected years

The large span of applicable values can be explained by the importance of the cyclonic pattern. Førland et al. (1997) found this very important to the precipitation distribution and it changes from year to year and probably also from summer to winter. At one station, 202 m.a.s.l., at the glacier they found that the precipitation was increased by 33% in 1994

URN:NBN:no-6348

and 78% in 1995, compared to measurement in Ny-Ålesund. Tests in this study show that a high precipitation correction gives better results during the early years relative to measurements of snow accumulation on the glacier. From the late eighties this trend seems to change and a lower correction is better. Here a value of 14% is used. The altitude correction suggested by Hagen and Lefauconnier (1995) is based on measured precipitation (not corrected for catch loss) and is therefore higher than values used here.

Table 2 Optimal parameter values used in the model compared to values found in literature.

Parameter	Optimal value	Values from literature
Precipitation corrections - Liquid - Solid	1.15 1.65	1.05 - 1.10 1.65 – 1.75
Precipitation increase with altitude	14 % pr 100 m	14 – 25 % pr 100 m
Threshold temperature rain/snow	1 ^{o}C	1 ^{o}C
Temperature lapse rate	- 0.65 ^{o}C pr 100 m	-0.6 – 1.0 ^{o}C pr 100 m

The average winter accumulation in the period 1971 to 1998 is 698 mm water equivalent. For the same period the average of the modelled winter accumulation is 634 mm or 9% lower. The years 1994 to 1996 stand out from the other (Fig. 7). In 1994 and 1996 the modelled winter accumulation are 37% and 48% higher than observed at the glacier, respectively. This is probably due to heavy rainfalls in November the previous years. On 30th November 1993 the largest ever observed precipitation event in Ny-Ålesund occurred with 57 mm recorded at the meteorological station. The average temperature was 3.3 °C. Temperatures the previous days and the following days were down to – 20°C. This caused the creation of a thick and solid ice layer over most of the Brøgger peninsula. It was observed in snowpits at lower altitudes in May the following year as an up to 20 cm thick solid ice layer. A tick ice layer can not be penetrated by normal snow sounding and it could easily be mistaken for the surface from previous year. 86% of the observed precipitation this winter fell before this date and due to the ice layer, a large portion of this is probably not included in the observations. A similar event occurred in the winter 1995 – 1996. On two occasions, 3rd of December 1995 and 12th of March 1996, heavy rainfall was observed at days with positive air temperatures. Also in May 1996 a thick ice layer was observed in the snowpits. In contrast 1995, the year in between these years, shows the opposite case. The observed accumulation is 20% lower than the average accumulation while the observed precipitation and simulated accumulation is 51% and 58% lower than average, respectively. Snow sounding above the equilibrium line is difficult because it can be hard to distinguish between snow - firn interface. With abnormally shallow snow depths, even an experienced observer may believe that the first hard layer encountered formed during the winter and not observed as last year's surface. He sounding could be made more forcibly and would penetrate into last year's snow stopping at the solid ice layer in the 1993-1994 snow pack. Hence, a larger snow accumulation would be estimated. This effort shows how the model could be used to detect years where the observations are questionable.

URN:NBN:no-6348

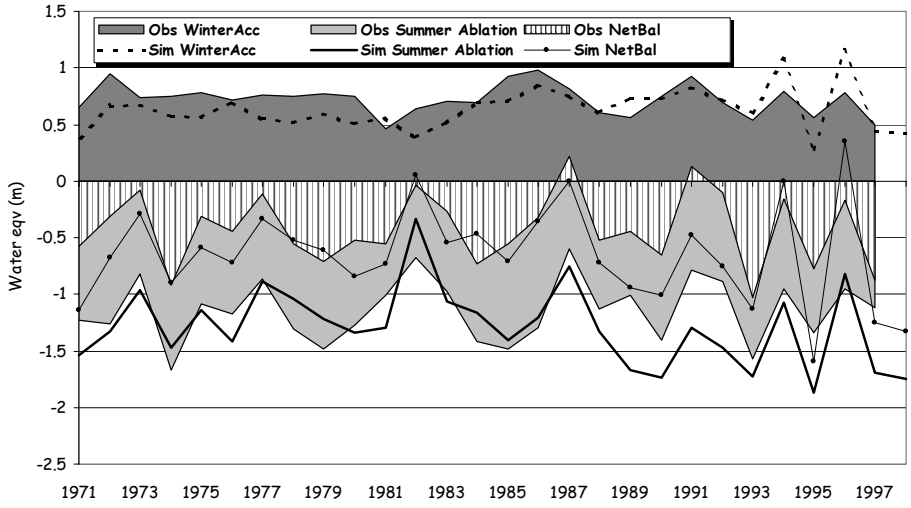

Figure 7 Observed and simulated summer ablation, winter accumulation and net balance of Austre Brøggerbre

The snowmelt dominates the spring flood. As the snow disappears during June and July the glacial melt gradually becomes the dominant component of the runoff. Albedo, threshold temperature for snow and ice melt, temperature lapse rate, snow distribution and the parameters with influence on the effect of wind, controls the snow and glacier melt. Albedo is a very important parameter in the energy balance calculations (Fig. 8). Due to a generally shallow snow cover, an uneven snow distribution and strong winds, substantial amounts of dust from bare patches can be carried long distances by wind and deposited at snow surfaces far away from the origin. In snow pits dust has been observed at several layers in the snow. When exposed they lead to strong drops in the albedo, which the model can not account for. At the higher elevations on the glacier these effects are reduced. The deviations seen at Fig.8 during the late ablation at location 2 can be explained by another effect the model does not account for. When the snow cover become shallow and translucent, and as the observations in Fig. 8 is from locations on the tundra below the glacier, the underlying dark soil is reducing the albedo. At the glacier this effect is substantially reduced as the base is ice with higher albedo than soil.

The average observed summer ablation in the period 1971 to 1998 is 1140 mm water equivalent. The model calculates snowmelt and glacial melt separately, the sum of these at Austre Brøggerbreen is compared to the observed summer ablation. The modelled average of the sum over the years 1971 to 1998 is 1330 mm water equivalent or 17% higher than the observed summer ablation. Simulated net balance was in average for the period 696 mm while the observed was 442 mm. As mentioned the model is not calibrated against the glacier mass-balance but to the runoff from the entire catchment. This includes the runoff from both Austre and Vestre Brøggerbreen. Summer ablation and winter accumulation can vary over the area. The mean altitude of Austre Brøggerbreen is approximately 100 m higher than the mean of Vestre Brøggerbreen and the exposition and

URN:NBN:no-6348

surroundings is different. By modelling the Austre Brøggerbreen explicit the parameters could be further calibrated to optimise the mass balance calculations. Førland et al. (1997) found surprisingly high precipitation in the upper areas of the glaciers, concluding that spillover and "seeder" and "feeder" effects was the explanation and not a generally high precipitation gradient. This effect and also snowdrift from the surroundings will accumulate more snow in the upper areas than the model with a linear precipitation gradient of 14%. Higher accumulation in the uppermost areas of the glacier would not effect the runoff calculation since these areas rarely are free of snow in the model. The albedo and thereby the melt rate would be unchanged. The winter accumulation would however be improved. The map, from which the hypsographic curve of the glaciers is found, is old and the surface level and the extent of the glaciers has changed since this map was created. With a lower glacier surface higher winter accumulation would probably be necessary not to change the timing of the ice melt and simulated runoff. In turn this would reduce the summer ablation but not necessarily the total runoff. This could be tested in a further work.

Since the late 1960's, when mass balance observations began Svalbard glaciers have generally retreated. A higher average summer air temperature, less precipitation or a combination of these in the period since the little ice age that culminated just before year 1900, might be the explanation. By manipulating the input data to the model these possible explanations can be tested. Looking at temperature alone, simulations indicate that the summer temperature has to be 1.2 to 1.3 °C cooler on average to maintain Austre Brøggerbreen in balance with the climate for the years 1971 - 1998. The same result would be achieved by a 100% increase of the snow precipitation. These are substantial changes probably only possible in a completely different climatic regime than we have today. A combination of lower air temperatures and more precipitation would to some extent give a synergistic effect since more precipitation then will fall as snow. With a 50% increase of the precipitation the glaciers would be in balance with an only 0.3 °C lower summer temperature. Radiation, cloudiness, relative humidity, wind speed and number of days with precipitation have not been changed. It is likely that increased precipitation would not only be induced by increased intensity, but also by an increased number of precipitation events. This would suggest more clouds, less radiation and higher relative humidity. For example, reducing the incoming short wave radiation by 10% by increasing the cloudiness, but keeping both temperature and precipitation unchanged, the ablation was reduced in average by only 1.5%.

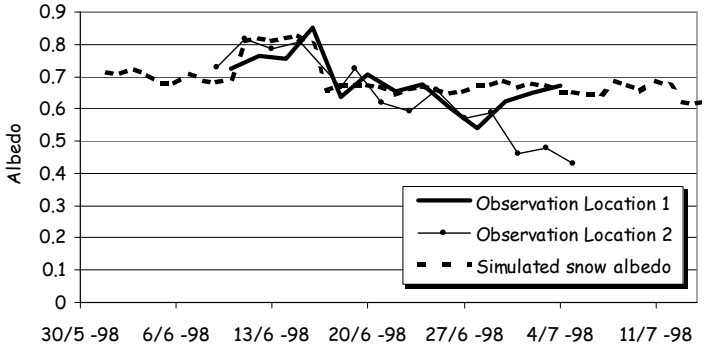

Figure 8 Simulated and albedo observed at two locations in lower parts of Bayelva catchment.

URN:NBN:no-6348

Conclusions

Based on the available meteorological input data from Ny-Ålesund the HBV-energy balance model could satisfactory reproduce the observed glacier mass balance at Austre Brøggerbreen glacier. The value of the parameters controlling snow accumulation and snowmelt were found through calibration and they were consistent with values found in the literature. In average over the period the simulation gave a negative net balance of 696 mm. The observation gives an average of 442 mm. The simulated winter accumulation was in average for the same period 9% lower and the summer ablation 17% higher than the observed. These differences could be reduced if calibration of the mass balance calculation was given higher priority than calibration of the runoff calculation. Higher accumulation rate than simulated in the upper areas of the glaciers is also likely and this would improve the winter accumulation calculation. Further would more up to date maps probably improve the calculations. The glacier surface and extent has changed since the map was created. A lower altitude of the glacier would require higher winter accumulation, which in turn would reduce the summer ablation.

The years with significant deviation between the modelled and observed results can probably be explained by thick ice layers in the snow pack caused by rain events during the winter. These layers disturb the observations perhaps causing significant errors. Changes in an order of -1 to -1.5 °C of the mean summer temperature or 100% increase of the winter (snow) precipitation is necessary for Austre Brøggerbreen to be in balance with the local climate. A combined change in temperature and precipitation such as -0.3 °C and 50% increased precipitation induce a synergistic effect and would also achieve glacier balance.

Acknowledgement

The authors acknowledge the financial support of the Norwegian Research Council, the Meteorological data supplied by the Norwegian Meteorological Institute and the Glacial mass-balance data and the radiation data supplied by the Norwegian Polar Institute. Last but not least the authors want to thank Kings Bay in Ny-Ålesund for the superb accommodation, their help and positive attitude.

URN:NBN:no-6348

References

Ashton, G. D. (ed.) 1986: *River and Lake Ice Engineering.* Book Crafters Inc., Michigan, USA. pp. 216–233.

Bengtsson, L. 1976: Snowmelt estimates from Energy budget studies. *Nordic Hydrology.* Vol. 7 , pp. 3–18.

Bergström, S. & Forsman, A. 1973: Development of a conceptual deterministic rainfall-runoff model. *Nordic Hydrology. Vol 16 , pp 89-104.*

Bergström, S. 1975: The development of a snow routine for the HBV-2 model. *Nordic Hydrology. Vol 6 , pp 73-92.*

Bergström, S. 1976: *Development and application of a conceptual runoff model for Scandinavian catchments*. SMHI Rep. Hydrology No.7. Norrköping Sweden.

Bergström, S. 1992: *The HBV model – its structure and applications*. SMHI Rep. Hydrology No.4. Sweden, pp 32.

Bruland, O. & Killingtveit, Å. 2001: An energy balance based HBV- model applied in an arctic watershed at Svalbard, Spitsbergen. Submitted to Nordic Hydrology feb 2001.

Bruland, O., Maréchal, D., Sand, K., Killingtveit, Å. 2001: Energy and water balance studies of a snow cover during snowmelt period at a high arctic site. Theoretical and Applied Climatology. LAPP/WINTEX Special Issue "Land-surface/atmosphere exchange in high-latitude landscapes". In press.

Bruland, O. & Maréchal, D. 1999: Energy- and Water Balance of Active Layer 1991-1994, Understanding Land Arctic Physical Properties 1996-1998. SINTEF Report STF22 A98417.

Førland, E.J., Hansen-Bauer, I., Nordli, P.Ø. 1997: Orographic precipitation at the glacier Austre Brøggerbre. DNMI-report 2/97 KLIMA. Norwegian Meteorological Institute, Oslo.

Haeberli,W. & Hoelzle, M. 1995: Application of inventory data for estimating characteristics of and regional climate-change effects on mountain glaciers: a pilot study with the European Alps. *Annals of Glaciology. Vol 21, pp 206-212.*

Hagen, J.O. & Liestøl, O. 1990: Long term glacier mass balance investigations in Svalbard 1950-1988. *Annals of Glaciology*, 14, 102-106.

Hagen, J.O. & Sætrang, A. 1991: Radio-echo soundings of sub-polar glaciers with low-frequency radar. *Polar Research* 9(1), 99-107.

Hamlin, L., Pietroniro, A., Prowse, T., Soulis, R., Kouwen, N. 1998: Application of indexed snowmelt algorithms in a northern wetland regime. *Hydrological Processes,* Vol. 12: 1641–1657.

Hansen-Bauer, I., Førland, E.J., Nordli, P.Ø. 1996: *Measured and true precipitation at Svalbard*. DNMI-report 31/96 KLIMA. Norwegian Meteorological Institute, Oslo, pp 44.

Harstveit, K. 1984: Snowmelt modelling and energy exchange between the atmosphere and a melting snow cover. Scientific report no 4, Geophysical Institute, University of Bergen. 119 pp.

Hinzman, L. D. & Kane, D. L. 1991: Snow Hydrology of a headwater arctic basin-2. conceptual analysis and computer modelling. *Water Resources Research,* Vol. 27, No 6, pp. 1111–1121.

Hisdal, V. 1993: *Svalbards nature og historie*, Polar håndbok nr 11. Norsk Polarinstitutt, Oslo

Kane, D.L., Gieck, R.E., Hinzman, L.D. 1997: Snowmelt modelling at Small Alaskan Arctic Watershed. *Journal of Hydrologic Engineering,* Vol. 2, No. 4, October 1997, pp. 204–210

Killingtveit, Å. 1978: A new approach to snow accumulation modelling. Nordic hydrological conference and second Nordic IHP meeting. Hanasaari

URN:NBN:no-6348

Cultural Centre July 31– august 3, 1978. Session 1a, pp. 1–12.

Killingtveit, Å., Petterson, L.E., Sand, K. 1994: Water balance studies at Spitsbergen, Svalbard. Proceedings, Tenth international Northern Research Basins Symposium and Workshop, Spitsbergen, Norway, SINTEF Report STF22 A96415, pp. 77-94.

Killingtveit, Å. & Sælthun, N.R. 1995: *Hydrology.* Hydropower Development, Vol. 7. Norwegian University of Technology and Science. Divison of Hydraulic Eng. Trondheim. 213 pp.

Lefauconnier, B., Hagen, J.O., Ørbæk, J.B., Meldvold, K., Isaksson, E. 1999: Glacier balance trends in the Kongsfjord area, western Spitsbergen, Svalbard, in relation to the climate. Proceedings of the International Symposium on Polar Aspects of Global Change, Tromsø, Norway, 24-28 August 1998, *Polar Research* Vol. 18 No. 2, pp. 113-400.

Lefauconnier, B. & Hagen, J.O., 1990: Glaciers and climate in Svalbard: statistical analysis and reconstruction of the Brøggerbreen mass balance for the last 77 years. *Annals of Glaciology*. 14, pp 148-152.

Lindström, G., Johansson, B., Persson, M., Gardelin, M. and Bergström, S. 1997: Development and test of the distributed HBV-96 hydrological model. *Journal of Hydrology* (201)1–4: pp. 272–288

Male, D.H. & Gray, D.M. 1981: Snow ablation and Runoff. *Handbook of Snow*. Ed. D.H. Male and D.M. Gray. Pergamon Press, N.Y., pp. 360–436.

Nash, J.E. & Suthcliffe, J.V. 1970: River flow Forecasting trough Conceptual Models, Part 1-a. *Journal of Hydrology,* Vol 10, No 3.

Partridge, G.W. & Platt, C.M.R. 1976: *Radiative Processes in Meteorology and Climatology.* Elsevier Scientific Publishing Company, Amsterdam.

Paterson, W.S.B, 1994: *The Physics of Glaciers*. 3rd ed. Elsevier Science. Ltd. England.

Repp, K. 1978: Breerosjon, glaciohydrology og materialtransporti et høyartktisk miljø, Brøggerbreen, Vest Spitsbergen. Final Thesis, Univ. of Oslo. (in Norwegian)

Sand, K. 1990: Modelling snowmelt runoff processes on temperate and arctic environments. Dr. Ing Thesis, IVB-report b-1990-1. Norwegian University of Technology and Science, Division of Hydraulic Eng. Trondheim. 176 pp.

Swinbank, W.C. 1963: Longwave Radiation from Clear Skies. *Qurterly Journal of the Royal Meteorological Society*. No 89, pp. 339–348.

Sælthun, N. R. 1996: The "Nordic" HBV Model. Description and documentation of the model version developed for the project Climate Change and Energy Production. Norwegian Water Resources and Energy Administration. NVE Pub. 7. 26 pp.

Tveit, J. & Killingtveit, Å. 1994: Snow surveys studies of water budget on Svalbard 1991-1994. Proceedings, Tenth international Northern Research Basins Symposium and Workshop, Spitsbergen, Norway, pp. 77-94.

U.S. Army corps of Engineers 1956: *Snow Hydrology.* Summary report of Snow Investigations, Corps of Engineers, North Pacific Division, Portland, Oregon, pp. 141–191 and plates.

Vehvilänen, B. 1992: *Snowcover models in operational watershed forecasting*. Publications of the Water and Environment Research Institute. National Board of Waters and Environment, Finland. No 11. 112 pp.

Winther, J.G., Bruland, O., Sand, K., Killingtveit, Å., Maréchal, D. 1997: Snow accumulation distribution on Spitsbergen, Svalbard, in 1997. *Polar Research*, Vol 17, No 2, pp 155–164

URN:NBN:no-6348

Paper 4:
Meltwater production in Antarctic blue-ice areas: sensitivity to changes in atmospheric forcing. Polar Research, Vol. 18 (2), pp. 283-290.

URN:NBN:no-6348

URN:NBN:no-6348

Paper 5:
Snow Distribution at a High Arctic Site at Svalbard. Nordic Hydrology, Vol. 32 (1), pp. 1-12.

URN:NBN:no-6348

Nordic Hydrology, 32 (1*)* 2001, 1-12

Snow Distribution at a High Arctic Site at Svalbard

Oddbjørn Bruland[1], Knut Sand[2]
Ånund Killingtveit[1]
[1]Norwegian Univ. Of Science and Tech., N-7491 Trondheim
[1]Univ. Courses on Svalbard, N-9170 Longyearbyen, Norway

In the Arctic regions snow cover has a major influence to the environment both in a hydrological and ecological context. Due to strong winds and open terrain the snow is heavily redistributed and the snow depth is quite variable. This has a significant influence to the duration of the melting season, on the possibilities of greenhouse gas exchange, the plant growing season and therefore the arctic terrestrial fauna. The aim of this study is to describe the snow depth variability by detailed measurement of snow distribution in a 3 km^2 site near to Ny-Ålesund at 79^o north at Svalbard and to link this to topography and climate at the location. The measurements were carried out in a grid of 100 m by 100 m cells using the SIR-2 Georadar from Geophysical Survey System Inc. (GSSI). Differential GPS was used to create a detailed Digital Elevation Model (DEM) and the snow depth data were correlated to topographic data. The average snowdepth in the area was about 70 cm with a standard deviation of 40 cm. Statistical distribution and spatial correlation for the snow depths were found. The method was found acceptable for snow distribution mapping. The main observation was the major accumulation in the west facing slopes due to easterly winds that are dominant in this area.

Introduction

As long as a thick layer of snow covers the surface of the arctic tundra the temperature of soil underlaid by permafrost is kept well below 0^{o}C and the processes within the active layer are retarded. During the period of snowmelt the

URN:NBN:no-6348

snow cover gets thinner and the temperature of the soil rises with increased biological activity. The processes producing the greenhouse gases, Carbon dioxide and Methane become more active, the plants prepare for the growing season, and the active layer starts to develop. The snow cover is both a limiting factor and during early spring an important water resource for several processes in the arctic environment. It is therefore important to have knowledge of its distribution and the main governing processes.

Due to the large effort it takes to collect snow depth data manually over a large area, different methods have been used to describe the snow distribution. Numerical modelling (Liston and Sturm 1997) has in many cases shown good results but leads to high model complexity and long computer run time. Remote sensing (Andersen 1982; Engman and Guerney 1991; Kønig and Sturm 1998; Rango 1980) is efficient to detect snow covered area but can not be used directly to find snow depths. Other methods such as extracting topographic parameters from maps (Tveit 1980) to estimate snow depth variability has also been used. Since the introduction of digital terrain models and Geographical Information System this method has become more efficient. In hydrological modelling where snow distribution is taken into account information on distribution is usually based on information from satellite images (Andersen 1982; Martinec 1985) or by using snow distribution curves (Killingtveit and Sælthun 1995). As distributed hydrological models with more correct physical description of the processes replace lumped models, there is a need for better temporal and spatial snow data.
New measuring methods have made it possible to measure snow depth over large areas with far less effort than earlier (Sand and Bruland 1998). By using Georadar connected to a snowmobile it is possible to measure snow depths down to more than 7 m depth with 25 cm interval at a travelling speed of 20 km/h. This makes it possible to make detailed snow depth maps over large areas based on measured data.

In this study radar surveys have been made in a 2 km x 1.5 km area outside Ny-Ålesund at 79^{o} north at Svalbard (Fig.1) in order to describe the snow distribution in this area. After snowmelt the same terrain was mapped using highly accurate differential GPS and a detailed digital terrain model was constructed. These data sets are combined and the correlation is studied and commented.

Study Area

The study was conducted close to Ny-Ålesund, the centre for Norwegian arctic research, at 78^{o}55'N, 11^{o}56'E at Svalbard. The 3 km^2 study area is located in the lower part of Bayelva catchment. The topography and vegetation within the measurement grid is representative for most lowland areas at Svalbard. It consists of a flat riverbed in the centre, on the west side an east-facing slope towards the Schetelig mountain and some small but sharp ridges in the north-west corner.

At the East side there are two east-west oriented ridges, Rabben and Kolhaugen, with the lakes Storvatnet and Tvillingvatnet in between (Fig.1) The steepest slopes are found around Kolhaugen with an inclination up to 10 deg.

URN:NBN:no-6348

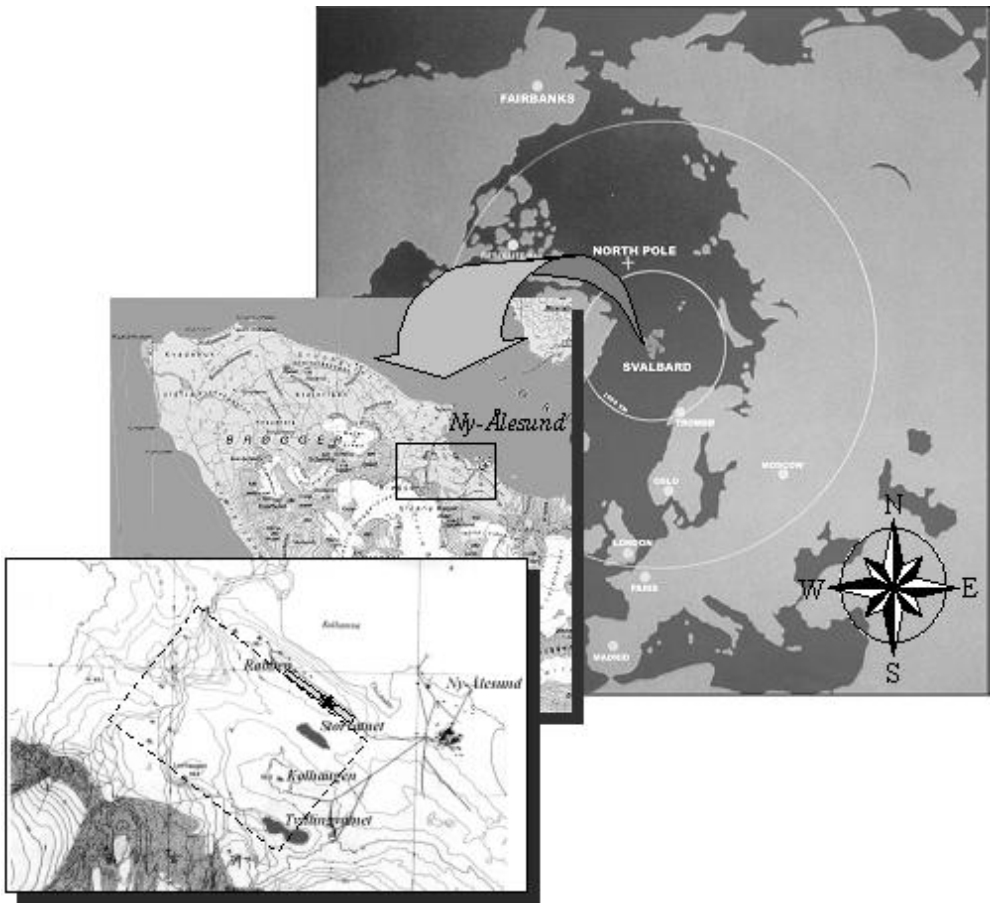

Fig. 1. Ny-Ålesund is located at the Brøgger peninsula Northwest at Svalbard. The study area is located between the terminal moraines of the Brøgger glaciers (the shaded area) and the airstrip at Rabben.

Except from the riverbed with only gravel, the area has a uniform lichen cover and areas with Rock Sedge (Carex rupestris) and Mountain Avens (Dryas octopetala).

As for the rest of Svalbard there is no tall vegetation that has any influence on the snow accumulation. The study area is surrounded by tall steep mountains in southeast and southwest, the Zeppelin and Schetlig Mountain, the terminal moraines below the Brøgger Glaciers in south and a open horizon to Kongsfjorden to the north. The dominant wind direction (Fig.2) is longitudinally to the Kongsfjord from the East. The long time average precipitation for a year in Ny-Ålesund is 372 mm. Approximately 65 % this falls as snow during the period from mid September to end of May (Hanssen-Bauer 1990)

URN:NBN:no-6348

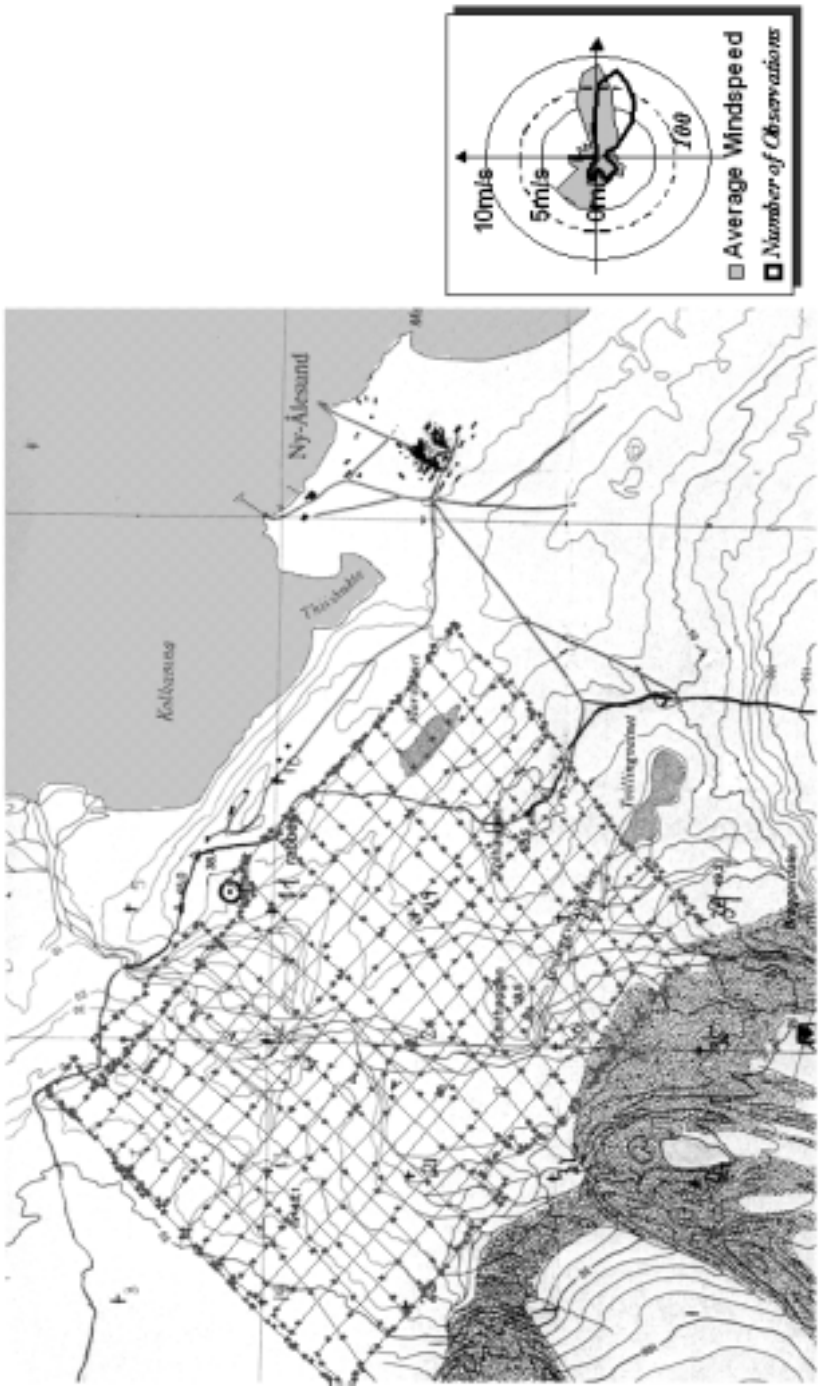

Fig. 2. The measured grid where the markers at the lines are positions logged at a GPS. The graph at the low right corner shows the average wind speeds and the number of wind observations for every 10o section during the winter 1997 to 1998.

URN:NBN:no-6348

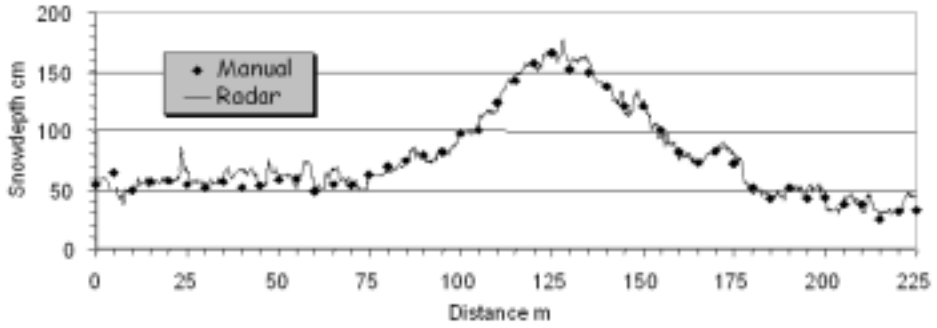

Fig. 3. Verification of Radar Measurement by comparing digitalized radar data to manual snow depth measurement at every 5 meter along a test line.

Measurements and Method

The objective of the study is to quantitatively describe the snow distribution for the 3 km^2 area. In order to achieve this it is necessary to have a strategy with very dense measurements. To avoid systematic errors caused by biased sampling due to accessibility, snow mobile driving conditions and snow accumulation features, a grid of straight profiles perpendicular to each other was chosen. Due to the relatively gentle topography in the study area it was assumed that a sufficient accuracy would be achieved with 100 m distance between the profiles. The mileage recorder on the snowmobile was used to set the endpoints of the profiles, and a GPS was used to keep the course along the profile and to log positions along the tracks.

A GSSI SIR-2 Georadar with a 500 MHz antenna was used to measure the snow depth. This instrument has earlier shown high efficiency and good accuracy in snow surveying (Sand and Bruland 1998). The principle of the radar measurement technique is described by Hamran (1996) and Sand and Bruland (1998). The radar measurement was calibrated and verified by doing 45 manual depth and 3 density control measurements along a 225 m long test line (fig.3). The radar sends an impulse trigged by a survey wheel and records the TwoWayTraveltime (*TWT*) the signal uses trough the snow pack and back to the receiver antenna. The radar was set to measure at every 25 cm. The recorded travel time is converted to snow depth (*d*) by using the empirical formula for the permittivity, κ'_{ds}, of dry snow found in Ulaby et al. 1986.

$$v = \frac{TWT}{2d} = \frac{c}{\sqrt{\kappa'_{ds}}} \qquad (1)$$

and

$$\kappa'_{ds} = 1 + 1.2\,0.51\rho_s^3 \qquad (2)$$

where ρ_s is snow density in g/cm^3, v is pulse velocity and c is the velocity of light. The temperature was below 0^{o}C in the entire snow pack during the measuring period and the formula for the permittivity of dry snow could be used.

URN:NBN:no-6348

During 2 days in early June in total 268783 snow depths where measured with approximately one half in each of the two directions along a total distance of approximately 67 km (Fig.2). Positions along the profiles were logged with a Global Positioning System (GPS).

A topographic map was constructed by the data collected after the snowmelt by the use of a differential GPS system with high accuracy. These data sets were combined in order to visualise the correlation between topography, dominant wind direction and snow distribution. The Norwegian Polar Institute in Ny-Ålesund measures wind speed and wind direction four times a day. The dominant wind direction (Fig.2) is found by averaging wind speed observations and by counting number of observations for every 10^{o} sector trough the snow accumulation period.

Results

The position of every measurement was found from the positions logged at the GPS and a snow depth map could be constructed by using the surface mapping system Surfer. By combining information about the wind during the accumulation period and an overlay of these maps, snowdrift formation and snow erosion pattern can be explained (Fig.4).

The average snow depth was found to be 70 cm with a maximum of 308 cm and a standard deviation of 40 cm. There was a difference of 4 cm in the average depth between measurements along the NW-SE profiles and NE-SW profiles. Areas with snow depths a half standard deviation less than mean snow depth (< 50 cm) are defined as erosion areas, those with depth a half standard deviation larger than mean (> 90 cm) are defined as accumulation areas and those with snow depths in between are called equilibrium areas. The erosion areas amount to 34%, the accumulation areas to 22% and the areas in equilibrium to 44 %. Two large snowdrifts were found, both in the bottom of long west facing slopes. Erosion dominated more along the Rabben ridge in Northeast, than in the rest of the area were the erosion features is more scattered. There is a higher spatial correlation between measurements along the NW-SE running profiles than along the profiles running NE-SW (Fig.5). This can be explained by lower topographically variation in the NE-SW direction and that the wind smoothes the snow surface to a larger extent in this direction.

Fig. 4. Contour map and visualised map of the snow distribution at the study area in May 1998. Accumulation and erosion areas are defined as areas with snow depths a half standard deviation higher/lower than average snow depth. The dotted line at the lower map

URN:NBN:no-6348

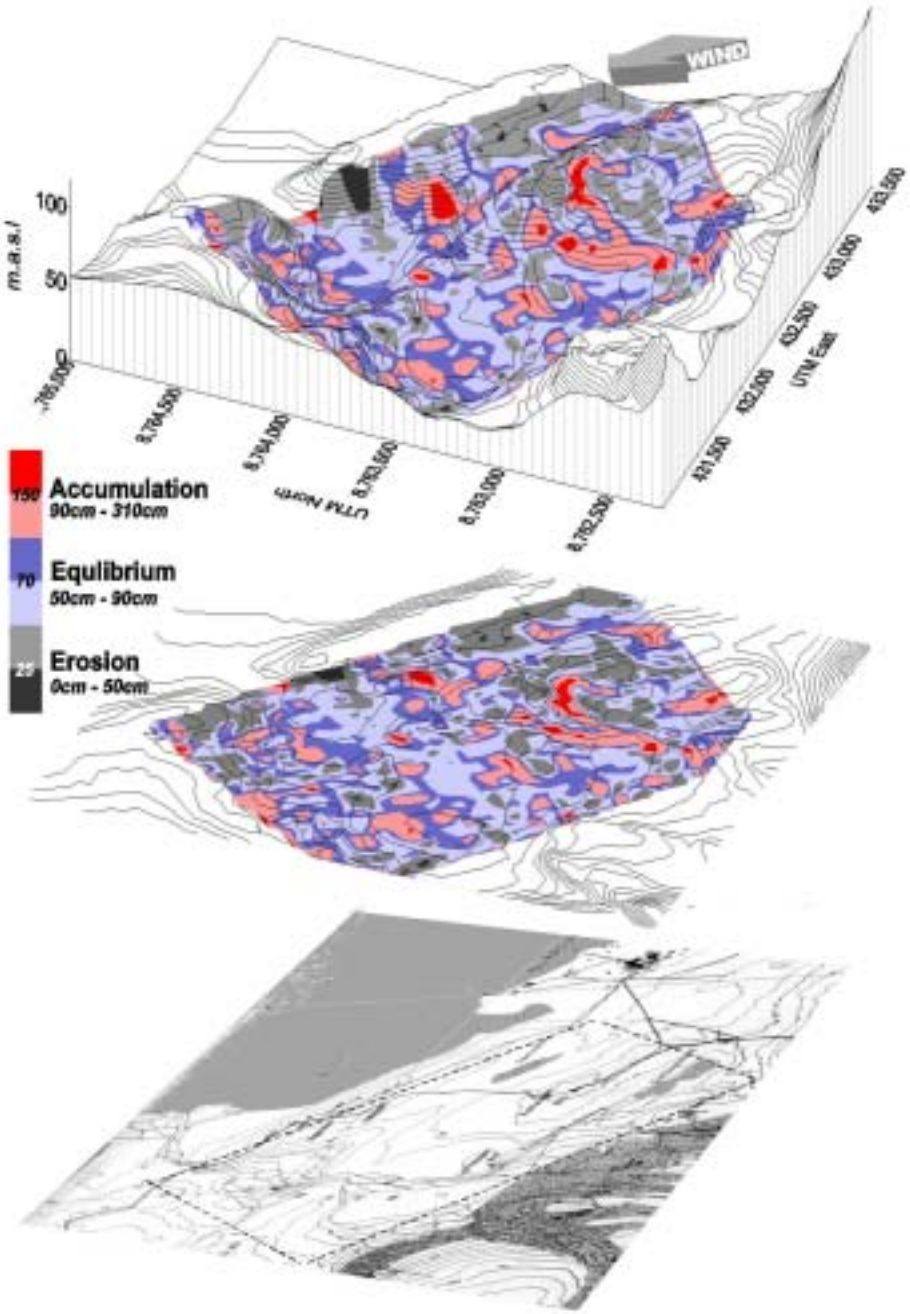

URN:NBN:no-6348

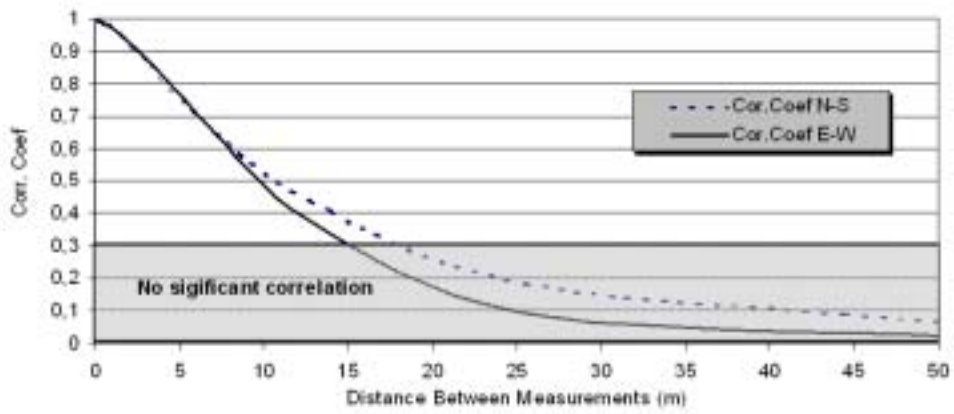

Fig. 5. Spatial correlation between adjacent measurements along snow profiles. A correlation coefficient higher than 0.3 indicates significant correlation.

Statistical Analysis

In this study the statistical distribution and spatial correlation is analysed. This data set is extensive compared to manually collected snow depth data sets and therefore a better basis for further analyses. The statistical distribution of the measurements will give a very reliable estimate of the variation in snow depth in the area. Analysis of spatial correlation will reveal correlation between individual measurements and show if the grid cells are small enough to ensure representative sampling. In further studies the snow depth measurements can be combined with the topography data in a Geographical Information System in order to study correlation between erosion and snow accumulation pattern and topographic features. This can be compared to results from simulations in a dynamic numerical snow transport model where the end of season snow distribution can be found by the model based on the climatic data for the accumulation season.

The spatial correlation between adjacent snow depth measurements along the profiles was calculated by the following formula:

$$r(k \div L) = \frac{1}{N - k - 1} \frac{\sum_{i=1}^{N-k} (x_i - \sigma)(x_{i+k} - \sigma)}{\omega^2} \qquad (3)$$

where x_i and x_{i+k} is measured snow depth number i and $i+k$ with k·÷L interval, σ and ω is average snow depth and standard deviation based on N observation,. Fig. 5 shows that snow depths within a distance of around 15 m to 20 m are significantly correlated to each other.

The variation coefficient of the snow depths, C_v, was calculated by the following equation to be 0.58.

$$C_v = \omega / \sigma \qquad (4)$$

URN:NBN:no-6348

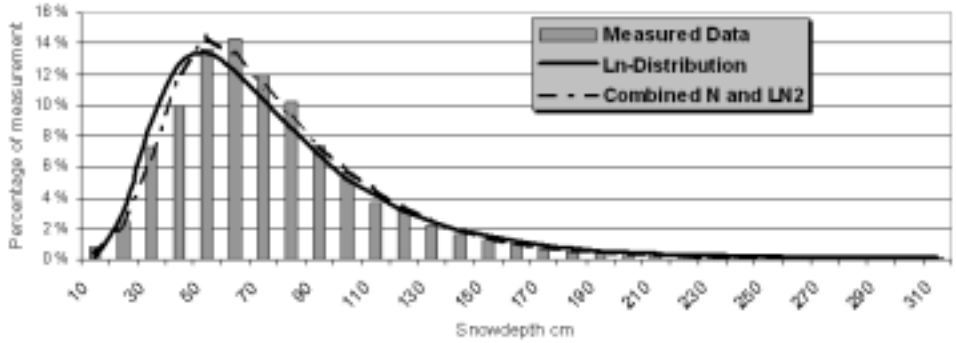

Fig. 6. Frequency distribution of the measured snow depths compared to a Log Normal Distribution and a combined Normal and LogNormal Distribution with the same mean value and standard deviation.

The distribution of the measured snow depths was computed and a Log Normal distribution was fitted to this empirical distribution (Fig.6) by applying the lognormal cumulative distribution function:

$$f(x) = \frac{1}{\sqrt{2\phi}\omega x} e^{-(\ln(x)-\sigma)^2/2\omega^2}, \qquad x > 0 \qquad (5)$$

where x is snow depth, σ and ω is average snow depth and standard deviation. The adaptation is good at the lower and upper end of the distribution, but there is a difference between the medians of the distributions. A weighted combination between a Log-Normal and a Normal distribution (eq.6) gave a better result.

$$f(x) = \frac{1}{\sqrt{2\phi}\omega}\left(a e^{-(x-\sigma)^2/2\omega^2} + 2\frac{b}{x} e^{-(\ln(x)-\sigma)^2/2\omega^2}\right), \qquad x > 0 \qquad (6)$$

where a and b are the best combination of weights found for this data set.

URN:NBN:no-6348

Discussion and Conclusions

Fig. 4 shows that most areas with accumulation and erosion features can be explained by slope exposure towards the dominating wind. Though, there are some areas where one would expect different results. This is especially true at some exposed ridges and slopes where it seems more likely to find erosion than an equilibrium condition. Ny-Ålesund is, as is Svalbard in general, exposed to strong winds and one should expect the snow to be strongly redistributed. From the map we can see that this is not necessarily the case. A variation coefficient for the area of 0.58 is close to what Tveit and Killingtveit (1994) reported from measurements in DeGeer valley close to Longyearbyen on Svalbard, but low compared to normal values ranging from 0.5 to 1.5 found in Norwegian mountainous catchments (Andersen et al 1982). A snow surface exposed to strong winds turns rapidly into a hard crust and prevents further erosion. The results indicate that this process possibly is more effective on Svalbard with its arctic climate than in Norwegian mountains. Some of the features can also be explained by the fact that the map is a result of interpolation between the measurements. This can give incorrect results over a hill with deeper snow depths measured at each side. If the latter is the case it shows that a finer grid is necessary to describe the distribution more exactly. The difference in average snow depth along the NW-SE and NE-SW profiles also indicates that result would benefit of a finer grid. This difference also shows the need for having profiles in both directions.

The snow distribution found in this investigation can be a useful tool for understanding the flora in this area and it can also be used to explain differences in thaw depths of the active layer. The distribution found in this study will be compared with distributions found for a larger area and for other years in the same area. If this distribution can represent a larger area and it is found to be similar every year, it can be a useful tool for estimation of snow depth variability in the arctic regions. The data will also be very valuable for calibrating and verifying numerical models for snow transport.

References

Andersen, T. (1982): *Operational Snow Mapping by Satellites, Hydrological Aspects of Alpine and High-Mountain Areas*, edited by J.W.Glen., IAHS Publication, Vol 138: 149-154.

Engman, E. T., and Gurney, R. J. (1991): *Remote Sensing in Hydrology*, Chapman and Hall.

Hamran, S. E. (1996): Radar in Glaciology. Lecture notes presented at University Studies at Svabard (UNIS) Spring 1996.

Hanssen-Bauer, I., Solås, M. K, Steffensen, E. L. (1990): The Climate of Spitbergen. *DNMI Report 39/90.* The Norwegian Meteorological Institute, Oslo, Norway.

URN:NBN:no-6348

Killingtveit, Aa., and Sælthun, N.R. (1995): *Hydrology*. Hydropower Development, Vol 7. Norwegian University of Technology and Science.

Kønig, M., and Sturm, M. (1998): Mapping Snow Distribution in the Alaskan Arctic using aerial photography and topographic relationships. *Water Resources Research, Vol 34*, No 12, pp. 3471-3483.

Liston, G. E, and Sturm, M. (1997): A snow-transport model for complex terrain, *Journal of glaciology, 44 (148)*: 498-516

Martinec, J. (1985): Snowmelt Runoff models for Operational Forecasts. *Nordic Hydrology, Vol. 16*: 129-136.

Rango, A. (1980): Operational application of Satellites snow cover observations. *Water Res. Bull*. Vol.16: 1066-1073.

Sand, K. and Bruland, O. (1998): Application of Georadar for Snow Cover Surveying. *Nordic Hydrology, 29 (4/5)*: 361-370.

Tveit, J., Killingtveit, Aa. (1994): Snow surveys for studies of Water Budget on Svalbard. *Proceedings Tenth International Northern Research Basins Symposium and Workshop*. Svalbard, Norway, pp. 489-509.

Tveit, J. (1980): Representativitet av Snømålesystem ut frå topografiske og morfometriske parametrar. Ph.D report. Dep. of Hydraulic and Environmental Engineering, Norwegian University of Technology and Science (in Norwegian).

Ulaby, F. T., Moore, R. K. and Fung, A. K. (1986): *Microwave Remote Sensing. Active and Passive*, Vol III, Addison-Wesley Pub. Company.

Received: 10 December, 1999
Revised: 16 June, 2000
Accepted: 16 June, 2000

URN:NBN:no-6348

URN:NBN:no-6348

Paper 6:
Snow accumulation distribution on Spitsbergen, Svalbard, in 1997. Polar Research, Vol. 17 (2), pp. 155-164.

URN:NBN:no-6348

URN:NBN:no-6348

Paper 7:
Modelling of the snow distribution at two high arctic sites at Svalbard, Norway, and at a sub-arctic site in central Norway. Submitted to Nordic Hydrology Nov 2001.

URN:NBN:no-6348

Submitted to *Nordic Hydrology* Nov 2001

MODELLING THE SNOW DISTRIBUTION AT HIGH ARCTIC SITES AT SVALBARD, NORWAY, AND AT A SUB-ARCTIC SITE IN CENTRAL NORWAY.

Oddbjørn Bruland[1], Glen E. Liston[2], Jorien Vonk[3], Knut Sand[4] and Ånund Killingtveit[1].

[1]Norwegian University of Science and Technology, 7491 Trondheim, Norway.
[2]Department of Atmospheric Science, Colorado State Univ., Fort Collins, Colorado 80523, U.S.A.
[3]University Courses on Svalbard, Longyearbyen, Svalbard, 9170 Norway.
[4]SINTEF Energy Research, Energy Systems, S Sælandsvei 11, 7491 Trondheim, Norway.

In Arctic regions snow cover has a major influence to the environment both in a hydrological and ecological context. Due to strong winds and open terrain the snow is heavily redistributed and the snow depth is quite variable. This has a significant influence to the duration of the melting season, the snow cover depletion and thereby the land surface albedo, on the possibilities of greenhouse gas exchange, the plant growing season and therefore the arctic terrestrial fauna. The aim of this study is to test to what degree a numerical model is able to recreate an observed snow distribution in sites located on Svalbard and Norway and with size ranging form 1 km^2 to 250 km^2. Snow depth frequency distribution, a snow depth rank order test and location of snowdrifts and erosion areas were used as criterion for the model performance. SnowTran3D is the model used in the study. In order to allow for occasions during the winter with milder climate and temperatures above freezing, a snow settling calculation was included in the model. The topographic modification of wind speeds was also changed from treating the curvature of ridges and valleys independent of wind direction to let the influence of curvature on the wind speed depend on wind direction. The model result was compared to extensive observation dataset for each site and the sensitivity of main model parameters to the model result was tested. For all three sites the modelled snow depth frequency distribution was highly correlated to observed distribution and the snowdrifts and erosion areas were located correspondingly by the model to what was observed at the sites.

Introduction

As long as a thick layer of snow covers the surface of the arctic tundra the temperature of soil underlaid by permafrost is kept well below 0˚C and the processes within the active layer are retarded. During the period of snowmelt the snow cover gets thinner and the temperature of the soil rises with increased biological activity. The processes producing the greenhouse gases, for example Carbon dioxide (CO_2) and Methane (CH_4), become more active. Lloyd et al. (1999) found that in the process of global warming, the premise that the Arctic will become a net source of CO_2 is highly dependent upon the particular climate conditions, especially the depth of the summer snow cover, summer cloudiness and precipitation frequency. They also found that the length of the growing season is among the key factors for the variability of the CO_2 balance over mountain birch forest in Kevonen, North Finland. The land surface albedo has a large influence on the radiation balance of the earth and at higher latitudes at the northern hemisphere this closely linked to the snow cover. Colman et al. (1994, 2001) states that it is one of the most important parameterisation in global climate models and better description of the snow distribution and thereby the albedo can improve global climate modelling.

URN:NBN:no-6348

The snow cover is both a limiting factor and, during early spring, an important water source for several processes in the arctic environment. The effect of the snow cover on the production of CO_2 is also documented in Brooks et al. (1997). Bruland and Cooper (2001) found a high correlation between the snow distribution and vegetation distribution in an area close to Ny-Ålesund at Svalbard, Norway. Van Der Wal et al. (2000) found snow depth and timing of the snowmelt influenced the grassing behaviour of Svalbard reindeer as they seemed to prefer plots that had been snow-free longest. The importance of snow drifting in the magnitude and timing of snowmelt water inputs to the runoff is emphasized by Hartman et al. (1999). Referring to Blöshl et al. (2001) and to McLung and Scharer (1993), Marsh (1999) noted "redistribution of snow in mountainous environments is extremely important for both runoff calculation and avalanche forecasting".

Sublimation losses in blowing snow is also substantial in arctic regions and Pomeroy et al. (1998) stated that redistribution and sublimation can cause a difference of – 40% to +100% between accumulated measured snowfall and snow accumulation.

According to Marsh (1999), Gray and others (1979) noted that "it is evident, at the present time, because of the lack of knowledge of the snow transport and deposition processes and complex nature of the accumulation phenomenon, it is impossible for the hydrologist to define snow cover distribution patterns by a physically based, mathematical model". Since that time a lot of effort have been made to develop such models and physically based algorithms developed from process studies have been incorporated in models of blowing snow (Uematsu et al. (1991), Pomeroy et al. (1993), Liston and Sturm (1998), Déry et al. (1998)). Marsh (1999) summarized the development and content of several of these models and concluded that these models work reasonably well in terrain that is rolling or for single-species forest stands but they are not capable of modelling snow cover evolution in complex mountainous terrain or multi species forest stand.

In the current study, the Liston and Sturm model (SnowTran-3D) is applied to two high Arctic sites on Svalbard and to an alpine site in central Norway. The sites are ranging from 1 km^2 to 250 km^2 and from rolling to mountainous terrain. At the two smallest sites the modelling is based on high-resolution topographical data and the simulated result has been compared to very detailed measured snow distribution. The only available topographical data at the largest site has a resolution of 100m by 100m and the snow depth measurements were carried out along selected snow courses since complete coverage is impossible at this scale.

In order to meet the warmer climatic conditions at these locations compared to the interior of Alaska or Colorado where the model earlier has been applied, a new snow settling sub-model is incorporated to the model.

Bruland et al. (2001) mapped and described the snow distribution of the Ny-Ålesund site in detail. The main objective of this study is to test how well SnowTran-3D with an improved snow settling sub-model, can reconstruct this snow distribution and further to test the model at a site with completely different topographic characteristics and at a site with a different location and climate. The result of the model simulation is evaluated by visual comparison between plotted observed and simulated snow distribution and by comparing the frequency distribution of observed and simulated snow depths. If the model successfully passes these tests, we assume it can be used as a tool to explain how snow distribution might change with climatic changes and how this might influence vegetation distribution, grazing conditions and exchange of greenhouse gases. It can also be used as a tool to improve the estimates of the total volume and distribution of snow reservoir in catchments for hydropower production. This knowledge has a high commercial value in the hydropower stock market.

URN:NBN:no-6348

Study Area

Ny-Ålesund

The northernmost site is located close to Ny-Ålesund, the centre for Norwegian arctic research, at 78˚55'N, 11˚56'E at Svalbard. The 3 km^2 study area is located in the lower part of Bayelva catchment. The topography and vegetation within the measurement grid is representative for most lowland areas at Svalbard. It consists of a flat riverbed in the centre, on the west side an east-facing slope towards the Schetelig mountain and some small but sharp ridges in the north-west corner.

At the East side there are two east-west oriented ridges, Rabben and Kolhaugen, with the lakes Storvatnet and Tvillingvatnet in between (Fig. 1) The steepest slopes are found around Kolhaugen with an inclination up to 10 deg. Except from the riverbed with only gravel, the area has a uniform lichen cover and areas with Rock Sedge (Carex rupestris) and Mountain Avens (Dryas octopetala). As for the rest of Svalbard there is no tall vegetation that has any influence on the snow accumulation. The study area is surrounded by tall steep mountains in southeast and southwest, the Zeppelin and Schetlig Mountain, the terminal moraines below the Brøgger Glaciers in south and a open horizon to Kongsfjorden to the north. The dominant wind direction is longitudinally to the Kongsfjord from the East. The long time average precipitation for a year in Ny-Ålesund is 403 mm. Approximately 75% this falls as snow or sleet during the period from mid September to end of May (Førland et al., 1997).

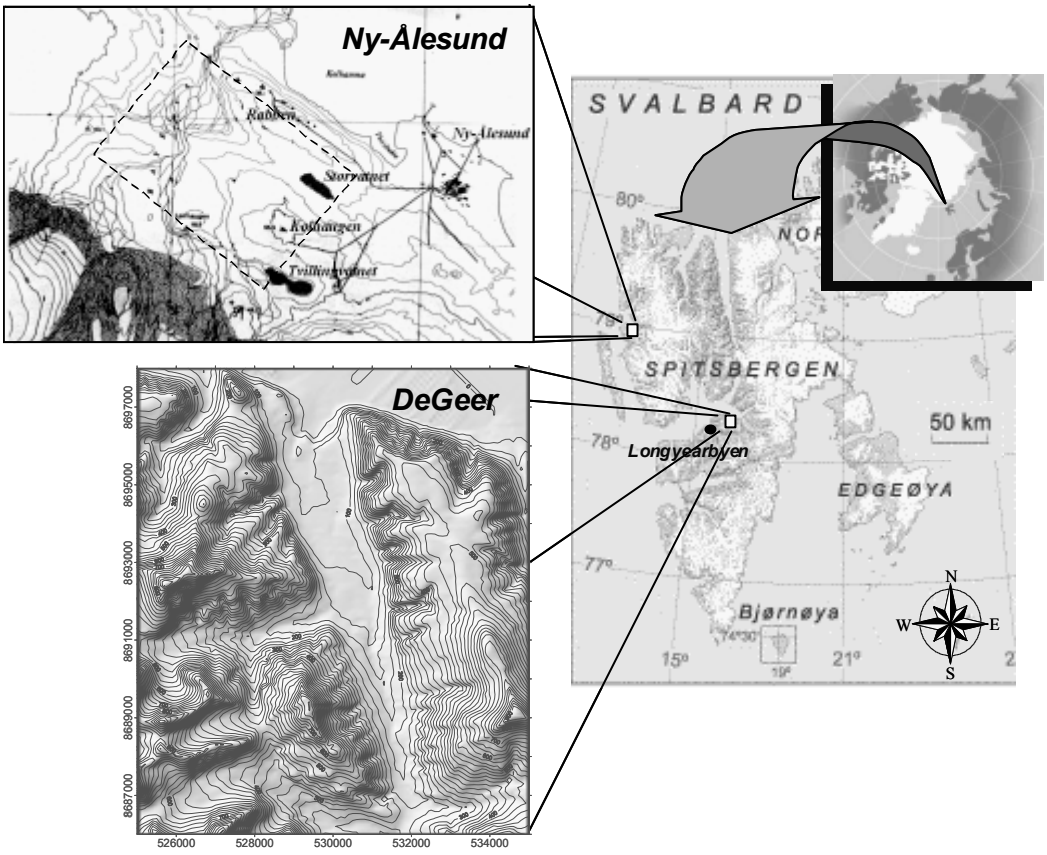

Fig 1. Location of the Ny-Ålesund Site and DeGeer valley

URN:NBN:no-6348

DeGeer

The DeGeer Valley is the largest of the sites and located at 78˚16'N, 16˚19'E also at Svalbard. The simulation is conducted in a 250 km^2 area covering the south-north oriented DeGeer valley, the surrounding mountains and adjacent valleys (Fig. 1). The site has a relief ranging from about 100 masl in the valley bottom up to 917 masl at Albert Bruntoppen. The vegetation in the lower areas is comparable to the vegetation at the Ny-Ålesund site. Moving to higher elevations the vegetation get sparser as gravel, stones and rock takes over. Fangenbreen, Blackbreen and Tellbreen are glaciers located in the adjacent valleys east of DeGeer. The closest meteorological input data for DeGeer is the Norwegian Meteorological Institutes observations at Svalbard Airport about 20 km west of DeGeer. Svalbard airport has a long time precipitation average of 182 mm/year, around 70% of this falls as snow or sleet (Førland et al. 1997).

Aursunden

The southernmost site is located at 62˚47'N, 17˚46'E close to Røros, Norway (Fig. 2). It is 1 km^2 and has an average elevation of about 1000 masl. The terrain and vegetation is typical to a Norwegian mountain plateau with small hills, ridges and precipices. It has a weak declination towards northeast. The nearest meteorological observations is conducted at a station, St 2, located 3 km northeast of the site below the timberline at 834 masl. Another station, St 1, run by the Norwegian road administration, is located 2 km further north at 920 masl. The latter station has a wind exposition more similar the experiment site but precipitation is not here observed. None of these stations has long records, but the long time average precipitation in Røros, 20 km to the south, is 504 mm/year, whereof about 40% falls during the winter months. The average temperature over the year is 0.3˚C and –6.9˚C over the winter season (Statistics Norway, 2001).

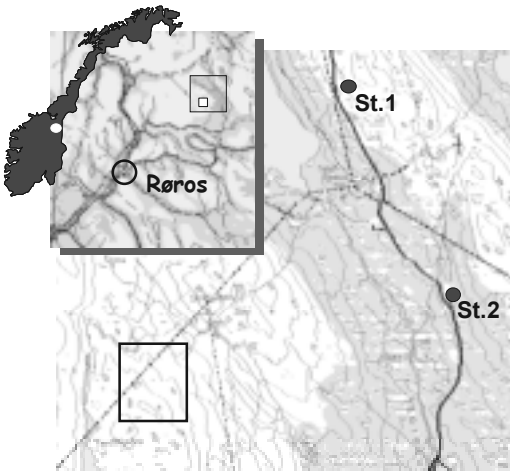

Fig.2 Location of Aursunden site

Measurements

The snow distribution at the end of the snow accumulation season at the 3 km^2 Ny-Ålesund site was extensively measured both in 1998 and 2000. The method and strategy used was the same both years. This and the 1998 results are described in Bruland et al. (2001). By pulling a GSSI georadar with a 500 Mhz antenna after a snowmobile along straight profiles perpendicular to each other on a grid (Fig. 3a) and logging positions using a GPS. Snow depths were measured every 25 cm along a total distance of approximately 67 km in 1998 and along twice this distance in 2000 as the grid cell size was decreased from about 100m by 100m in 1998 to about 50m by 50m in 2000. A topographic map was constructed by the data collected by the use of a differential GPS system with an assumed accuracy in kinematic mode of ±3cm horizontally and ±5cm vertically.

The same method was used to map the snow distribution at the Aursunden site (Fig. 3c). Due to a rougher topography compared to the Ny-Ålesund site the size and shape of the grid cells is less uniform. In DeGeer valley the snow measurements was carried out along 17 selected transects with a total length of 24 km (Fig. 3b) (Vonk, 2001).

URN:NBN:no-6348

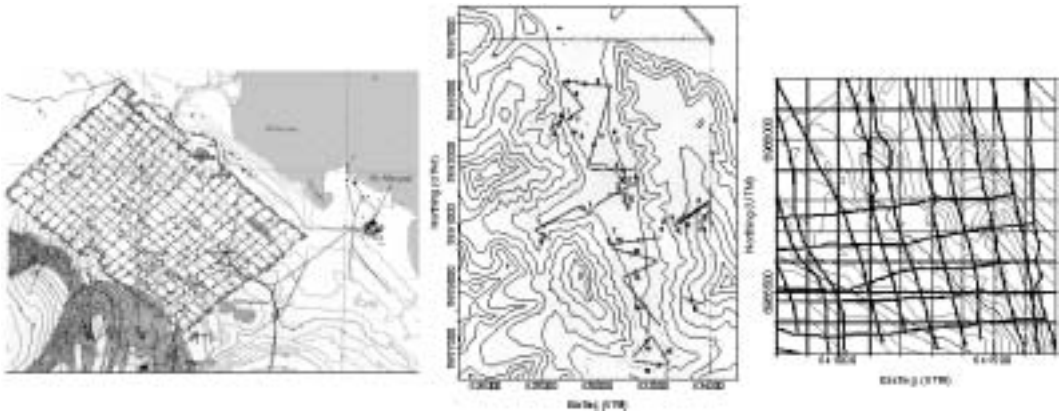

Fig 3. Snow depth measurement transects at Ny-Ålesund , DeGeer and Aursunden site

Model description and changes made to the model

A physically based numerical snow transport (SnowTran-3D) is described by Liston and Sturm (1998). This is a mass-transport model which includes processes related to snow holding by vegetation, topographic modification of wind speeds, snow cover shear strength, wind induced surface shear stress, snow transport resulting from saltation and suspension, snow accumulation and erosion, and sublimating of blowing and drifting snow. Fig. 4 illustrates the key input parameters (solar radiation, precipitation, wind speed and direction, air temperature, humidity, topography and vegetation snow holding capacity), the key processes (saltation, turbulent suspension and sublimation) and the key outputs (spatial distribution of snow erosion and deposition) from the model. The six primary components of the model are: (1) the computation of the wind-flow forcing field; (2) the wind shear stress on the surface; (3) the transport of snow by saltation; (4) the transport of snow by turbulent suspension; (5) the sublimation of saltating and suspended snow, and (6) the accumulation and erosion of snow at the surface a lower boundary that is allowed to move with time. Even though the average temperature over the winter months both at Svalbard and at Røros, are several degrees below freezing, occasionally during the winter warm humid air masses arrive and lead to air temperatures several degrees above freezing, often followed by precipitation.

Rain, warm air and eventually melting changes the properties of the snow surface and increase its resistance to wind shear stress and erosion. Previously this was not accounted for in the model. In the application presented her, the SnowTran-3D snowpack is modified and defined to be composed of two layers instead of one; a "soft" surface layer that includes snow that is able to be moved by the wind, and a "hard" layer that is unavailable for transport.

To determine the threshold friction velocity, u*t, of this soft snow, the temporal evolution of the snow density is related to the strength and hardness of the snow, which is then related to u_{*t}.

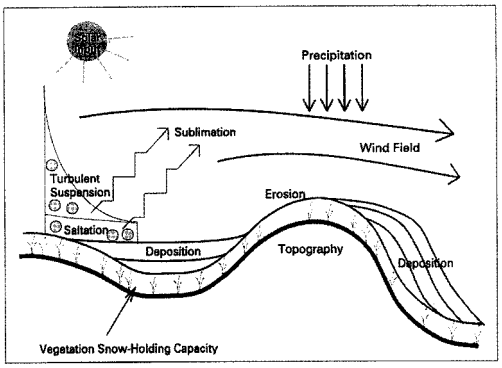

Fig 4. Key features of Snowtran3D

Density changes in the soft layer occur by two mechanisms. First, snow precipitation is added to the soft snow layer using a new snow density of 200 kg/m^3. The second mechanism increases the density by

URN:NBN:no-6348

compaction, and includes the influence of temperature, wind-speed, and the weight of the snow in the layer. Following Anderson (1976) with the addition of a wind-speed influence, the temporal change in snow density, ρ_s, is given,

$$\frac{\partial \rho_s}{\partial t} = A_1 U W_s \rho_s \exp\left(-0.008\left(T_f - T_s\right)\right)\left(-A_2 \rho_s\right) \quad (1)$$

where T_f is the freezing temperature, T_s is the soft snow temperature (defined in this application to be equal to lesser of the air temperature), U is the wind sped at 2 meters height, W_s is the weight of snow in the top half of the soft-snow layer and expressed in water equivalent depth; and A1 and A2 are constants set equal to $0.00013 m^{-1}s^{-1}$ and $0.021 m^3/kg$, respectively, based on Kojima (1967)

This density is related to the snow strength using the uniaxial compression measurement of Abele and Gow (1975). An equation fitted to their results describes the variation of hardness, σ, with density,

$$\sigma = 1.36 \exp\left(\rho_s / 76\right) \quad (2)$$

where σ is in kPa, and ρ_s is in kg/m^3. A relationship between hardness and u_{*t} is provided using the data of Kotlyakov (1961),

$$\sigma = 267 \cdot u_{*t} \quad (3)$$

Combining Equation (2) and (3) yields,

$$u_{*t} = 0.005 \exp\left(\rho_s / 76\right) \quad (4)$$

$$W = 1.0 + \gamma_s \Omega_s + \gamma_c \Omega_c \quad (5)$$

where Ω_s and Ω_c are the topographic slope and curvature, respectively, and γ_s and γ_c are positive constants which weight the relative influence on Ω_s and Ω_c on modifying the wind speed. The slope and curvature are computed such that lee and concave slopes produce Ω_s and Ω_c less than zero and windward and convex slopes produce Ω_s and Ω_c greater than zero. Thus, decrease and increase wind speed respectively. Previously the wind direction has only influenced the effect of the slope index. With this original curvature calculation (OrigCurve) the convexity of a ridge or concavity of a valley, have the same effect on the wind speed whether the ridge or valley is parallel or perpendicular to the wind direction. In this study the direction of the curvature in respect to the wind is accounted for as the effect of curvature is gradually increasing from zero when the curvature is parallel to the wind, to full effect when perpendicular to the wind (WCurve).

Results

The extensive observation dataset for the Ny-Ålesund site is suitable for testing the sensitivity of the model parameters and the effect of the changes made to the model. Curvature (γ_c) and Slope (γ_s) weights, temperature and density thresholds for snow settling in the two layer model, are parameters used to optimise the model and the sensitivity to changes is these are tested. At the sites in DeGeer valley and in the Aursunden area the observations are less extensive and a less extensive optimisation is performed. The simulation results where interpolated and visualized in the surface mapping system SURFER. Visually comparison of plotted observed and simulated snow distribution, correlation between the simulated and observed frequency distribution of the snow depths and a sorted rank order test suggested by Prasad et al. (2001) were used as criterion for optimising the model. The sorted rank order test (V_f) is a measure of the residual error between the distribution of modelled and observed snow depth (Eq. 6). A value of zero for V_f would indicate a perfect match between observed and modelled snow depth distribution

$$V_f = \frac{\sum_{i=1}^{n}\left(SnD^{i}_{obs} - SnD^{i}_{sim}\right)^2}{\sum_{j=1}^{n}\left(SnD^{j}_{obs} - \overline{SnD}_{obs}\right)^2} \quad (6)$$

URN:NBN:no-6348

where SnD^{i}_{obs} is the observed snow depth at the *i*-th location, $\overline{SnD_{obs}}$ is the mean observed snow depth, and *i* refers to the *i*-th largest value in the set of observed or modelled snow depths, and n is the numbers of grid cells.

The atmospheric forcing data for the three sites is presented in Fig. 5. In the model the precipitation is corrected due to catch losses using a dynamic correction factor (Eq. 7).

$$P_{corr} = P_{obs} \cdot \exp(0.02 \cdot U) \qquad (7)$$

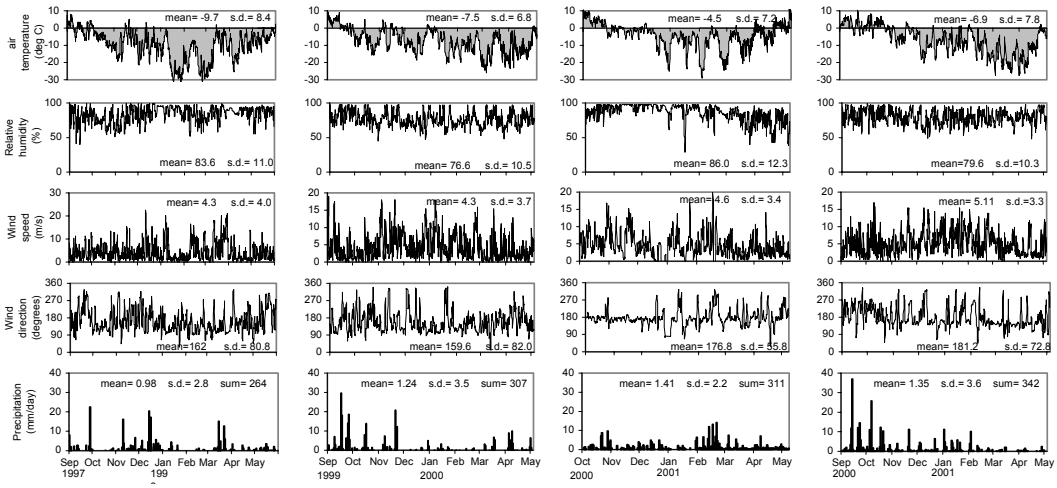

Fig 6. Meteorological forcing data for Ny-Ålesund 1998 and 2000, Aursunden and DeGeer

Ny-Ålesund site

Model simulations were run from 1 September through 15 May, for the winters 1997–98 and 1999–00, in the following referred to as 1998 and 2000, respectively. The simulation was run both with 100m by 100m and 50m by 50m model grid spacing and a 6 hours time step.

Optimisation and sensitivity testing of the model parameters were carried out on the 100m by 100m grid spacing with curvature and slope weights 0 – 200 and 0 to 40 respectively, and with temperature and density thresholds 0-10ºC and 200-300 g/cm^3, respectively. For the WCurve model optimal ∂_c and ∂_s for the two years together was in the range from 130 to 150 and 5 to 10, respectively. The modelled snow distributions for the WCurve model and the OrigCurve model are plotted together with observed snow distribution for 1998 and 2000 in Fig.6.

URN:NBN:no-6348

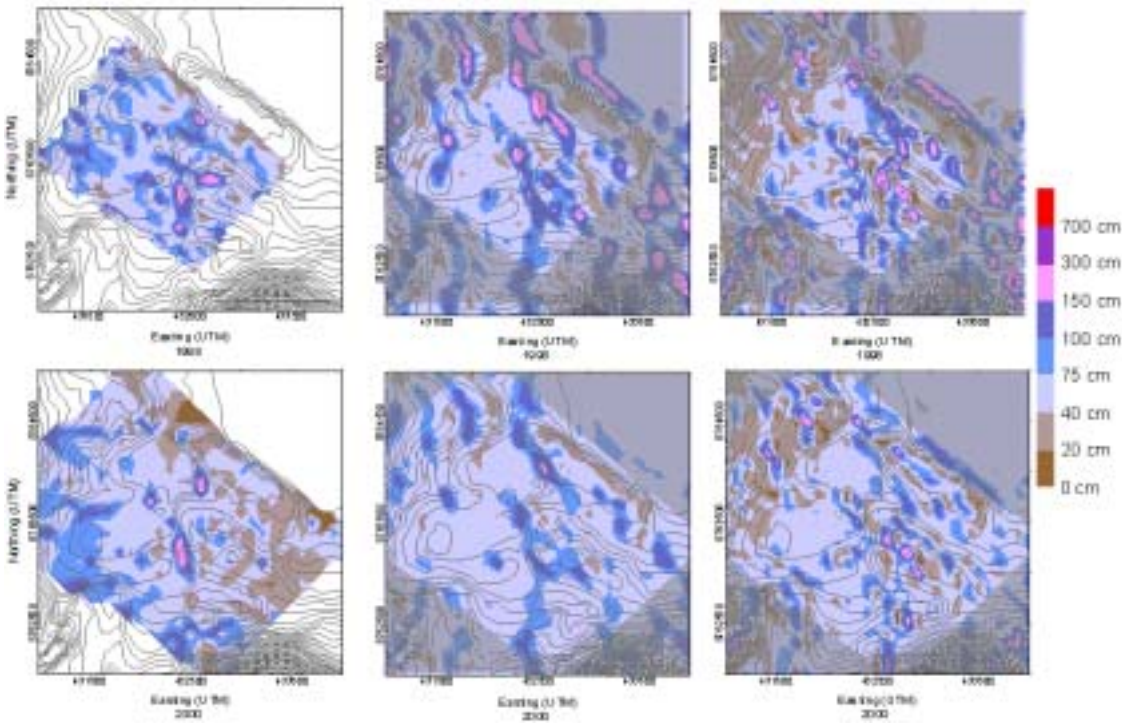

Fig. 6 Observed (left) snow distribution and modelled snow distribution using WCurve model (centre) and OrigCurve model (right).

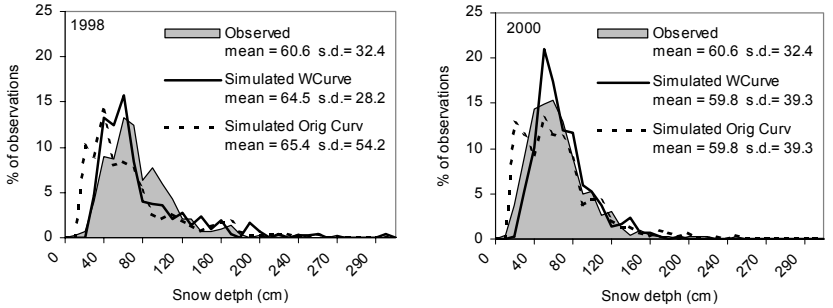

Fig.7 Observed and modelled Snow frequency distribution for Ny-Ålesund site 1998 and 2000

The correlation between the snow depth frequency distributions (Fig. 7) were more sensitive to changes in the model parameters than the sorted rank order test. A diagram showing the sensitivity of $ɔ_c$ and $ɔ_s$ is presented in Fig 8. Optimal temperature and density threshold was found to be 5 ºC and 250 g/cm^3, respectively. The highest correlation between the modelled and simulated snow depth frequency distributions (0.89) and lowest V_f –value (0.025) was achieved for year 2000. With the OrigCurve model the optimal $ɔ_c$ was reduced to 12 while $ɔ_s$ was in the same range as for the WCurve model.

The optimal parameter range was not as unambiguous for the two years when using the OrigCurv model as for the WCurve model and the correlation between the modelled and simulated snow frequency distribution and V_f were poorer. This indicates that at least for this site the WCurve model performs better than the OrigCurv model.

Fig. 9 shows how the observed and modelled accumulation and erosion areas are distributed as a function of the aspects. The observations show that the snow is more

URN:NBN:no-6348

uneven distributed in 2000 than in 1998. The WCurve simulations tend to place too much snow at southern slopes while the OrigCurv model erodes too much at the eastern slopes. Neither the frequency distribution nor the location of snow at the aspects where improved by increasing the resolution from 100m by 100m grid spacing to 50m by 50m.

The residual plot at Fig. 10 shows that the errors in the simulated snow distributions are largest in the steep SSW facing slopes west of Rabben where the model place too much snow, west of Kolhaugen were it does not accumulate enough and in the ENE facing slopes up towards the Schetlig mountain. A more complex wind model where topographic modification of wind direction and not only wind speed is included, would probably reduce these errors as the ESE-WNW oriented valleys in the site probably redirect the wind and lead to more erosion in e.g. the slope SSW of Rabben.

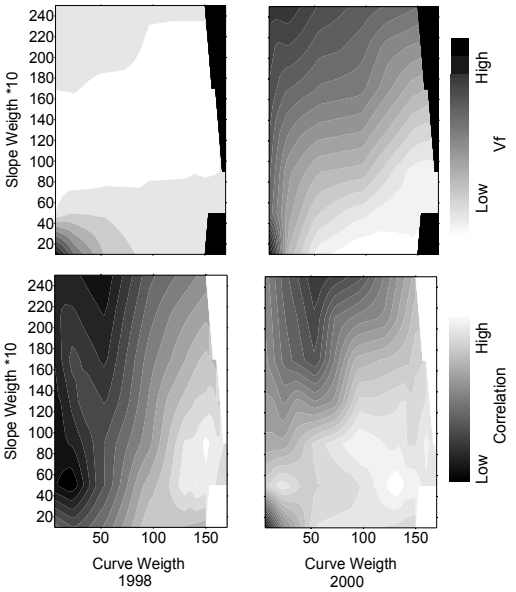

Fig. 8 Sensitivity of the correlation between observed and modelled snow depth frequency distributions and of Rank Order Coeffisient V_f with changing σ_c and σ_s.

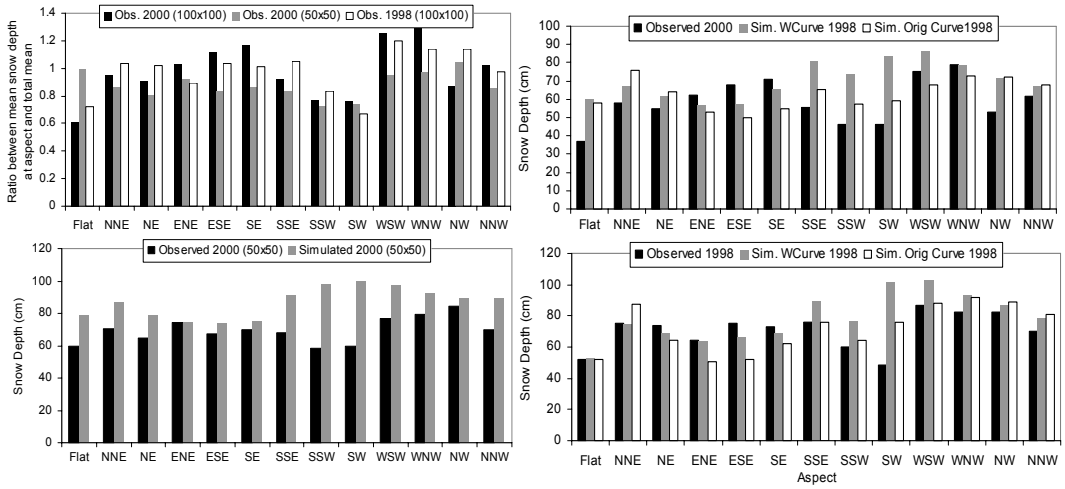

Fig. 9 Observed and modelled snow depths at different aspects

URN:NBN:no-6348

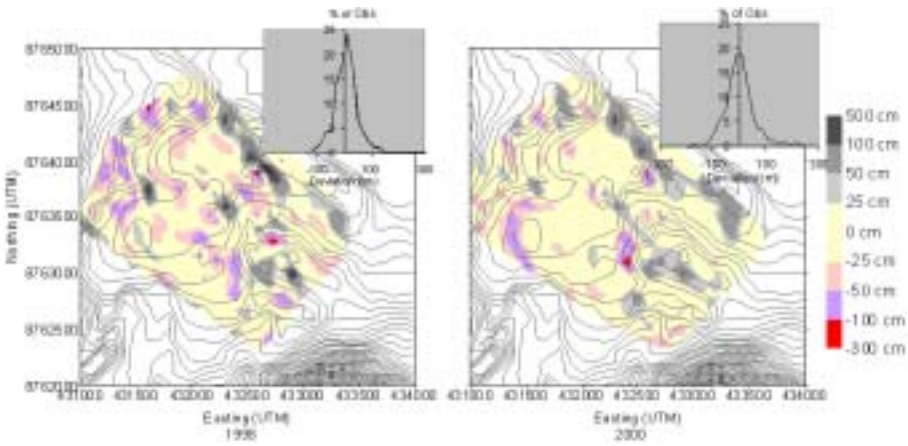

Fig.10 Residual plot of modelled – observed snow depths with it's frequency distribution

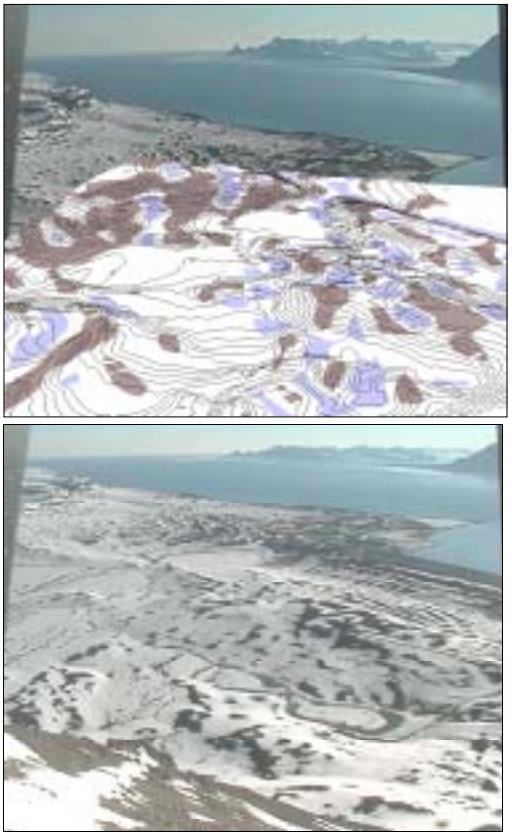

Fig.11 Oblique photo of the site end of June 2000 compared to aerial view with shallow snow cover marked brown and deeper snow in white and blue.

In Fig. 11 an oblique photograph from a video camera monitoring the snow cover depletion in the site from it's location at Zeppelin mountain, is compared to the modelled snow distribution. The photograph shows the snow cover in the end of June 2000 when most of the shallow snow is melted and the deeper snowdrifts are exposed. Both the location and extent of the accumulation and erosion areas are to a high degree coincident with the model result.

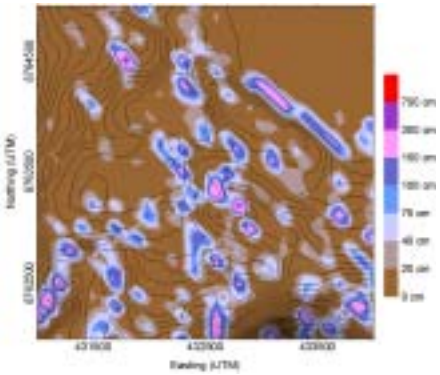

Fig. 12 Modelled snow distribution using the original model without snow settling

Fig. 12 shows the result of simulations using the original model without the snow settling two layer calculation included. This model does not create the crust on the snow surface that prevents further erosion and the snow is eroded down to the vegetation threshold in large areas of the site. In this area with no scrub or taller vegetation the modelled snow cover it too shallow compared to the observation.

URN:NBN:no-6348

Aursunden site

For this site the model simulation was run only for one winter, from 1 of October 2000 through 9 May 2001. The simulation was run with 25m by 25m grid spacing and a 6-hour time step. Meteorological observation station St 1 has a more representative location, but since it's data series has some large gaps, these data sets are used only to correct the data from St 2. The model was run with the original curvature calculation and the optimal ∂_c and ∂_s was found to be 8 and 12, respectively. This is consistent with what was found for the Ny-Ålesund site with the OrigCurve model. The result of the model simulation were plotted and compared visually to the measured data (Fig. 13)

.

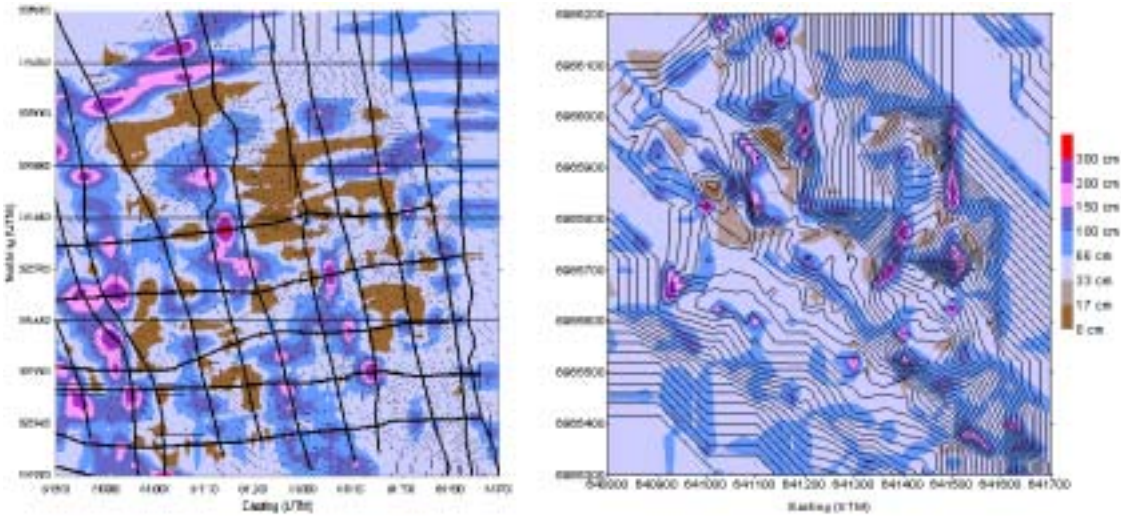

Fig.13 Observed (left) and modelled snow distribution at Aursunden site. Measured grid is included on observation plot.

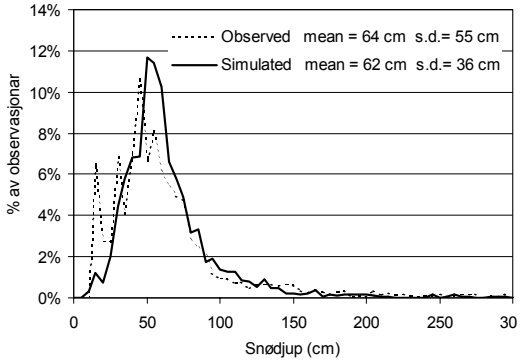

Fig. 14 Frequency distribution of modelled and observed snow depths at Aursunden

Frequency distribution of simulated and observed snow depths are presented in Fig. 14. The residual plot (Fig. 15) shows that the snow drifts in some areas are displaced compared to the observations. These deviations are probably due to a poorer resolution of the topographic model and/or snow depth measurements in these areas. The topographic model is composed of data with 100m by 100m grid spacing and manual observations using DGPS (Differential Global Positioning System) along topographic features. Along the western and northern edge of the site there are few or none manual observations and the topographic model is thus less accurate. In some places a combination of fog and difficult terrain made snowmobile driving difficult. Here snow depth measurements are more scattered and the interpolated values between these are not necessarily representative. This is the case for a larger area in the centre of the site where interpolation of the observed snow depths indicates erosion and the model on the contrary and probably correctly, accumulates snow. The frequency distribution of the observed snow depths is more peaked than for the distribution of the simulated snow depths.

URN:NBN:no-6348

The correlation between the snow depth frequency distributions was 0.9 and the V_f – value of 0.002. The frequency distribution of the residuals between observed and simulated snow depths (Fig. 15) shows that the residuals are nearly symmetrically distributed around 0 and that close to 45% of the grid cells has no deviation between observed and simulated snow depth.

These factors and visually comparison of the plot showing observed and modelled snow distributions, indicates that the snow depths in and location of snowdrifts and erosion areas with a few explainable deviations, are acceptable.

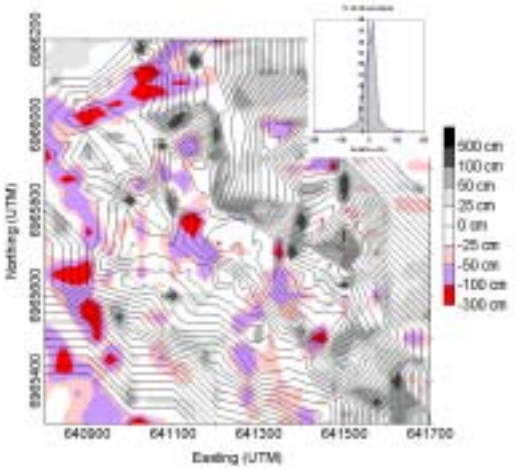

Fig.15 Residual of modelled-observed snow depths at Aursunden site

DeGeer site

The model simulation was run from 1 of September 2000 through 11 May 2001 on a 100m by 100m grid and with a 6-hour time step. The simulated snow distribution is presented in Fig. 16.

Due to the much larger basin scale it is impossible to have verification data for the entire site and the model simulation is compared only to snow depths measured along a set of selected transects crossing the DeGeer Valley.

These transects have a total length of 24 kilometres and snow depths were measured every meter by Georadar.

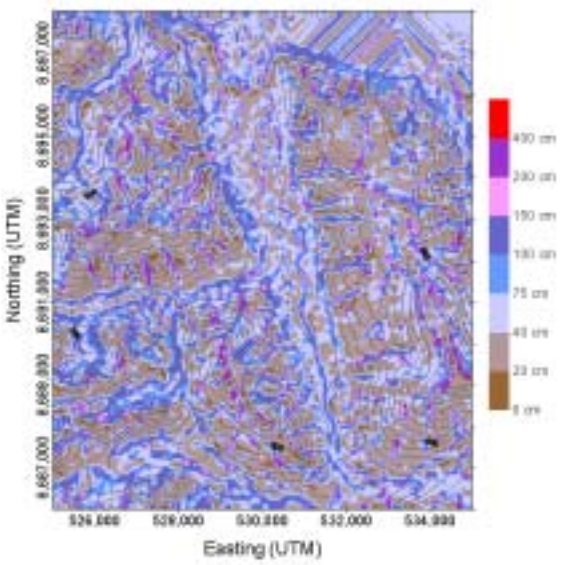

Fig. 16 Modelled snow distribution in DeGeer

Fig. 17 shows the frequency distributions of observed and simulated snow depths for all transects in DeGeer and observed snow depths along four of these transects compared to simulated values found by interpolation in SURFER.

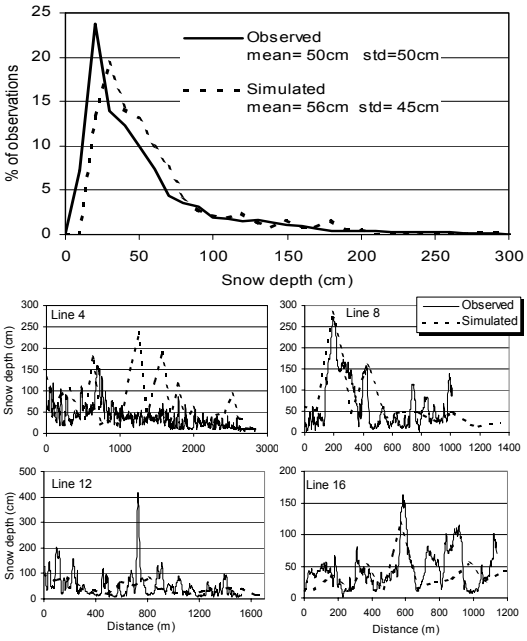

Fig. 17 Modelled and observed: - snow depth frequency along all transects; - snow depths along 4 of the 17 transects

URN:NBN:no-6348

The snow depth observations are not extensive enough to validate whether the WCurve model performs better than the original model for this site. A short period with observation of wind speed and direction in DeGeer shows also that the direction of the wind in this valley in several occasions deviates considerably from what is measured on Svalbard airport (Fig. 18).

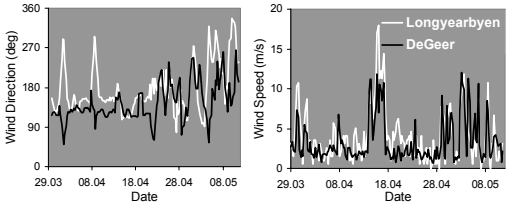

Fig. 18 Wind observation at Longyearbyen airport compared to local observations in DeGeer Valley

The original curvature calculation is therefore used here. In order to reproduce the snowdrifts observed at the eastern side of the valley, the curvature weight gc was increased to 18 while the slope weight gs was reduced to 4. Fig. 19 shows two oblique aerial views of the DeGeer valley. Seen from Southwest the large areas with shallow snow depths are visible. The view from Northeast gives a different impression as the accumulation areas is more visible. Pictures of the west and east facing valley sides shows the same features (Fig. 19). This and comparison of frequency distributions and snow profiles, indicates that the model is capable of reproducing the snow distribution also at this scale and with the rather poor quality and representativity of the data available.

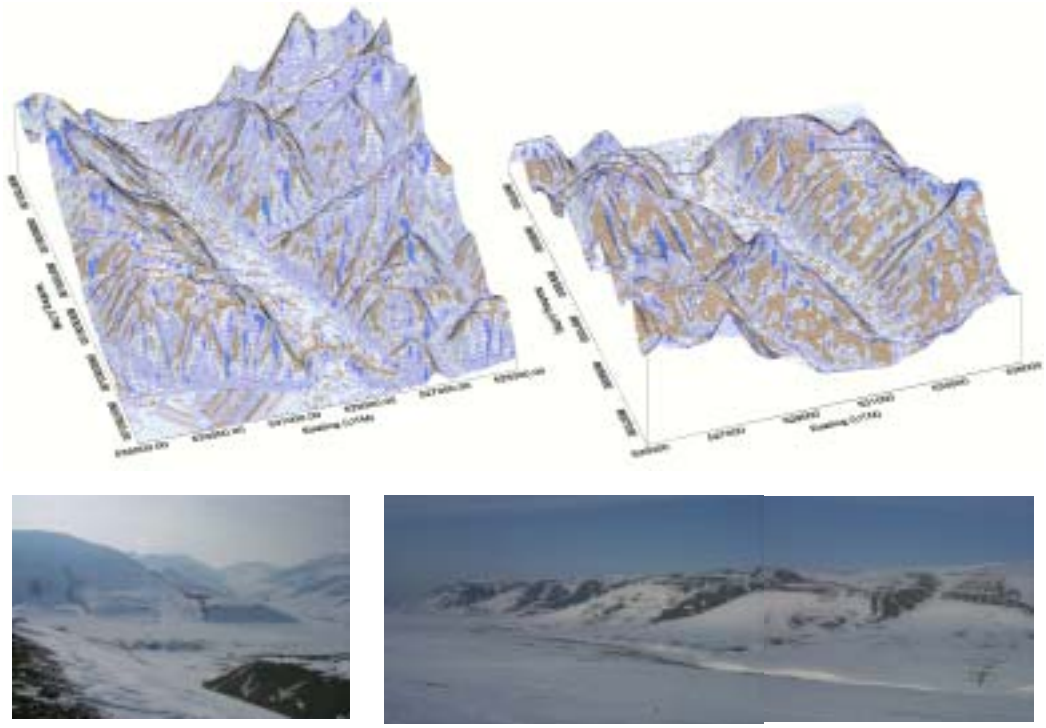

Fig. 19 Oblique areal view of the DeGeer valley from SSW (right) and from NNE (left) and photos showing a section of the west facing side of the valley (right) and a typical view of the east facing slopes (left).

URN:NBN:no-6348

Summary and Conclusions

SnowTran-3D was applied at three different sites with size ranging from 1 km^2 to 250 km^2 and location from 62ºN to 79ºN. In order to allow for events during the winter with mild climate and temperatures above freezing, a snow settling calculation was included in the model. The topographic modification of wind speeds was also changed from treating the influence of curvature independent of wind direction to increase it gradually from zero to full effect as the wind direction changes from longitudinally to perpendicular to the topographic curvature. The model result was compared to extensive observation dataset for each site and the sensitivity of main model parameters to the model result was tested.

For the Ny-Ålesund site the different variants of the model was tested. Without the snow settling calculation the model eroded the snow cover down to the vegetation threshold over most of the site. In the two layered model the erosion threshold depends on the climatic conditions and the snow settling and the result was thereby significantly improved.

The improvement by the wind direction dependent curvature calculation (WCurve) was less significant but it led to a more unambiguous parameter range for the two years it was tested. Snow depth frequency distribution was also slightly improved by the WCurve model compared to the original curvature calculation. Optimal curvature ($ↄ_c$) and slope weights ($ↄ_s$), temperature and density thresholds for the WCurve model was found to be around 150 and 8, 5ºC and 250 g/cm^3, respectively. For the OrigCurve model optimal $ↄ_c$ was 12, the other parameters were unchanged. In both years the modelled snow distribution had a snow depth frequency distribution and location of snowdrifts and erosion areas with a satisfactory coincidence with the observations.

The Aursunden site is located 17º latitude south of Ny-Ålesund and thus has a different climate. Modelled snow depth frequency distribution was highly correlated (0.9) with the observed. Displacements of snowdrifts and erosion areas are explained partly by too poor resolution in the topographic model basis and in some places with poor coverage of snow measurements.

The DeGeer valley site is about 100 times larger than Ny-Ålesund site and the climatic observations has a poorer representativety. Still the modelled snow depths compared to snow depths measured along carefully selected transect has a high coincidence. Both the frequency distribution of the snow depths and the location of snowdrifts and erosion areas are comparable to observation.

These tests and applications proofs that a numerical model is capable of recreating the snow distribution in sites with different size, topographic variability and location. Snow depth frequency distribution and location of snowdrifts and erosion areas a satisfactory recreated. The model can thereby produce snow distribution basis that can improve snow ablation calculation without extensive measurement campaigns, it can be used to study consequences of climatic change scenarios with higher precipitation and temperatures on the snow cover and it can be a helpful tool to study correlation between snow depth and vegetation distribution.

Acknowledgement

The authors acknowledge the financial support of the Norwegian Research Council, the support of topographic data and logistics in field from the Norwegian Polar Institute, UNIS and University of Colorado in Forth Collins for the residencies and last but not least the authors want to thank Kings Bay in Ny-Ålesund for the superb accommodation, their help and positive attitude.

URN:NBN:no-6348

References

Andersen, T., Gottschalk, L., Killingtveit, Å., and Aam, S. (1982) Snømålinger for kraftverksdrift. Rapport til Rådet for den kraftverkshydrologiske tjenesten. Prosjekt A-113. Trondheim (in Norwegian), 116 pp.

Andersen, T., Lundteigen Fossdal, M., Killingtveit, Å., and Sand, K. (1987) The snow radar: A new device for areal snow depth measurements. "Hydropower '87" Int. Conf. on Hydropower in Norway, Trondheim 30 June-2 July 1987, 16 pp.

Beek, L. K. H. van (1967) Dielectric behaviour of heterogeneous systems, *Progress in Dielectrics, Vol. 7*, pp. 69-114.

Glen, I. W., and Paren, I. G. (1975) The electrical properties of snow and ice, *J. Glaciol., Vol. 15, No. 73*, pp. 15-37.

Hamran, S. E., Hjelmstad, J., and Aarholt, E. (1986) Tofrekvens radar for snødybdemålinger. Sluttrapport med prototyp testresultater. Technical note NT-75/86. Norwegian research council for technical research – Programme for environment monitoring (in Norwegian).

Kennett, M. (1994) Uttesting av georadar for snømålinger – status pr. oktober 1994. HB-notat 11/94. Norwegian Water Resources and Energy Administration. Oslo (in Norwegian) 3 pp.

Killingtveit, Å., and Sælthun, N. R. (1995) Hydrology. Hydropower development. Vol. 7, Norwegian Institute of Technology, Division of Hydraulic Engineering. Trondheim. 213 pp.

Sand, K., and Killingtveit, Å. (1983) Snøforholdene i Orklafeltet. Studie av snøfordeling og forslag til snømåleopplegg. Rapport STF60 A83016. Norges hydrodynamiske laboratorier, Trondheim (in Norwegian), 76 pp.

Sand, K., and Killingtveit, Å. (1988). Snow-radar: An efficient tool for areal snow pack assessments, Proc. 7th Northern Research Basins Symp. and Workshop, May 25-June 1 1988, Ilulissat, Greenland, pp. 145-157.

Ulaby, F. T., Moore, R. K., and Fung, A. K. (1986) *Microwave Remote Sensing, Active and Passive, Volume III,* Addison-Wesley Pub. Company.

Ulriksen, P. (1989) Radar measurement of equivalent water content in snow measured from a helicopter. EARsel Workshops and Symp., Helsinki University of Technology, Espoo, Finland, 27 June – 1 July 1989, 6 pp.

Received: November, 1997
Revised: August, 1998
Accepted: August, 1998

Address:
Knut Sand,
The University Studies on Svalbard,
P. O. Box 156/157,
N-9170 Longyearbyen,
Norway.
Email: knut@unis.no

Oddbjørn Bruland,
SINTEF, Civil and Environmental Eng.,
N-7034 Trondheim,
Norway.
Email: oddbjorn.broland@civil.sintef.no

URN:NBN:no-6348

References

Abele, G. and Gow, A.J. (1975) Compressibility characteristics of undisturbed snow. Research report 336, U.S. Army Cold Regions Research and Engineering Laboratory (CRREL), Hanover New Hampshire.

Anderson, E.A. (1976) A point energy and mass balance model of s snow cover. NOAA Tecnical Report NWS 19, Office of Hydrology, National Wheater Service, Slver Spring.

Brooks, P.D., Schmidt, S.K. and Williams, M.W. (1997) Winter production of CO_2 and N2O from alpine tundra: environmental controls and relationship to inter-system C and N fluxes. Oecologia, Vol. 110 , pp. 403-413.

Bruland, O. and Cooper, E. (2001). Snow distribution and vegetation. In: P. Kuhry (Editor), Proceedings of Arctic Feedbacks to Global Change. Rovaniemen Paintuskeskus Oy, Rovaniemi, Finland, pp. 110.

Bruland, O., Sand, K. and Killingtveit, Å. (2001) Snow Distribution at a High Arctic Site at Svalbard. Nordic Hydrology, Vol. 32 (1), pp. 1-12.

Colman, R.A., McAvaney, B.J., Fraser, J.R., Rikus, L.J. and Dahni, R.R. (1994) Snow and cloud feedbacks modelled by an atmospheric general circulation model. Climate Dynamics, Vol. 9 (4/5), pp. 253-265.

Déry, S.J., Taylor, P.A. and Xiao, J. (1998) The thermodynamic effects of sublimation, blowing snow in the atmospheric boundary layer. Boundary-Layer Meteorology, Vol. 89 , pp. 251-283.

Førland, E., Hanssen-Bauer, I. and Nordli, P.Ø. (1997) Climate statistics & longterm series of temperature and precipitation at Svalbard and Jan Mayen. DNMI Report 21/97, Norwegian Meteorological Institute, Oslo.

Gray, D.M. and others, a. (1979). Snow accumulation and distribution. In: S.C. Colbeck and M. Ray (Editors), Proceedings of Meeting on Modeling of Snow Cover Runoff. US Army Cold Regions Research and Engineering Laboratory, Hanover, New Hampshire, pp. 3-33.

Hartman, M.D. et al. (1999) Simulation of Snow Distribution and Hydrology in a Mountain Basin. Water Resources Research, Vol. 35 (5), pp. 1587-1603.

Kojima, K. (1967). Densification of seasonal snow cover. Physics of Snow and Ice., Proceedings of International Conference on Low Temperature Science - Sapporo. The Institute of Low Temperature Science, Hokkaido University, Sapporo, pp. 929-952.

Kotlyakov, V.M. (1961). Results of study of the ice sheet in Eastern Greenland, Proceedings of International Geodetical Geophysical General Assembly. Scientific Publication. International Association of Hydrology, Helsinki, pp. 88-89.

Liston, G. and Sturm, M. (1998) A snow transport model for complex terrain. Journal of Glaciology, Vol. 44 (148), pp. 498-516.

Lloyd, C.R. et al. (1999) Final Report of the Land Arctic Physical Processes (LAPP) Project. Contract No. ENV4-CT95-0093, EC DG XII Climate and Environment, Brussels.

Marsh, P. (1999) Snowcover Formation and Melt: Recent Advances and Future Prospects. Hydrological Processes, Vol. 12 , pp. 2117-2134.

McLung, D. and Scharer, P. (1993) The Avalanch Handbook. The Mountaineers, Seattle, 271 pp.

Norway, S. (2001) Statistical Yearbook of Norway 2001. NOS C671, Statistics Norway, Oslo.

Pomeroy, J., Gray, D.M. and Landine, P.G. (1993) The Prairie Blowing Snow Model: characteristics, validation, operation. Journal of Hydrology, Vol. 144 , pp. 165-192.

Pomeroy, J.W. et al. (1998) An evolution of snow accumulation and ablation processes for land surface modelling. Hydrological Processes, Vol. 12 , pp. 2339-2367.

URN:NBN:no-6348

Prasad, R., Tarboton, D.G., Liston, G., Luce, C. and Seyfrid, M. (2001) Application of a Wind Blowing Model to Reynolds Creek Experimental Watershed. Water Resource Research, Vol. 37 (5), pp. 1341-1357.

Ryan, B.C. (1977) A mathematical model for diagnosis and prediction of surface winds in mountainous terrain. Journal of applied meteorology, Vol. 16 (6), pp. 571-584.

Uematsu, T., Nakata, T., Takeuchi, K., Arisawa, Y. and Kaneda, Y. (1991) Three-dimensional numerical simulation of snowdrift. Cold Regions Science and Technology, Vol. 20 (1), pp. 65-73.

Van Der Wal, R. et al. (2000) Trading forage quality for quantity? Plant phenology and patch choice by Svalbard reindeer. Oecologia, Vol. 123 , pp. 108-115.

Vonk, J. (2001) Distributed snow modelling and verification in a High Arctic Catchment. Master Thesis, University Courses on Svalbard, Longyearbyen, 77 pp.

URN:NBN:no-6348

Paper 8:
Application of Georadar in Snow Cover Surveying. Nordic hydrology, Vol. 29 (4/5), pp. 361-370.

URN:NBN:no-6348

Paper 9:
Improved Measurements and Analysis of Spatial Snow Cover by Combining a Ground Based Radar System With a Differential Global Positioning System Receiver. Nordic Hydrology, Vol. 32 (3), pp. 181-194.

URN:NBN:no-6348

URN:NBN:no-6348